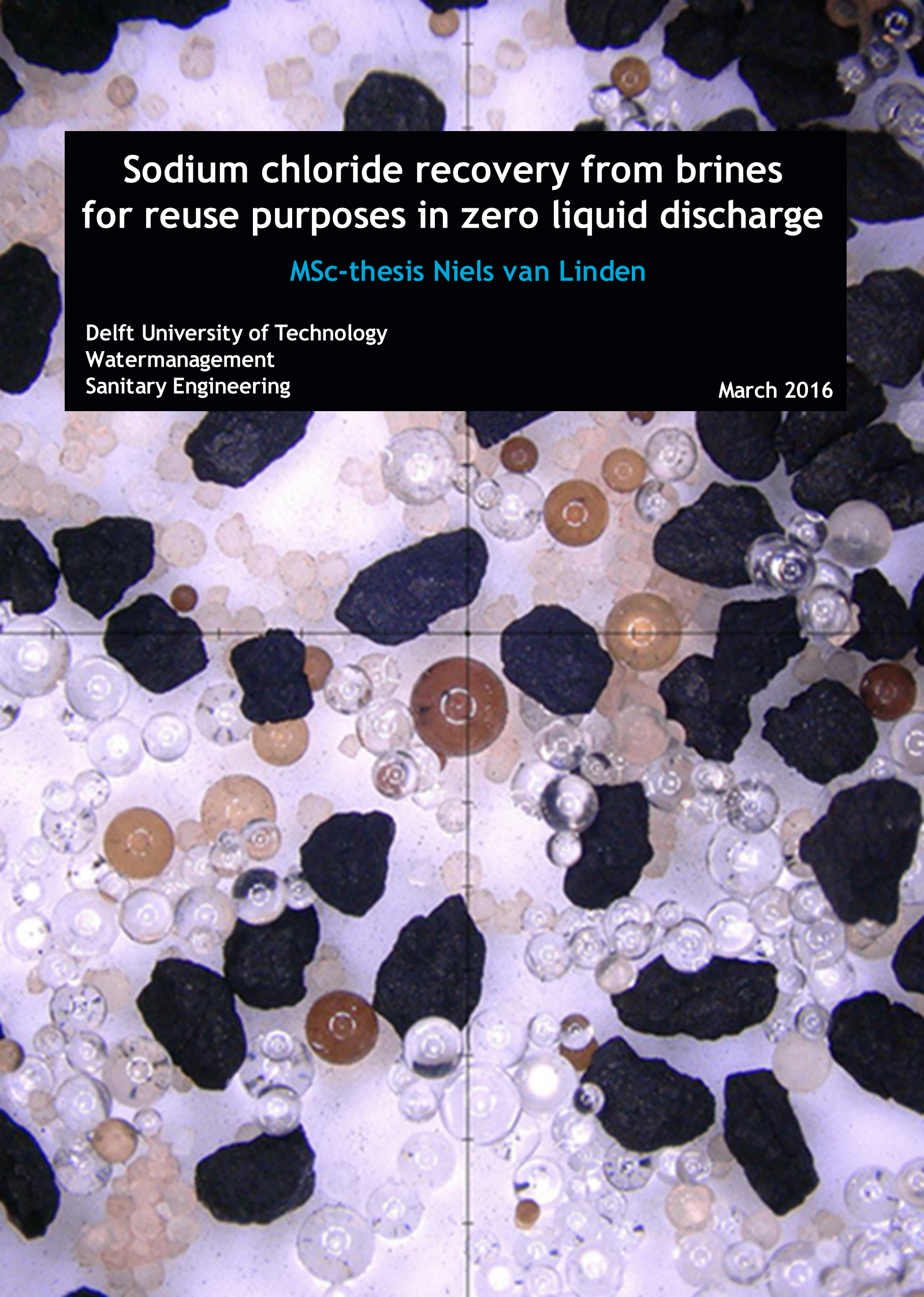

Sodium chloride recovery from brines for reuse purposes in zero liquid discharge

MSc-thesis Niels van Linden

Delft University of Technology
Watermanagement
Sanitary Engineering

March 2016

Colophon

Description	Final MSc-thesis	
Title	Sodium chloride recovery from brines for reuse purposes in zero liquid discharge.	
Date	Thursday, 31st of March 2016	
Author	Niels van Linden	
	N.vanLinden@tudelft.nl	
Supervision	Prof. Dr. Ir. L.C. Rietveld	TU Delft – Watermanagement
	Prof. Dr. Ir. G.J. Witkamp	TU Delft – Process & Energy
	Dr. Ir. H. Spanjers	TU Delft – Watermanagement
	Dr. Ir. S.G.J. Heijman	TU Delft – Watermanagement
	Dr. Ir. R. Shang	TU Delft – Watermanagement
	G. Stockinger MSc.	Shell Global Solution International B.V.

Partners

Acknowledgements

I am very glad I made the switch to Watermanagement after a short study period at a different faculty. Before this switch, I conducted my BSc thesis partially in Portugal, which made me very enthusiastic about water treatment. But I already decided to start with a less-technical master, which did not last long. I wanted to continue treating water, since during my BSc thesis I encountered a problem I could not solve at the time: management of brines.

After one and a half years education, including two nice trips to Jakarta and Barcelona, I started looking for a MSc thesis topic. I believe I was picky, because I wanted to do something with experimental testing, various physical/chemical water treatment techniques and preferably something with zero liquid discharge. A certain topic was available, but not readily, since it was a project executed by a research group of the TU Delft and there were some difficulties with confidentially and thesis definition. Finally, I was allowed to pick this topic for my MSc thesis and the respective research group formed the majority of my committee. I could continue where I finished with my BSc thesis: management of brines.

Eight months of research finally results in this thesis. During this period, I was spoiled with the variety of physical/chemical water treatment techniques. Because I had quite some help during the last eight months and actually also during my entire MSc, I would like to thank a lot of people. Luuk Rietveld, I would like to thank you for your aid throughout my entire MSc: you inspired me to conduct my MSc in Watermanagement after my successful BSc thesis experience. Henri Spanjers, thank you for the many discussions during my internship, Fundamentals courses and especially my MSc thesis. I would also like to thank you for making it possible to do my MSc thesis on this topic and giving me the opportunity to work in the project as a team member. Subsequently, I would like to Bas Heijman, Ran Shang, Geert-Jan Witkamp and Georg Stockinger for your valuable contribution during the kick-off and intermediate meetings.

Additionally, I would like to thank the staff of the Waterlab: Armand, Tonny, Wanisha and Mohammed, for making experimenting go smoothly and thanks goes out to Waterapplicatiecentrum, for being responsible for part of the analysis of my samples. I would also like to thank Marjolein Vanoppen and Arne Verliefde for their time to discuss electrodialysis. Furthermore, I would like to thank Raluca Olariu, for helping me with the electrodialysis and nanofiltration experiments and guiding me through the lab the first weeks. Abel, Frans-Willem, Basak and Max, I would like to thank you for your presence and help in the Waterlab.

I would like to thank my family, for always supporting me, actually with everything. I would like to thank my friends, because hard work also comes with relaxing and fun. Finally, I would like to thank my girlfriend Loran, for always supporting me. We had a very rough year, but you have always been very patient and supportive. Thank you so much for that.

Niels van Linden

Vlaardingen, March 2016

Abstract

As a progressive strategy of brine management, ZLD is applied to recover all water in a full-scale WWTP, resulting in final solid stream. This stream consists of mixed solids, of which the bulk is NaCl. Currently, the NaCl is of low purity, because various contaminants are present and exceed the guideline limit in the mixed solids: NOM, silica and iron. Therefore, this solid stream is currently landfilled. If the purity of the NaCl can be improved, re-use opportunities arise, implying various benefits.

In order to improve the purity of the NaCl, the contaminants needed to be rejected from the NaCl. Rejection was considered to be feasible by isolation of dissolved NaCl and the extraction of the contaminants from the mixed solids. Therefore, the research objective was *to select the most suitable intervention technique(s) contributing to produce high purity NaCl in the ZLD WWTP*.

To this extent, initially, the presence in the solids was reviewed. Secondly. for the dissolved phase, the most concentrated dissolved solids stream (RO-brine) was topic of research for dissolved NaCl isolation in various bench-scale experiments: PNF and CNF with variable cross-flow application, ED using MVMs and STMs and IEX in various ionic forms. Finally, a bench-scale SALEX experiment was executed to purify the mixed solids. Based on these experiments, the performance of all techniques was determined based on the (dissolved) solids yield, the rejection of contaminants and finally the content of contaminants in the total solids (as [mg/g]). The contamination content was compared with NaCl re-use guidelines, serving as independent judgemental performance tool.

The presence of the contaminants proved to be inevitable, since NOM is a product of decay of micro-organisms present in the bio treaters in the ZLD WWTP and silica presence is caused by environmental influences. The presence of iron proved to be facilitated by the presence of NOM: organic iron complexation increased the solubility of iron up to fifty times in an additional experiment.

With regard to the isolation and purification of NaCl: all techniques proved to have a high yield of (dissolved) solids, but the rejection of contaminants deviated strongly. The rejection of NOM deviated: 0.14 – 0.77 [-] expressed as TOC. Generally, aromatic molecules were rejected to a higher extend than non-aromatic molecules. The rejection of silica deviated even more: 0.07 – 0.96 [-]. Both the variation in NOM and silica rejections can be related to the specific characteristics of these constituents and the working mechanisms of the used techniques. None of the NaCl isolation techniques was able to propose a sufficiently pure NaCl stream. The content of iron could not be determined, since no reliable iron results were measured. This is probably caused by the 10^5 times higher presence of sodium during simultaneous sodium and iron analysis, using ICP-MS.

On the contrary, the purification of the mixed solids using the SALEX technique, proved to be able to produce a NaCl stream meeting the guidelines. Enforced by positive outcomes of a SWOT analysis, this technique is recommended to be implemented in the ZLD WWTP, in order to contribute to produce high purity NaCl for reuse purposes.

Table of contents

Abbreviations

AEM	Anion Exchange Membrane
BV	Bed Volume
CDOC	Chromatographable Dissolved Organic Carbon
CEEM	Cation Exchange End Membrane
CEM	Cation Exchange Membrane
CNF	Ceramic Nanofiltration
DF	Diafiltration
DOC	Dissolved Organic Carbon
DVR	Dynamic Vapour Recompression
EC	Electrical Conductivity
ED	Electrodialysis
EFC	Eutectic Freeze Crystallization
HC	High Cross-flow
HMP	Hydraulic Membrane Permeability
HOC	Hydrophobic Organic Carbon
HPLC	High Performance Liquid Chromatography
ICP-MS	Inductively Coupled Plasma Mass Spectrometry
IEX	Ion Exchange
LC	Low Cross-flow
LCD	Limiting Current Density
LC-OCD	Liquid Chromatography Organic Carbon Detection
LMW	Low Molecular Weight
MAEM	Monovalent-selective Anion Exchange Membrane
MVM	Monovalent-selective Membrane
MW	Molecular Weight
MWCO	Molecular Weight Cut Off
NaCl	Sodium Chloride
NF	Nanofiltration
NOM	Natural Organic Matter
OIC	Organic Iron Complexation
PNF	Polymeric Nanofiltration
QVC	Qatar Vinyl Company
RO	Reverse Osmosis
SALEX	Extraction of impurities from SALt
STM	Standard Membrane
SUF	Submerged Ultrafiltration
TDS	Total Dissolved Solids
TMP	Trans Membrane Pressure
TOC	Total Organic Carbon
UV254A	Absorbance of Ultraviolet light at 254 nm
VMD	Vacuum Membrane Distillation
WWTP	Waste Water Treatment Plant
ZLD	Zero Liquid Discharge

1. Introduction

1.1. Background information

1.1.1. Generation of brines

In water treatment, undesired constituents are rejected from the feed water stream, which is often performed by exclusion based on size or charge. In case of physical separation of these constituents, a reject stream will inevitably be produced. This type of stream consists of high concentrations of undesired constituent and are produced during the application of, for example, membrane filtration. These concentrate streams are called **brine**, which typically contain high concentrations of dissolved salt(s) (Pérez-González et al., 2012).

Generated brines are considered hard to treat, because of their considerable volume (depending on the recovery in membrane processes: ranging 25 – 35% of the feed water volume for desalination of brackish and seawater (Ahmed et al., 2003)) and high concentration of various constituents. The actual composition of the brine depends on the composition of the feed water and applied strategy to the treatment process: pre-treatment, added chemicals, applied recovery for membrane processes or contaminants and volumes for spent regeneration solution in ion exchange. For this thesis, brine generation consists of the concentrate stream of membrane filtration with reverse osmosis (RO).

1.1.2. Management of brines

In order to process brines, various strategies have been developed. Conventional strategies for brine management include;

- Surface water discharge (seas and rivers),
- Deep-well injection,
- Sewer discharge
- Evaporation in evaporation ponds.

Roberts et al. (2010) showed that discharge of brine in seas has significant impact on marine environments. Deep-well injection has the restriction that the subsurface becomes clogged after repeating injection, because of scaling products in the (often supersaturated) brine and sewer discharge comes with high costs, because of high constituents loading (Mickley et al., 2008). Finally, evaporation ponds take large amounts of space for construction, which are not always available (Ahmed et al., 2003; Alberti et al., 2009; Jeppesen et al., 2009).

When the discussed conventional strategies do not suffice, because of the respective restrictions, advanced treatment strategies must be applied to process brines. Additionally, regulations are the most frequent reason to apply advanced brine treatment, because discharge is either fined or simply not allowed (Robert Y. Ning et al., 2010).

1.1.3. Zero liquid discharge

One of the most progressive brine treatment strategies is the application of **zero liquid discharge (ZLD)**: a generic name for technologies resulting in 100% water recovery. This strategy has been introduced in the 1970's and has subsequently been developed since the 1990's. Currently, more than 120 various ZLD systems are operative in the United States of America only, in a great variety of configurations achieving ZLD (Mickley et al., 2008). The most distinctive applied processes in the variety of configurations to achieve ZLD are the evaporation and crystallization process.

Evaporation process

Evaporation processes make use of techniques relying on thermal driven mechanisms: application of heat. Because the phase transition of water takes place at different temperatures than for the other constituents, the water evaporates and can be recovered after cooling as condensate. The residual stream, with a significant decreased water content, can be called Evaporation-brine.

Solar evaporation with possible enforcement of wind is a natural evaporation technique, which is applied as mechanism in evaporation ponds (Pérez-González et al., 2012). On the other hand, Dynamic Vapour Recompression (DVR) and Vacuum Membrane Distillation (VMD) are more advanced evaporation techniques where VMD is a synergy between membrane and evaporation techniques. These mechanisms are (extensively) discussed by Pérez-González et al. (2012) and Vaudevire et al. (2013) and not further discussed in this thesis.

Crystallization process

In order to produce a stream free of liquids, crystallization techniques are applied. In this process, solid salt crystals are produced by making use of continuous recovery of water, resulting in salt concentrations exceeding the solubility concentration: crystallization. A rough distinction of crystallization techniques can be made between *selective* and *unselective* crystallization techniques.

A specific selective crystallization technique, eutectic freeze crystallization (EFC), makes use of a staged process, where the temperature is gradually decreased: application of cooling instead of heating. In this process various constituents crystallize at their respective eutectic point, after water is reclaimed as ice and the solution becomes more concentrated. This results in sequential recovery of both high purity salts and water (Nathoo et al., 2009).

On the contrary, evaporative crystallization techniques make use of heating, similarly as DVR and VMD. Examples of these unselective evaporative crystallization techniques are presented in a technical paper of GE Power and Water, discussing the advantages of various mixed salt crystallizers in ZLD waste water treatment systems (Griffin et al., 2011).

Zero liquid discharge

A strategy to achieve ZLD is schematized in Figure 1, with in its centre: brine generated in a membrane process. The volume of brine is significantly reduced, because water is recovered as condensate by evaporation and crystallization processes. Because the initially generated permeate adds to the recovery of water, 100% water recovery of is realized. The residual stream in the ZLD process consists of solids: either separated or mixed, depending of the applied crystallization technique.

The discussed evaporation and crystallization processes (except EFC) require a lot of thermal energy. Therefore, for this thesis, it is assumed that applying a ZLD strategy is economically more interesting when waste heat is present and water scarcity is an issue.

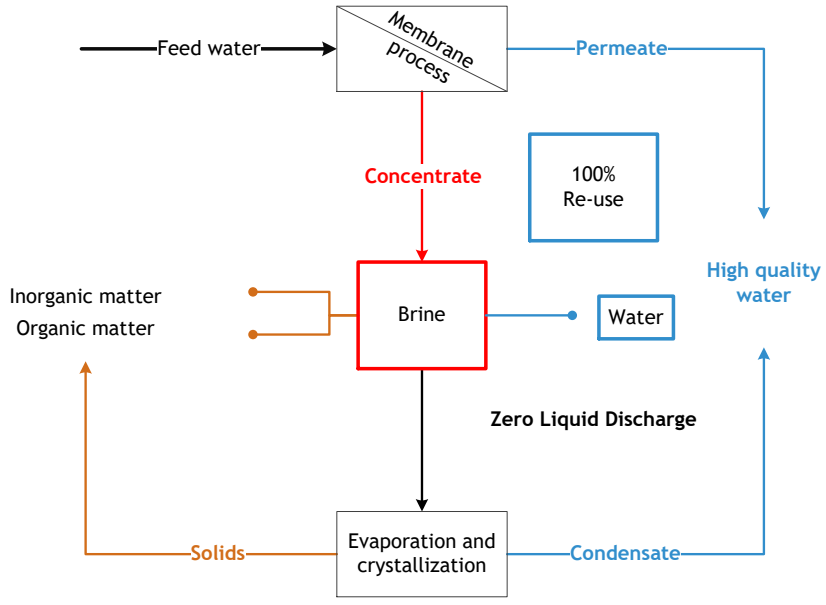

Figure 1 - Schematization of a strategy to achieve ZLD, with the brine as its centre. Water is recovered for 100%, whereas a residual solid waste stream is produced.

1.1.4. ZLD in petrochemical industry

The composition of feed water is unique for each water treatment facility and therefore the composition of brines is also unique for each situation. For this thesis, an actual existing full-scale ZLD waste water treatment plant (WWTP) serves as subject of research. The ZLD WWTP is operated by Shell.

The ZLD WWTP treats the waste water of a petrochemical facility, that produces a significant amount of water as a by-product in the production processes. The produced by-product is merged with effluent produced throughout the petrochemical facility.

Large amounts of waste heat are released in the production processes, whereas suitable cooling water is scarce. Additionally, local authorities are strict on (heat) emissions to the atmosphere and do not allow discharge of liquid streams on seas. Because water can be recovered and reused directly in the facility, ZLD was chosen as final achievement in the water management strategy (de Leeuw, 2013).

WWTP description

The WWTP combines conventional wastewater treatment processes with membrane processes and evaporation and (unselective) crystallization processes to achieve ZLD. The conventional wastewater treatment processes exist of coagulation-flocculation-flotation as pre-treatment and biological treatment as main treatment. Subsequently, sub-merged ultrafiltration (SUF) serves as a physical barrier for particulate and suspended solids and a two-step RO produces high quality permeate for cooling water purposes. In this process, initial RO concentrate is filtrated again, resulting in a concentrated concentrate in RO3: **RO-brine**, in this thesis.

Finally, the last liquid fractions are recovered from the RO-brine as condensate in evaporation and crystallization processes. This results in a stream of generated solids, leaving the crystallization process. Figure 2 presents a schematic overview of the ZLD WWTP, including all treatment steps.

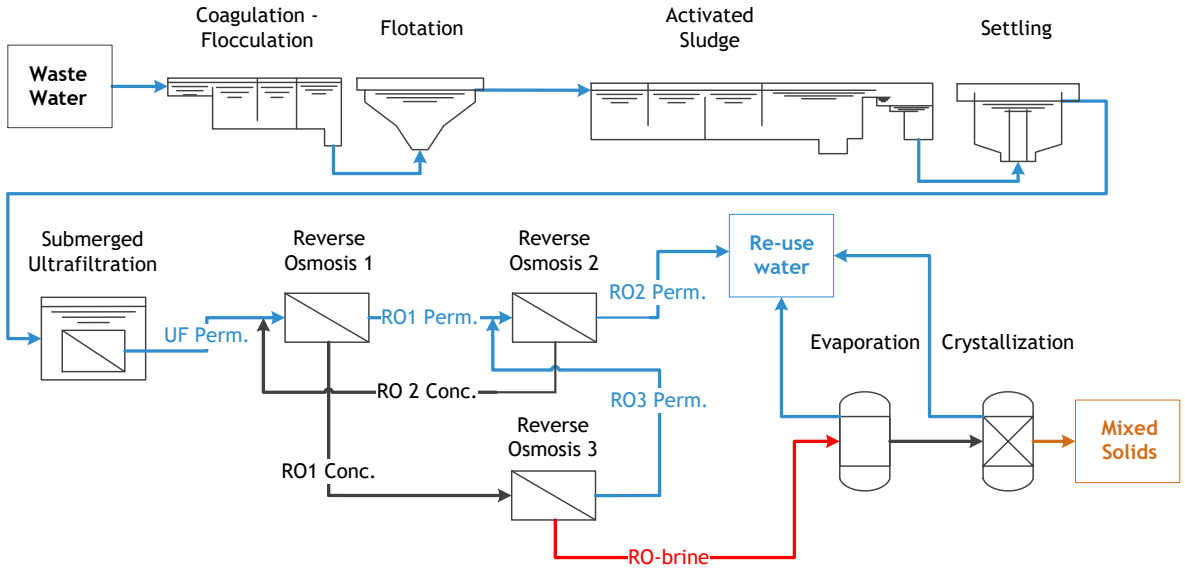

Figure 2 - A schematization of the ZLD WWTP. The water streams are indicated in blue and black and the RO-brine stream is indicated in red. A produced mixed solids stream is indicated in brown.

1.2. Problem description

The stream of solids generated in the ZLD WWTP consists of various solids (caused by unselective crystallization) and will therefore be called **mixed solids** in this thesis, as indicated in brown in Figure 2.

The mixed solids consist mainly of crystals, according to visual inspection. High purity sodium chloride (NaCl) crystals have a round-cubical shape and have a white and translucent appearance, see Figure 3. The crystals in the mixed solids have a similar shape as the NaCl crystals, but have a brown appearance, as presented in Figure 3.

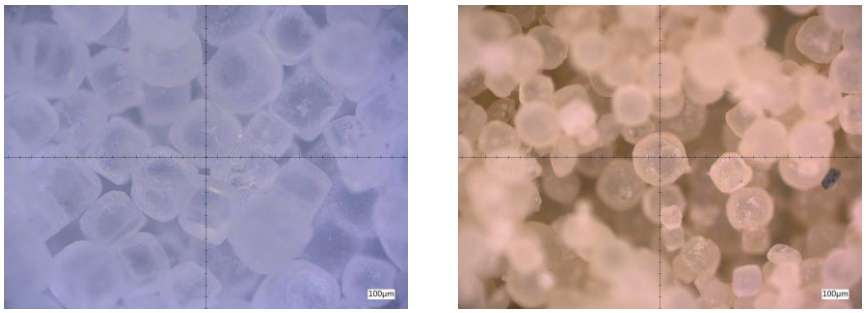

Figure 3 - Visible difference between commercial NaCl crystals (left) and NaCl crystals in the produced mixed solids (right). Pictures are taken at 100x magnification.

The composition of the crystals in the mixed solids was determined by chemical analysis and proved to consist mainly of NaCl: 0.94 [-] (as NaCl weight per weight of total solids), considering results from six various samples taken in a period covering 2013 – 2015. Because of the brown appearance, the mixed solids are unsuitable for re-use as solid NaCl. This statement is emphasized by comparison of the chemical analysis results to quality demands of a potential customer: a chemical company, producing PVC and chemicals such as hydrochloric acid (HCl) and caustic soda (NaOH) (QVC, 2013). The limits and chemical analysis results are presented in Table 1.

The results from Table 1 show that three various constituents are exceeding the restricting limit:

- Natural organic matter
- Silica
- Iron

These constituents will be referred as **contaminants** in this thesis. Nickel is exceeding the limit on average, but this is due to a single peak in the measurement: in five out of six measurements no nickel was measured. Therefore nickel is left outside of the scope of this thesis. Because potassium has very similar characteristics as sodium, it is assumed practically infeasible to be excluded from NaCl crystals and therefore also not considered as contaminant for the scope of this thesis.

When the contaminants are excluded from the mixed solids, the solid stream in the ZLD WWTP can potentially be re-used, as potentially high purity solid NaCl separately can be recovered. This adds value to the ZLD process as it will contribute to closing resource loops. At the moment, the mixed solids are landfilled. Therefore upgrading salt quality has the potential to avoiding costs of landfilling and even generate additional revenue from potential sales of the high purity NaCl.

Table 1 - An overview of constituents present in the mixed salts. The values in red represent the contaminants: constituents in the mixed solids exceeding the specifications, derived from (QVC, 2013).

Parameters	QVC Spec. for solid NaCl	Mixed solids AVG ± STD
All units in [mg/kg]		
Non metals		
Natural organic matter	**< 300**	**1,095 ± 141**
Silica (SiO_2)	**< 5**	**266 ± 251**
Cations		
Aluminium (Al)	< 1	0.21 ± 0.36
Barium (Ba)	< 1	0.02 ± 0.03
Calcium (Ca)	< 1,000	557 ± 538
Iron (Fe)	**< 10**	**64 ± 30**
Magnesium (Mg)	< 600	188 ± 101
Nickel (Ni)	< 0.20	0.81 ± 1.39
Potassium (K)	< 150	1,075 ± 1,793
Sodium (Na)	> 380,000	365,065 ± 16,547
Strontium (Sr)	< 60	0.17 ± 0.30
Anions		
Chloride (Cl)	> 590,000	574,978 ± 23,375
Bromide (Br)	< 200	-
Iodide (I)	< 1.2	-
Sulphate (SO_4)	< 1,500	574 ± 105

1.3. Research

1.3.1. Research objective

In order to finally yield high purity solid NaCl, modifications should be made in the ZLD WWTP. This is considered to be the main research topic for this thesis. To this extend, the objective of this thesis was:

"To select the most suitable intervention technique(s) contributing to produce high purity NaCl in the ZLD WWTP."

The main research of this thesis will therefore focus on various techniques that will *contribute* to produce high purity NaCl. It is stressed that these techniques are not solely responsible for the production of high purity NaCl. Additionally, these techniques should fit in the existing ZLD WWTP and are not considered to replace existing installations in the ZLD WWTP.

1.3.2. Research approach

The research was broken down into various steps, forming a structured approach to conduct the research.

Literature review

As a first step, a literature review was conducted on the *characteristics of the contaminants*, in order to explain their presence in the mixed solids and to relate their characteristics to the rejection mechanisms of the proposed treatment techniques. An extension of the literature review focused on constituent transport mechanisms, in order to gain more understanding of the techniques. Note: these mechanisms will not be verified in this thesis.

Isolation of dissolved NaCl

The second step was to determine *the most suitable water treatment techniques to isolate dissolved NaCl*. To this extend, isolation refers to separate dissolved NaCl from the contaminants. When a certain stream can be produced, it is assumed that subsequently all water can be recovered by the present evaporation and crystallization processes in the ZLD WWTP, resulting in high purity solid NaCl. For this step, a previous conducted research of de Ridder et al. (2014) served as a starting point. The proposed water treatment techniques originated from this research and include:

- *Nanofiltration* (using polymeric & ceramic membranes in various configurations)
- *Electrodialysis* (using standard & monovalent selective ion exchange membranes)
- *Ion exchange* (using resins in chloride & hydroxide ionic form)

The potential of dissolved NaCl isolation of the proposed water treatment techniques was determined with bench-scale experiments (flow rates up to 300 [L/h]), with RO-brine as feed.

Purification of mixed solids

The third step was *to purify the generated mixed solids in the ZLD WWTP*. This step considered mixed solids purification, to produce high purity solid NaCl using SALEX. The working mechanism of this technique was also subject of the literature review and its potential to produce high purity NaCl was determined with bench-scale experiments as well.

Comparison

To determine the performance of the proposed techniques, the purity of the NaCl was expressed as content of the contaminants per amount of total solids. The final contaminant contents were compared with the set specifications for solid NaCl reuse, to select the most suitable technique(s) based on their performance. Finally, the technique(s) was/were subject to a SWOT analysis, in order to address strength, weaknesses, opportunities and threat, with respect to implementation.

1.3.3. Research questions

The main research question was:

"What is/are the most suitable intervention technique(s) contributing to produce high purity NaCl in the ZLD WWTP?"

To answer the main question, the following three sub-research questions were formulated.

1. *How do the contaminants end up in the mixed solids?*
2. *What is the performance of the proposed water treatment technique(s) regarding dissolved NaCl isolation from RO-brine?*
3. *What is the performance of the proposed solid purification technique regarding purification of the mixed solids?*

Additional specific research questions concerning the performance of the techniques in the experiments are presented in 3 Materials and methods.

1.4. Thesis lay-out

The thesis is divided into six chapters as follows:

- Chapter 1 – Introduction: Discussing background information and cause of the problem central in the thesis and the research objective, approach and questions.
- Chapter 2 – Theoretical background: Providing relevant theoretical background information on the characteristics of the contaminants, with emphasis on organic iron complexation. Additionally the working principles of the proposed water treatment and mixed solid purification techniques are discussed.
- Chapter 3 – Materials and methods: Presenting the used experimental set-ups, configurations and followed procedures.
- Chapter 4 – Results and discussion: Presentation of the gained results during the experiments and comparison of the techniques, including relevance, remarks and additional comments.
- Chapter 5 – Conclusions: Overview of conclusions drawn based on the experimental results, the discussion and comparison of the techniques.
- Chapter 6 – Recommendations: Proposal for implementation of the suitable technique(s) and research topics to address in future research.

2. Theoretical background

2.1. Contaminants in mixed solids

2.1.1. Characteristics of natural organic matter

Natural organic matter (NOM) consists of a large variety of organic molecules and is a product of chemical reactions with and without involvement of organisms (NASA, 2014). In water treatment, NOM becomes present as a residual product of the biological treatment: decay of micro-organisms results in organic molecules in effluents, which are generally considered to be hardly biochemically degradable (Lee et al., 2004). The variety of organic molecules is related to amongst others: origin, age and fate (Grefte, 2013).

The great variety of organic molecules and diverse presence is hot topic in research, resulting in extensive research on NOM characterization and presence. Cause for this is the implications of NOM presence on raw water sources: giving colour, taste, potential disinfection by-products to water (Grefte, 2013).

NOM speciation and characterization

Matilainen et al. (2011) published an overview discussing the working principle of various characterization methods, such as: UV254A, TOC and LC-OCD. UV254A is the absorbance of ultraviolet (UV) light at a wavelength of 254 [nm], absorbed by *aromatic bonds* in organic molecules (Korshin et al., 1999). TOC is a measure of total organic carbon, the sum of particulate and dissolved organic carbon (DOC). In modern analysis equipment, various kinds of oxidation steps are used (burning, radiation and oxidising agents) to oxidize the organic carbon. Resulting CO_2 is measured mostly by infra-red (IR) spectroscopy, and is a measure of the TOC. A direct measurement for molecular weight (MW) and content of NOM in water is Liquid Chromatography - Organic Carbon Detection (LC-OCD): where detection is performed with both UV and organic carbon detection (Matilainen et al., 2011).

The variety of NOM characteristics can roughly be described from differences in *MW and molecular structure*. More specific NOM characteristics can be derived from the composition, such as electron donation resulting in *charge* of NOM, as the results of oxygen presence and the *hydrophobicity/hydrophilicity* (Grefte, 2013; Specht et al., 2000). Based on the MW and structure, five main categories can be distinguished and described, which are detected by various peaks in a LC-OCD analysis (Stefan A. Huber et al., 2011):

A. *Biopolymers*
B. *Humic substances (humic acids and fulvic acids)*
C. *Building blocks*
D. *Low molecular weight (LMW) acids*
E. *Low molecular weight (LMW) neutrals*

Figure 4 presents an example of the various detected peaks in an LC-OCD analysis, with corresponding NOM categories. Based on this analysis, MW, charge and the presence of aromatic molecules can be derived.

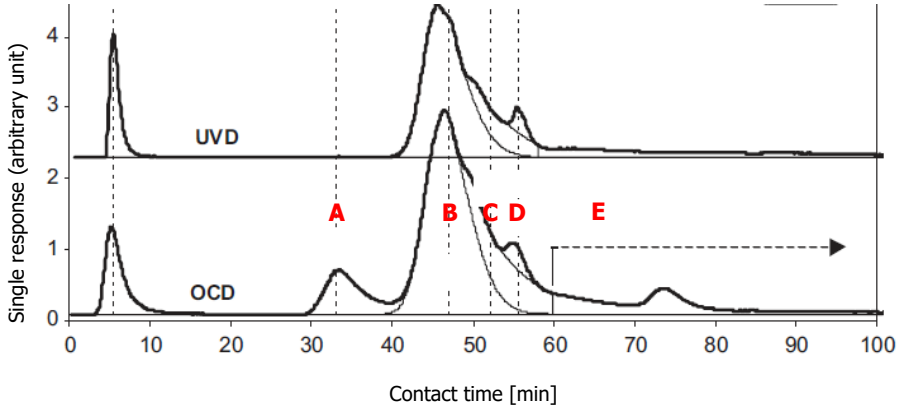

Figure 4 - Visual presentation of the various NOM categories, according peak distinction by both UV and organic carbon detection (Stefan A. Huber et al., 2011)

The NOM categories can be distinguished based on charge, MW and aromatic bond presence, of which information is acquired via multiple analyses in reference publications. A summary is presented in Table 2. The MW range of all NOM categories proves to be very widespread (arbitrary), according to various researches on NOM characterization in marine environments, fresh water lakes and rivers, drinking water sources and waste water effluents (Baghoth et al., 2008; Beckett et al., 1987).

Presence of NOM categories in water

It is generally accepted that biopolymers have the largest MW, followed by a great range of humic substances. Building block, LMW acids and neutrals are significantly smaller. In many conducted analyses on NOM characterization, humic substances proved to be the dominant category (S.A. Huber, 2002). Humic substances in water are negatively charged, resulting in stabilized *colloids*, giving colour to the water (Hendricks, 2006). The presence of aromatic bonds results from UV analysis as a quick detection method of certain NOM categories: humic substances, building blocks and LMW acids.

The variety of characteristics of NOM has consequences for water treatment, since various techniques rely on various mechanisms. Suitable treatment techniques should be assigned based on the presence and distribution of NOM categories and subsequently experiments are required to verify the potential of the respective technique to reject the NOM.

Table 2 - Summary of charge, MW and aromatic characteristic of the various NOM categories (Beckett et al., 1987; S.A. Huber, 2002; Stefan A. Huber et al., 2011)

	Charge	MW (arbitrary)	Aromatic bonds
Biopolymers	None	> 10,000 Da	No
Humic substances	Negative	350 – 3,000 Da	Yes
Building blocks	None	350 - 500 Da	Yes
LMW acids	Negative	< 350 Da	Yes
LMW neutrals	None	< 350 Da	No

2.1.2. Characteristics of silica species

Silica is earth's crust's most abundant mineral constituent and a common constituent of sand, to which its presence in water can be related to. Silica is a metalloid, showing characteristics of both metals and non-metals. The presence of silica in water is researched to high extend in membrane processes, where silica is considered as a severe and harsh potential scaling factor (White et al., 2010; Zaman et al., 2015).

Silica speciation

Silica can be present in various species, where again particulates play no significant role in water treatment. Silica is a molecule, consisting of silicon and oxygen atoms: SiO_2. In water, silica reacts with water molecules and forms orthosilicic acid: $Si(OH)_4$. Orthosilicic acid is in equilibrium with negative silicate ions: $H_3SiO_4^-$ and $H_2SiO_4^{2-}$, as a result of continuous hydrolysis reactions, depending on the pH (Meyers, 1999).

Characteristics of silica in water

At neutral pH and temperature of 25 [°C], silica is dominantly present as uncharged $Si(OH)_4$ and has a solubility of 120 [mg/L] (Alexander et al., 1954). When the pH increases to pH = 8.0 [-], charged silica species are formed, which are considered reactive. According to researches of Akhavan (2009) and Meyers (1999) unreactive silica tends to *polymerize*, forming larger molecules by covalent bonds. Additionally, R. Y. Ning (2003) reports on polymerization of reactive silica, resulting in silica polymers with colloidal proportions. Silica is referred as colloidal when the particle size exceeds 1 [nm], corresponding to 600 [Da] (Bergna et al., 2005). These particles are considered stabilized, as they tend not to agglomerate because of their repulsive interaction (Alexander et al., 1954; Bergna, 1994). Therefore, particulate silica (considering particle size > 450 [nm]) is not likely to be formed in water.

Because silica can be present in multiple states simultaneously, as demonstrated in the research of Belton et al. (2012) and Zaman et al. (2015), various properties should be addressed for its removal. The MW depends on the degree of polymerization and the charge of silica depends on both the pH and the polymerization mechanism, as described by R. Y. Ning (2003). In order to stimulate polymerization to have higher MW of the silica and potential charged silica, the pH is preferably > 8.0 [-], according to Figure 5, where dissolved silica speciation is depicted.

2.1.3. Characteristics of iron species

Iron is a well-studied, but complex metallic constituent in water, according to many studies reported since the 1950's.Presence of various iron species originates from iron containing minerals, present in earth's crust. The presence of iron is not straightforward, as iron can be present in various species.

Iron speciation

Particulate iron refers to solid iron species, present in clays. Iron in this state is unreactive, considerably large (particle size > 1000 [nm] (Bruland et al., 1999)) and plays no role in water treatment.

On the contrary, dissolved and colloidal iron do play an important role in water treatment, as it is undesired in drinking and process water, because of its potential to give colour and taste to the water. Dissolved iron can be present in various oxidation states: ferrous iron (Fe^{2+}) and ferric iron (Fe^{3+}). Dissolved Fe^{3+} can only be present in oxidized water (E > 0.8 [V]) at a very low pH (pH < 4.0 [-]), whereas dissolved Fe^{2+} presence is more likely because of its wider presence range (pH < 8.0 [-] and -0.4 < E [V] < 0.8) (Kopeliovich, 2012).

The solubility product of both Fe^{3+} and Fe^{2+} and hydroxide is very low ($K_{Fe3+,OH-} = 6.0 \cdot 10^{-38}$ & $K_{Fe2+,OH-} = 1.8 \cdot 10^{-15}$). When the maximum iron solubility concentration (for the respective pH) has been exceeded, iron hydroxides ($Fe(OH)_3$ and $Fe(OH)_2$) are formed rapidly, and can grow to both colloidal (particle size ranging 1 – 450 [nm]) and particulate proportions. The solubility of iron is affected when (in)organic ligands are present in the water: anions, forming dissolved *iron complexes* (Shapiro, 1964). The complexing mechanism prevents the production of iron hydroxides and affects the *iron solubility* (Albrektiene et al., 2011).

Presence of iron in water

When oxidized water without complexing ligands is occuring, the distribution of iron species is a function of the pH, as plotted in Figure 5. In oxidized water with pH-range = 7.0 – 8.5 [-], iron is assumed not to be *present* as free ions (Hem et al., 1959), but as iron hydroxides that can be removed easily from water with < 500 [nm] pore sized filters. In case of complexation of iron by organic matter, iron can be rejected by rejecting NOM (Keller, 2004).

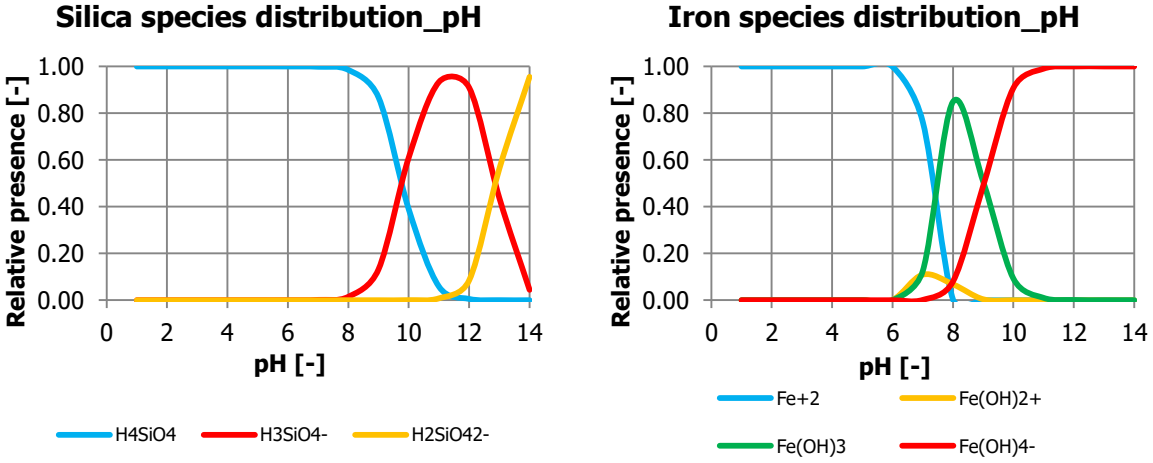

Figure 5 - Left: The relative presence distribution of solution of iron species, not accounting for polymerization of reactive and unreactive silica. Both figures (made using PHREEQC) consider oxidized water at T = 25 [°C]. Right: The relative presence distribution of s species, not accounting for presence of (in)organic ligands.

2.2. Organic iron complexation

The conditions for free dissolved iron ions absence described in 2.1.3 Characteristics of iron species are applicable for the ZLD WWTP considered in this thesis: oxidized water with pH = 7.0 – 8.5 [-], according to heat and mass balance data. In the ZLD WWTP, SUF is implemented, resulting in the assumption that potential undissolved iron is also absent in the SUF permeate. Since the SUF permeate is the feed water for the RO stages, iron was not expected to be present in the RO-brine. Unless there is a mechanism facilitating conditions for iron to stay dissolved.

Occurrence of OIC

The complexation of iron by NOM, hereafter referred as *organic iron complexation (OIC)*, has been briefly introduced in both 2.1.1 Characteristics of natural organic matter and 2.1.3 Characteristics of iron species. Fractions of NOM (humic substances and LMW acids) are negatively charged and potentially function as *ligand* for iron ions, which is schematized in Figure 6. **Because the *charge density* of humic substance varies per specific substance, the charge of the organic iron complex deviates.** For example, the organic iron complex in Figure 6 is monovalent negatively charged complex. The complexation of iron with a different organic molecule could lead to negatively multivalent charged or even to a positively charged complex.

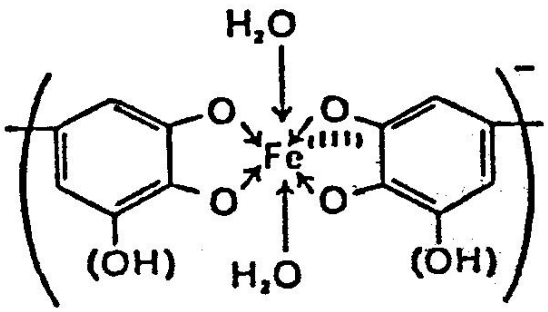

Figure 6 – A visualization of an organic iron complex: Fe^{3+} and tannic acid, serving as organic ligand (De Sacadura Bretes, 1985).

Implications of OIC

OIC has been researched for its various implications. Research has been conducted on the availability of iron, for potential uptake by organisms in environmental waters and specifically of iron speciation in seas and rivers. From these researches, it can be concluded that the influence of NOM on the speciation and solubility of iron is significant, because 0.93 – 1.00 [-] of iron proved to be dissolved as organic complex in various environments (Kawakubo et al., 2002; Rue et al., 1995) in concentrations up to 2.0 [mg/L], exceeding the maximum solubility concentration. The effect of NOM presence for iron removal in conventional drinking water treatment has been researched by Koenings et al. (1976). In this research, only 0.36 [-] of iron formed iron hydroxide flocs in the presence of NOM, whereas in absence of NOM 0.84 [-] of iron formed flocs. This implies significant that in presence of NOM, a significant fraction of iron remains dissolved, resulting in elevated iron concentrations, with respect to absence of NOM.

The strategy of iron removal by treating for NOM has successfully been applied in drinking water treatment, where 0.79 [-] NOM removal by coagulation simultaneously resulted in 0.98 [-] iron removal, according to the research of Albrektiene et al. (2011). This strategy will therefore be followed for the simultaneous removal of NOM and iron in this thesis, guided by recommendations of Keller (2004).

Relevance of OIC in this thesis

The dissolved iron concentration in the permeate of the UF is 0.6 [mg/L], in a TDS concentration of 800 [mg/L], according provided mass and heat balance data and analysis of the mixed solids and RO-brine. The maximum solubility of dissolved iron in oxidized water at pH = 8.0 [-] is << 0.6 [mg/L], according to the standard water wateq4f database used in chemical modelling software package PHREEQC.

Since iron was present in the mixed solids, it was interesting for this thesis to experimentally enforce the claim that iron can be complexed in the presence of NOM. To this extend, an additional experiment was included in the research: the OIC experiment.

2.3. Nanofiltration for dissolved NaCl isolation

The first proposed technique to isolate dissolved NaCl is nanofiltration (NF). NF is well-established and is used for the rejection of multivalent ions and organic matter in both drinking and process water production (Cob, 2014). For this thesis, the NF permeate stream was of main subject of research, as it was assumed that dissolved NaCl ended up in this stream.

2.3.1. Working principle of nanofiltration

During the application of NF, *high pressures* are applied in order to push water through a semi-permeable membrane. NF produces a permeate stream, free of rejected constituents, as well as a concentrate stream, containing the concentrated rejected constituents. The actual transport model of water (*water flux:* flow rate per unit of membrane surface) and dissolved constituents is neither straightforward nor generally accepted (Hendricks, 2006). The build-up of NF membranes is considered to be a-symmetrical (the composition and characteristic vary over the thickness of the membrane), implying that water cannot flow through open pores (Vandezande et al., 2008). Various researches tried to narrow down the respective transport mechanism of water and dissolved constituents, resulting in the now commonly accepted theory that water is transported by *advection* and dissolved constituents *diffuse* through membranes. This is supported by various literature sources discussing the water transport mechanism in NF by Vandezande et al. (2008) and Baker (2000).

Constituent transport mechanisms in NF

Whereas water transport is promoted during NF, the transport of dissolved constituents is intentionally opposed. The rejection of constituents is subject of various mechanisms. Very small constituents, such as small monovalent ions, are assumed to pass the NF membrane at a high rate by diffusion. Larger constituents are rejected based on *size exclusion*, when the MW is larger than the cut-off characteristics of the NF membrane: *molecular weight cut-off* (MWCO). Additional constituent rejecting mechanisms consider *charge repulsion* (rejection of multivalent ions) and *hydrophobicity/hydrophilicity*, according the research of Bellona et al. (2004). Complete rejection cannot be assured, because various constituents are able to diffuse slowly through the NF membrane. For more detailed information on NF operation, performance and development, further reading of Hendricks (2006) and Baker (2000) is advised.

NF configurations

NF can be carried out in *dead-end* or *cross-flow configuration*. In a dead-end configuration, there is no continuous concentrate flow, facilitating *concentration polarization* near the membrane: accumulation of dissolved constituents, resulting in increased diffusion (Hendricks, 2006). Whether this phenomenon is desired, depends on the objective of the application of NF. When membrane fouling becomes severe, backwashing can be applied to remove the fouling layer temporarily.

In order to avoid concentration polarization, a continuous concentrate flow can be facilitated (high cross-flow), in order to have turbulent flow over the membrane and prevent concentration polarization. This results in lower diffusion of constituents through the membrane and thus lower constituent concentration in the permeate. Both the dead-end and cross-flow configuration are presented in Figure 7 and Figure 8, including advection of water and diffusion of constituents. Another way to decrease permeate constituent concentration is by *dilution*. The diffusion rate is considered to remain equal, whereas the water flux is increased and thus equal contaminants and more water and yielded in the permeate: concentration decrease.

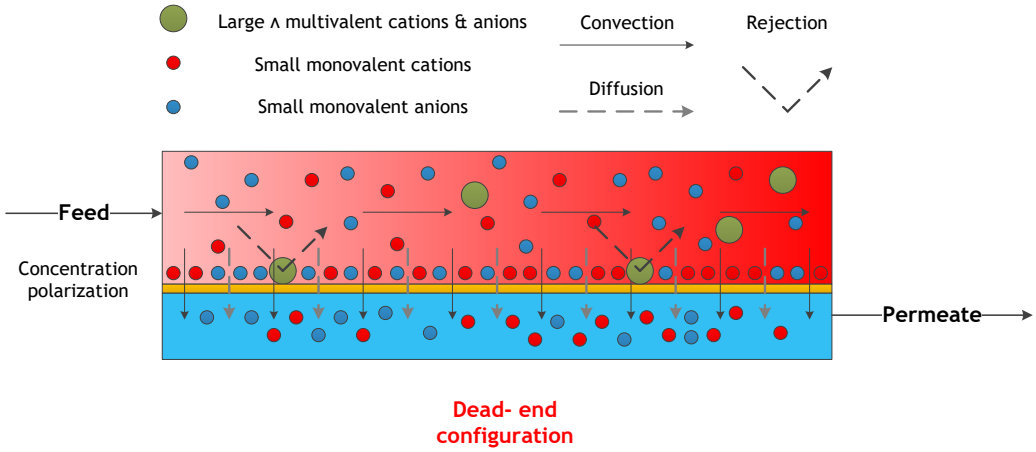

Figure 7 – An assumptive schematic presentation of active mechanisms in a dead-end NF configuration, considering convection, diffusion and rejection based on constituents' and membrane characteristics.

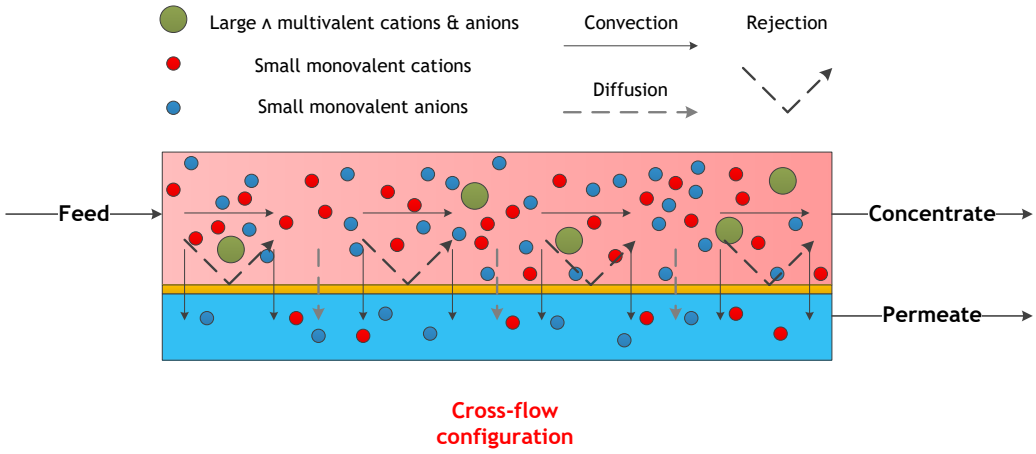

Figure 8 – An assumptive schematic presentation of active mechanisms in a cross-flow NF configuration, including convection, diffusion and rejection based on constituents' and membrane characteristics.

NF membranes

In NF, multiple types of membranes are applied, which are fabricated of various materials. The most often applied material is Thin Film Composite, also referred as *polymeric NF (PNF)* membranes: an ultrathin active layer on microporous support and reinforcing fabric. The ultrathin barrier layer is made of polyamide and serves as the actual semi-permeable layer (Baker, 2000). The active layer can be tailored, by giving it specific MWCO or electrostatic characteristics to reject constituents by size and charge, respectively. For example, DOW NF90 (MWCO ~ 200 [Da] and NF270 (MWCO ~ 400 [Da]) membranes have the required characteristics to achieve isolation of NaCl in the permeate, according to DOW (2006a).

Additionally, recently upcoming are ceramic NF (CNF) membranes that function similarly, but the active layer is made of ceramic materials, having high mechanical strength and thermal and chemical resistance (Shang, 2014). Furthermore, the active layer can be tailored by application of additional coated layers to improve (selective) rejection of various constituents. More detailed information on NF membranes manufacturing and characteristics is described in detail by Vandezande et al. (2008). According to specifications, these membranes are considered applicable for NaCl isolation (de Ridder et al., 2014).

2.3.2. Performance of NF

Hydraulic NF membrane permeability

The performance of NF depends partially on the water flux through the membrane. When excessive high pressures are required for the production of a permeate, the process can be considered inefficient. The applied pressures are required to overcome *resistance* (expressed as pressure) of the membrane itself, and potential *osmotic pressure difference*. To this extend, the *hydraulic membrane permeability (HMP)* has been assigned as parameter for water flux as a function of pressure difference over the membrane and *viscosity* (Hendricks, 2006). This parameter is also used for the indication of fouling, resulting in either a lower flux or an increased pressure difference. This performance indicator is expressed as in Equation 1.

$$HMP = \frac{J \cdot \mu}{TMP} \qquad \textbf{Equation 1}$$

Where HMP = hydraulic membrane permeability [m], J = water flux [$m \cdot s^{-1}$], μ = dynamic viscosity [$kg \cdot m^{-1} \cdot s^{-1}$)] and TMP = trans membrane pressure [$kg \cdot m^{-1} \cdot s^{-2}$)].

NaCl yield and rejection of contaminants by NF

The rejection of the contaminants is not straightforward, because the characteristics of contaminants are not clearly specified and NF membrane are not considered absolute barriers: diffusion of constituents through the membrane occurs, although it is not desired (Vandezande et al., 2008). More specifically, the paper of Bellona et al. (2004) shows an elaborative decision tree on whether or not NOM passes the membrane. Many factors, such as pH, membrane charge and hydrophilicity are influencing this process. Despite this given, some researches succeed to isolate NaCl from a with NOM contaminated IEX-brine, using NF270 membranes. Vaudevire et al. (2013) rejected 0.80 [-] of DOC, whereas 0.80 and 1.00 [-] of sodium and chloride passed the membrane. Furthermore, Kabsch-Korbutowicz et al. (2011) achieved 0.99 [-] reduction in NOM induced colour, while approaching complete recovery of NaCl from an IEX-brine as well. Silica rejection proved to be less successful, according to results in the thesis of (Cob, 2014): 0.16 [-] using Dow PNF membranes. In contrast, a UF membrane removed up to 0.28 [-] of silica from a RO-brine, as reported by Zaman et al. (2015). This indicates that tighter membranes can be less effective than looser membranes, depending on the silica species and form.

Similarly as for ED, the performance of NF on the isolation of dissolved NaCl can be expressed by the yield of TDS and the rejection of contaminants in the permeate, as in Equation 2 and Equation 3, respectively.

$$Y_{TDS\_NF} = \frac{c_{TDS\_perm.}}{c_{TDS\_feed}} \qquad \textbf{Equation 2}$$

Where Y_{TDS_NF} = TDS yield for NF [-], $c_{TDS\_perm.}$ = TDS conc. in the permeate [g/L] and c_{TDS_feed} = TDS conc. in the feed [g/L].

$$R_{cont\_NF} = 1 - \frac{c_{cont\_perm.}}{c_{cont\_feed}} \qquad \textbf{Equation 3}$$

Where R_{cont_NF} = contaminant rejection for NF [-], c_{cont_perm} = contaminant conc. the permeate [mg/L] and c_{cont_feed} = contaminant conc. in the feed [mg/L].

2.4. Electrodialysis for dissolved NaCl isolation

The second proposed technique for the production of an isolated dissolved NaCl stream was electrodialysis (ED). Typically, ED is applied for desalination in the production of drinking and process water, but it is also upcoming in waste water treatment and brine processing (Valero et al., 2011). In this thesis, the ED concentrate stream was used as subject of research, as dissolved NaCl was aimed to end up in this stream.

2.4.1. Working principle of ED

By applying an electrical current, perpendicular to the flow direction through an ED cell, charged constituents *migrate* to the electrodes through ion exchange membranes (IEMs) with opposite charge *functional groups*: cations migrate through membranes with a negatively charged functional groups (cation exchange membranes: CEMs) and anions migrate through membranes with a positively charged functional groups (anion exchange membranes: AEMs), as presented in Figure 9. The ions migrate from the diluate stream to the concentrate stream. A more detailed description of the composition and specific properties of these membranes is presented in the research of Strathmann (2010) and the book of Baker (2000).

ED stacks and membranes

The CEMs and AEM are placed in an alternating way in an ED cell to form a stack, containing multiple flow cell(s). A stack of membranes without charge selectivity is referred as standard ion exchange membranes (STMs). A cell pair consists of a cell where ions migrate from (*diluate cell*) and a cell where ions migrate to (*concentrate cell*). Because ions are repelled by membranes with equally charged functional groups and alternating membrane placing, the cell pairs are formed. As only ions migrate through the membranes, uncharged constituents are considered to remain in the diluate, see Figure 10 (Strathmann, 2010).

Constituent transport mechanisms in ED

In order to promote selective ion migration, monovalent selective membranes (MVMs) have been developed. Monovalent anion exchange membranes (MAEMs) only allow small, monovalent anions passing through, as a positively charged thin layer has been coated on the membrane surface. This results in repulsion of larger or multivalent anions, as depicted in Figure 9. The same principle holds for monovalent cation exchange membranes (MCEMs), but with opposite charge. More detailed information on development and functioning of MVMs can been found in researches of Saracco et al. (1994) and Firdaous et al. (2007).

Rejection of undesired constituents to the concentrate is based on various mechanisms described by Strathmann (2010) and Tanaka et al. (2012). Rejection is achieved by *size exclusion*, *adsorption* and *charge repulsion*. Adsorption is an undesired mechanism, as it results in membrane fouling. Application of MVMs contributes to this topic, because the additional charged layer facilitates charge repulsion instead (Tanaka et al., 2012). The various mechanisms for AEMs are schematized in Figure 9, including the fate of anions.

Isolation of dissolved NaCl was assumed to be achieved by migration of NaCl (small monovalent ions) and rejection of contaminants. The actual rejection of the contaminants depends on the specific characteristics of these constituents: especially charge and size. A schematization of the ED process with MVMs is presented in Figure 10, including the various rejection mechanisms.

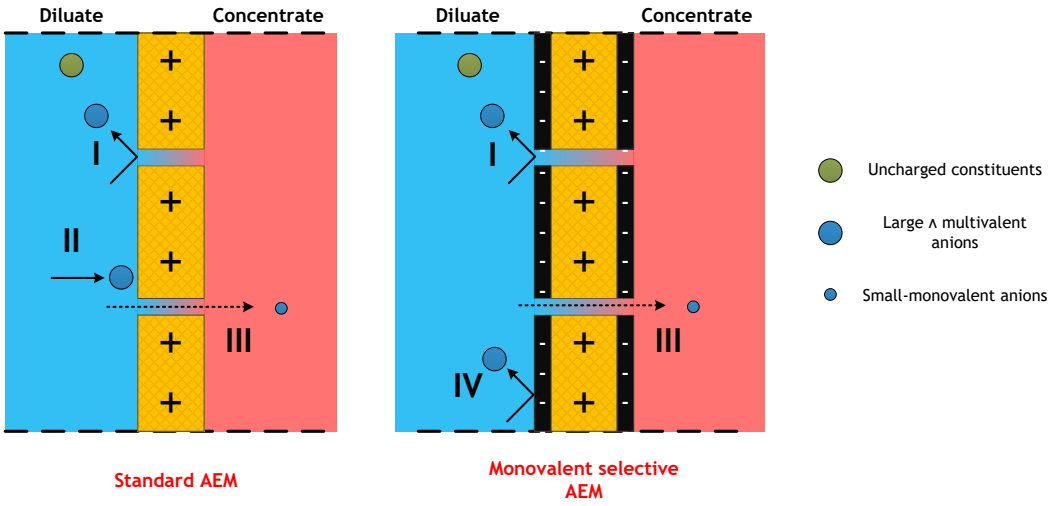

Figure 9 - An assumptive schematization of the fates of anions in ED with both standard and monovalent selective AEMs under influence of various mechanisms: size exclusion (I), adsorption (II), migration (III) and charge repulsion (IV). Similar mechanisms are applicable for CEMs and the fate of cations, but with opposing charges of the functional groups and additional layers.

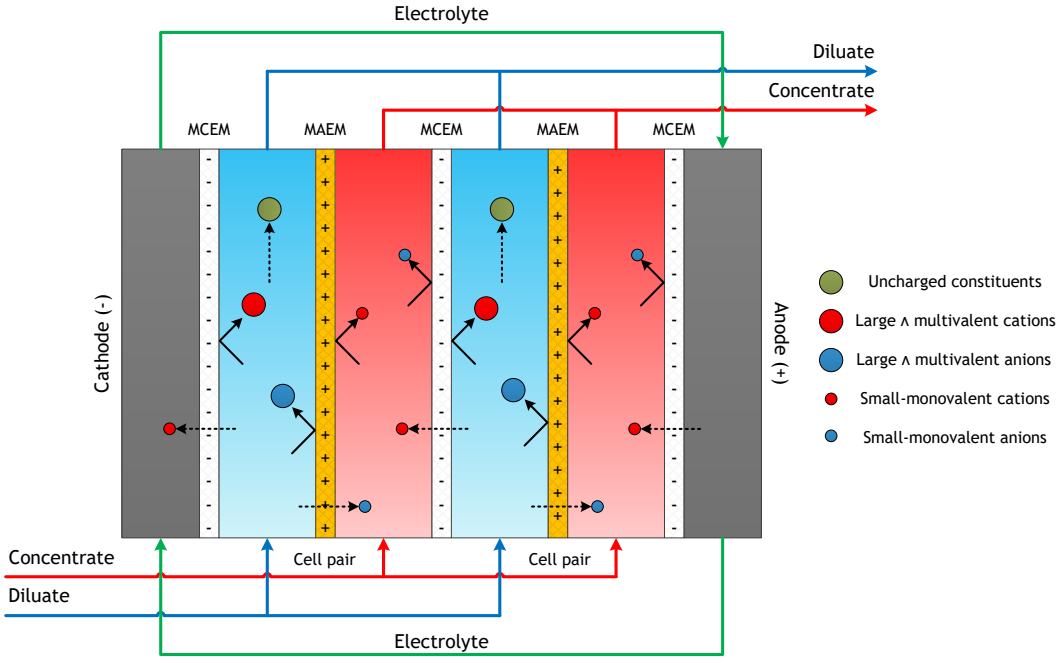

Figure 10 - An assumptive schematic overview of transport mechanisms in ED with MVMs. Small monovalent ions migrate to the concentrate, whereas uncharged constituents remain in the diluate. Larger and/or multivalent anions and cations are rejected and remain in the diluate as well, based on the various discussed mechanisms. The additional layers on MVMs are not projected in this schematization.

2.4.2. Performance of ED

Next to permeability and perm-selectivity of ED membranes, ion migration depends on the *applied electrical current*, according to the relationship between ion migration and electrical current presented in Nikonenko et al. (2014) and Xu et al. (2008).

Limiting current density in ED

The applied current must always be corrected for the *limiting current*, to avoid *water splitting*. This phenomenon arises when the ion migration through the membranes is faster than ion migration in the bulk solution and water is split to establish an electrical current between the electrodes (Cowan et al., 1959; Nikonenko et al., 2014; Strathmann, 2010).

NaCl yield and rejection of contaminants by ED

A scientific review of Andrade Becheleni et al. (2015) focussed on desalination of the diluate, resulting in the conclusion that near complete ion migration can be established. To determine the performance of ED, the *ion migration flux* and total yield of dissolved NaCl are key parameters and are expressed as in Equation 4 and Equation 5. These equations are specifically applicable for equal diluate and concentrate volumes.

$$J_{TDS} = \frac{\Delta c_{TDS.dil} \cdot V_{dil.}}{A_{membrane} \cdot \Delta t}$$ **Equation 4**

Where J_{TDS} = ion migration flux [mg·m^{-2}·s^{-1}], $\Delta c_{TDS,dil}$ = ion conc. difference (as TDS) [mg], V_{dil} = diluate volume [L], $A_{membrane}$ = effective membrane migration area [m^2] and Δt = time difference [s].

$$Y_{TDS\_ED} = \frac{\Delta c_{TDS.conc.}}{c_{TDS.dil.i}}$$ **Equation 5**

Where Y_{TDS_ED} = *dissolved TDS yield* for ED [-], $\Delta c_{TDS,conc.}$ = *TDS conc. difference in the concentrate* [g/L] and $c_{TDS,dil.i}$ = *initial TDS conc. in the diluate* [g/L].

A second topic on ED performance is the rejection of contaminants. A relevant reference research was performed by Zhang et al. (2011), where RO-brine was desalinated for increased water recovery. They achieved 0.87 [-] rejection of NOM in the concentrate, whereas 0.70 [-] of the ions migrated. Additionally, the research of Kabsch-Korbutowicz et al. (2011) focussed on NaCl recovery from spent IEX-brines and NOM rejection up to 0.91 [-], at 0.79 [-] yield of NaCl. 0.35 [-] rejection of silica was achieved in NOM isolation from RO-brine using ED, according the research of Koprivnjak et al. (2006).

To determine the performance of ED on contaminants rejection, the rejection performance indicator was expressed as Equation 6. These equations are specifically applicable for equal diluate and concentrate volumes.

$$R_{cont\_ED} = 1 - \frac{\Delta c_{cont.conc.}}{c_{cont.dil.i}}$$ **Equation 6**

Where R_{cont_ED} = *contaminant rejection* for ED [-] and $\Delta c_{cont.conc.}$ = *contaminant conc. difference in the concentrate* [mg/L] and $c_{cont.dil.i}$ = *contaminant conc. in the initial diluate* [mg/L].

2.5. Ion exchange for dissolved NaCl isolation

The final proposed technique to isolate dissolved NaCl was ion exchange (IEX). According to the potential negative charge of the contaminants, ion exchange was narrowed down to anion exchange in this thesis (but still abbreviated as IEX). IEX in chloride ionic form is found to be one of the most applied techniques for the removal of NOM in the preparation of drinking water (Bolto et al., 2002), whereas IEX hydroxide ionic form is applied for polish treatment of process water (Ben Sik Ali et al., 2013). For this thesis, the IEX effluent stream was of subject of research, as it was assumed that dissolved NaCl ended up in this stream.

2.5.1. Working principle of IEX

Anion exchange facilitates the exchange of anions, by differences in *affinity* of dissolved anions and solid fixed *counter-ions*, initially present on IEX resins. IEX resins often exist of cross-linked polystyrene matrix with attached functional groups, either in positive or in negative form. In case of positively charged functional groups, fresh IEX-resins contain negatively charged counter-ions. When the affinity of anions in the feed water (considered as contaminants) is higher than the counter-ion, exchange of these anions occurs. During this process, the *ionic strength* of the water is unaffected (Hendricks, 2006). The operation of IEX is schematized in Figure 11, where the fed stream is called the feed and the treated stream is called the (IEX) effluent. The counter-ions represent the specific ionic form of resin and often consider chloride or hydroxide. Similar ions in the feed water as the ionic form are referred as *co-ions*.

Anion exchange can be applied for all kinds of anions, as long as the affinity for the contaminant is higher than for the counter-ion. In order to apply IEX as technique, the resin can be place in a column to have either an up-flow or a down-flow configuration. Additionally, IEX can be applied in a completely mixed system or plug-flow configuration, which has successfully been applied by PWN in the Netherlands (Galjaard et al., 2010). Additional background information on application, functioning and variation in IEX can be found in Hendricks (2006) and the papers of Miller et al. (2009) and Alchin et al. (2002).

Breakthrough of IEX resins

A down-flow configuration aims at complete rejection of contaminants, when the contact time is high enough to facilitate exchange of anions. When in a down-flow column configuration the first contaminants appear in the effluent, *breakthrough* is reached. As from this point, the resin saturates starting at the top until operation is stopped when the contaminant concentration in the effluent exceeds the limits: *practical breakthrough*. When breakthrough has been reached, the resin can be *regenerated*: the desired ionic form is restored by *eluting* the resin with highly concentrated solution, containing the desired anions. This principle is discussed in various reports by (Miller et al., 2009) and schematized in Figure 11. Figure 12 presents a schematic presentation of the ionic form of fresh resin, saturated resin and regenerated resin, for a regeneration efficiency < 1.0 [-].

Constituent affinities in IEX resins

Silica can be exchanged when it is in ionic form, whereas IEX with NOM is strongly dependent on the charge of the respective NOM species (Bolto et al., 2002; Meyers, 1999). Hydroxide has the lowest resin affinity, according to Alchin et al. (2002) and is therefore a suitable ionic form for silica rejection. Chloride has higher resin affinity than silica and was therefore assumed to be less suitable for silica rejection (Meyers, 1999). No references could be found on simultaneous IEX of NOM and silica with either hydroxide or chloride, where chloride remains in the effluent. In order to isolate dissolved NaCl in the effluent, both discussed ionic forms can be applied.

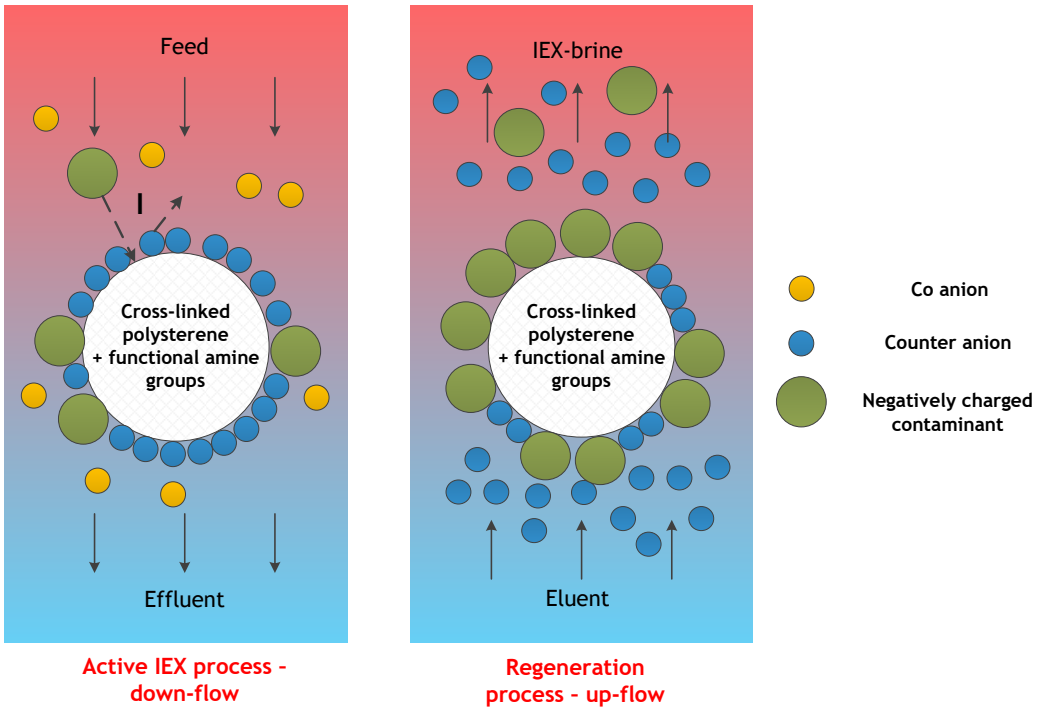

Figure 11 - An assumptive schematic presentation of the active transport mechanism in IEX (left), including the exchange of counter ions and contaminants (I), co-ion concentrations remain unaffected. On the right, the regeneration process is schematized, with excessive concentrations of counter ions to replace the adsorbed contaminants.

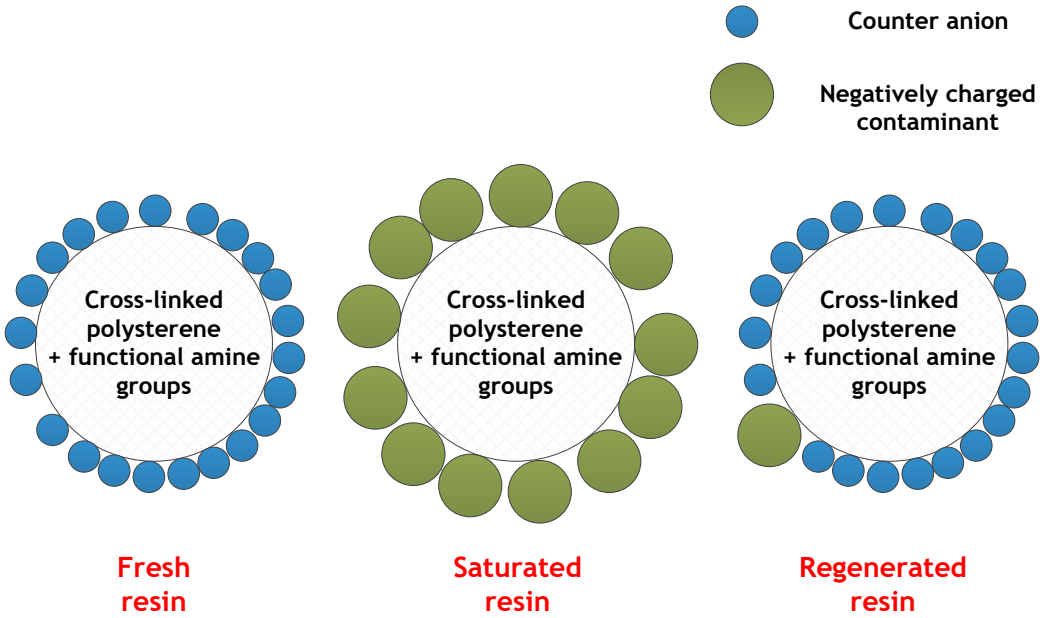

Figure 12 - A schematic presentation of the present ions on fresh resin, saturated resin and regenerated resin (for < 1.0 [-] successful regeneration).

2.5.2. Performance of IEX

Performance of IEX on NOM rejection varies strongly in the reported research. Grefte (2013) found rejection up to 0.90 [-], whereas the research of Audenaert et al. (2015) only succeeded to remove 0.61 [-] using fresh resins in chloride form. The difference in performance of NOM rejection appeared to be dependent on presence of anions with higher resin affinity, such as multivalent anions. Silica rejection by IEX resin in hydroxide form in NF-brine showed to be related to the specific characteristics of silica: at pH > 8.5 [-], the rejection was 0.80 [-], whereas at pH < 8.5 [-] the rejection was 0.05 [-] (Acevedo et al., 2010). Based on these results, it can be stated that the performance of IEX is dependent on its initial ionic form, the resin affinity of the contaminants and especially the presence of competing anions.

NaCl yield and rejection of contaminants by IEX

The performance of IEX on isolation of dissolved NaCl can be expressed as the yield of dissolved solids and the rejection of contaminants in the effluent. Multiple researches show that the TDS of the effluent does not change significantly (Acevedo et al., 2010; Audenaert et al., 2015) during IEX processes, resulting in the assumption that high dissolved NaCl can be achieved. Similar performance indicators as for NF and ED are expressed as in Equation 7 and Equation 8.

$$Y_{TDS\_IEX} = \frac{c_{TDS\_effluent.}}{c_{TDS\_feed}} \qquad \textbf{Equation 7}$$

Where Y_{TDS_IEX} = dissolved NaCl yield by IEX [-],$c_{TDS\_effluent.}$ = TDS conc. in the effluent [g/L] and c_{TDS_feed} = TDS conc. in the feed [g/L].

$$R_{cont\_IEX} = 1 - \frac{c_{cont\_effluent.}}{c_{cont\_feed}} \qquad \textbf{Equation 8}$$

Where R_{cont_IEX} = contaminant rejection by IEX [-], $c_{cont\_effluent}$ = contaminant conc. the effluent [mg/L] and c_{cont_feed} = contaminant conc. in the feed [mg/L].

Regeneration efficiency

Next to the yield of dissolved NaCl and the rejection of contaminants, the performance of IEX depends on the *regeneration efficiency* of IEX-resin. Audenaert et al. (2015) showed that regeneration of the IEX resin could only be achieved by approximately 0.60 [-], because the performance of re-used resin resulted in 0.40 [-] lower NOM rejection than for fresh resins. Additional researches on the regeneration of broken through resins in multiple contaminant rejection were not found.

The performance indicator on regeneration efficiency can be expressed as in Equation 9.

$$E_{regeneration} = 1 - \frac{\left(c_{cont.\_IEX-brine} \cdot V_{IEX-brine}\right)}{\sum_{t=1}^{n} (c_{cont.\_feed\_t} - c_{cont\_effluen\_t}) \cdot V_{feed\_t}} \qquad \textbf{Equation 9}$$

Where $E_{regeneration}$ = regeneration efficiency [-], $c_{cont\_IEX-brine}$ = contaminant conc. in the IEX-brine [mg/L], $V_{IEX-brine}$ = IEX-brine volume [L], c_{cont_feed} = contaminant conc. in the feed at time 't' in hours [mg/L] and $c_{cont\_effluent}$ = contaminant conc. the effluent at time 't' in hours [mg/L].

2.6. SALEX for mixed solids purification

The proposed technique for the purification of the mixed solids is SALEX, an acronym for ***EX****traction of impurities from* ***SAL****t*. This technique is developed by Krebs Swiss as a cost-effective alternative to application of dissolution and recrystallization for salt purity improvement.

SALEX-C is typically applied for the purification of solar salt (obtained by evaporation) and SALEX-F is applied for the purification of more valuable rock salt (obtained by mining). The technique has been installed on full-scale, for example in Spain, where a 130 [t/d] SALEX-C plant has been commissioned (Sedivy, 1996).

The application of SALEX typically refers to various inorganic *impurities*, such as calcium sulphate and magnesium chloride and to organic impurities, referred as insolubles. These constituents are present in produced salt with environmental origins. Because these impurities bring down the value of the raw salt, they need to be *extracted* from the salt. The considered impurities in the SALEX technique are represented by the contaminants considered in this thesis, whereas the raw salt is represented by the mixed solids.

2.6.1. Working principle of SALEX

The working principle is derived from a paper published by Sedivy (1996). The principle is based on two mechanisms: diffusion of contaminants to a washing solution and *advection* of small particulate contaminants in the washing solution (hereafter referred as *eluent*). The combination of these two processes is called *washing:* yielding *washed solids*. The principle assumes that the contaminants are not incorporated, but are located on the outside of the NaCl crystals in the mixed solids.

In order to facilitate contaminant diffusion and prevent the dissolution of NaCl, a saturated solution should be used as eluent. The eluent can be prepared from the least valuable NaCl fraction. The spent eluent is referred as *SALEX-brine*, which should be used efficiently. This can be achieved by staged washing, where the initial washing stage is performed with the most contaminated SALEX-brine as eluent. Recovery of NaCl in the SALEX-brine can be achieved using nanofiltration, as presented by Vaudevire et al. (2013).

When the contaminants diffuse to the eluent, cavities in the NaCl crystals appear. When the eluent exists of a saturated NaCl solution, *recrystallization* by dissolved NaCl is possible in the cavities, resulting in a higher efficiency of the process in terms of salt yield. The diffusion and recrystallization process are schematized in Figure 13.

The second mechanism is advective transport of the contaminants. When a down-flow configuration is applied, there is no advective transport possible of contaminants, because the solid salt serves as a filter bed. Therefore, an *up-flow* configuration is advised, to achieve a certain degree of *bed expansion*, facilitating conditions for the eluent to catch and discharge the contaminants by advection. The advection of contaminants is called *elutriation*, leaving purified NaCl crystals behind, as they settle. These processes are presented in Figure 13 as well, representing the SALEX principle.

Supported by visual inspection of the mixed solids in 1.2 Problem description, it is assumed that the contaminants in the mixed solids are situated on the outside of the NaCl crystals in the mixed solids. Therefore, SALEX is proposed as potential mixed solids purification technique.

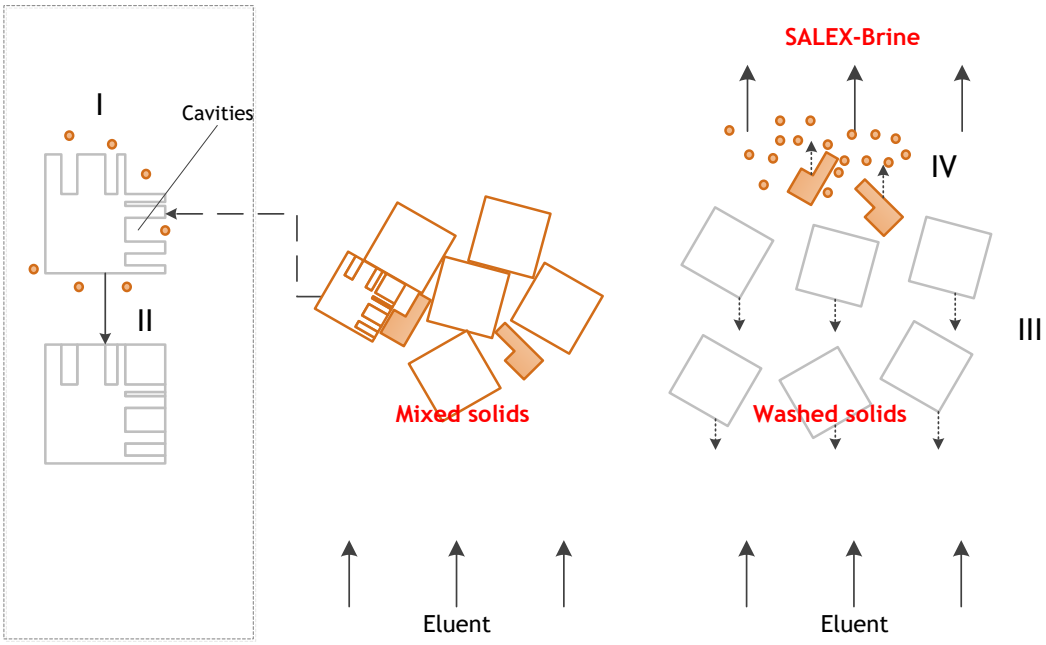

Figure 13 - A schematic presentation of the active transport mechanisms in SALEX, including the diffusion (I) and elutriation (IV) of contaminants at facilitated bed expansion (III). Additionally, recrystallization (II) of appeared cavities is visualized.

2.6.2. SALEX performance

With the SALEX technique, it is claimed that 0.9995 [-] purity of NaCl can be achieved. Additionally, it is claimed that conventional salt elution processes typically have an efficiency of 0.60 [-] and salt losses of 0.10 [-] (Sedivy, 1996). The performance of the SALEX technique is subject of various parameters, according the paper of Sedivy (1996): contact time for diffusion and elutriation and the initial content of contaminants. Additionally, it was assumed that the degree of bed expansion and eluent volume had high impact on the performance. These two parameters are not mentioned in the research of Sedivy (1996).

To determine the potential of the SALEX technique to purify the mixed solids, two performance indicators were defined for this thesis specifically, concerning both the *net yield ratio of solids* (taken the spent NaCl in eluent into account) and contaminant *extraction efficiency*, expressed as Equation 10 and Equation 11:

$$Y_{solids.net} = \frac{m_{solids\_washed} - c_{NaCl} \cdot V_{eluent}}{m_{mixedsolids}}$$ **Equation 10**

Where $Y_{solidsnet}$ = net solids yield ratio [-] and m_{solids_washed} and $m_{mixedsolids}$ = mass of mixed solids and the washed solids [g], c_{NaCl} = concentration of NaCl in the eluent [g/L] and V_{eluent} = eluent volume [L].

$$E_{ext.} = 1 - \frac{c_{solids\_washed}}{c_{solids\_mixed}}$$ **Equation 11**

Where $E_{ext.}$ = extraction [-] and $c_{mixed\ solids}$ and c_{solids_washed}= content of contaminant per gram of mixed solids and the washed solids [mg/g].

3. Materials and methods

3.1. RO-brine and mixed solids

Preparation of feed water

The RO-brine used in the dissolved NaCl isolation experiments was a solution of RO-brine solids, which were shipped from the ZLD WWTP as a batch of dried solids. Dissolving these solids in demineralised water (hereafter referred as *demi-water*), with an EC of < 0.010 [mS/cm] in the corresponding proportion, resulted in the representative RO-brine, because it was assumed that in the evaporation process only water is recovered. Based on heat and mass balance data of the ZLD WWTP, the total dissolved solids (TDS) concentration of the RO-brine is 6.8 [g/L].

Because HCO_3 is removed before the evaporation process (indicated in Figure 2) in the ZLD WWTP, by gas stripping after acid dosage, additional HCO_3 needed to be added to prepare RO-brine. Therefore, 3.6 [g/L] Sigma Aldrich sodium bicarbonate ($NaHCO_3$) was dosed for RO-brine preparation. Subsequently, 3.2 [g/L] solids from the evaporated brine was dosed, to have a final TDS concentration of 6.8 [g/L]. Because the NOM dissolved slowly in the solution, a mixing time of 24 hours was applied for the preparation of RO-brine at all time.

Preparation of mixed solids

The mixed solids (final stream in Figure 2) produced in the ZLD WWTP were shipped as a batch dry solids and could be readily used in the SALEX experiment.

3.2. Analytical equipment and procedures

For the various experiments, a wide range of analytical measurements was performed. The description of the analytical procedures and associating equipment is applicable for each experiment where the respective measurement has been performed.

All other measurements were performed in the Waterlab of the Delft University of Technology (Delft, the Netherlands), unless noted otherwise.

For the OIC experiment, the following parameters were measured:

- *pH*, *temperature* and *electrical conductivity (EC)*, representing physical water quality parameters. The total amount of dissolved solids (TDS) can directly be derived from EC.
    - Using an Inolab® Multi-parameter meter 3410 with calibrated TetraCon 925 EC-sensors and a calibrated Sentix 940 pH-sensor. Data was directly exported continuously (every second) to an attached laptop and stored in a Microsoft Excel spreadsheet.
- *Total organic carbon (TOC)*, as a measurement for the presence of *dissolved NOM*.
    - Using a Shimadzu TOC-L analyser, according to the procedure described by Shang (2014) and Olariu (2015).
- *Total iron (Fe)*, as a measurement for the presence of iron.
    - Using a Hach-Lange LCK321 test-kit (range: 0.2 – 6.0 [mg/L] Fe), according to its manual (Hach-Lange, 2013) and a Hach-Lange Spectrophotometer DR3900.

For the dissolved NaCl isolation experiments and the mixed solids purification experiment, the before mentioned pH, temperature, EC and TOC measurements were performed. Additionally, the following parameters were measured:

- *UV254A*, as a measure of NOM using UV-light:
    - Using a Thermo Scientific Evolution 60S UV-Visible Spectrophotometer and a 60 [mm] quartz cuvette, according to the procedure described by Olariu (2015).
- *Inductively Coupled Plasma Mass Spectrometry (ICP-MS)*, for the determination of *cations/metals (and silica)*: aluminium (Al), barium (Ba), calcium (Ca), chromium (Cr), copper (Cu), Iron (Fe), lead (Pb), magnesium (Mg), sodium (Na), nickel (Ni), potassium (K), silica (Si) and strontium (Sr).
    - Using a Thermo Fisher Scientific iCAP-Q ICP-MS. The analyses were performed by Waterapplicatiecentrum (WAC), Leeuwarden, the Netherlands, according to the supplied procedure of the supplier.
- *High Performance Liquid Chromatography (HPLC)*, for the determination of *anions*: chloride (Cl), nitrite (NO_2), nitrate (NO_3), phosphate (PO_4) and sulphate (SO_4).
    - Using a HPLC 1200 Infinity, Agilent Technologies and OpenLAB software. The analyses were also performed by WAC, according to the procedure of the supplier.
- *Total inorganic carbon (TIC)* for the determination of *bicarbonate (HCO_3)*.
    - Using a Shimadzu TOC-L analyser, by acidification with 1M HCl and coupled CO_2 analysis by NDIR.

Finally, for visual inspection two different devices were used:

- HTC M8S for pictures, using a 13 MP camera.
- VHX 5000 Digital microscope, using Keyence VH-Z00R / Z00W / Z00T (0 – 50x magnification) and VH-Z20R / Z20W / Z20T (20 – 200x magnification) lenses.

3.3. Organic iron complexation experiment

The in 2.2 Organic iron complexation introduced OIC experiment was designed to determine the potential of NOM to facilitate conditions to keep Fe in a dissolved state in oxidized water at a pH of 8.0 [-]. The specific research question for this experiment was therefore:

- *What is the effect of ZLD WWTP NOM presence on the solubility of iron?*

3.3.1. Experimental OIC set-up

For the OIC experiment, a batch configuration was applied. The experiment was executed in a glass 0.5 [L] bottle, that was placed on a mixing plate to guarantee complete mixing at all time. The volume of the solutions was 0.2 [L] for all different applied settings.

The used Fe^{3+} addition solution was a Prolabo 0.41 [-] ferric chloride ($FeCl_3$) solution, with a Fe^{3+} content of 0.21 [kg/L]. For the dosage of Fe^{3+}, a $1.0 \cdot 10^{-6}$ [L] Eppendorf pipet with associating pipet tips was used. In order to correct the pH, a 20 [mg/L] Sigma Aldrich NaOH solution was prepared and dosed with the same type of pipet as for Fe^{3+} addition. The solutions were buffered with a 30 [g/L] Sigma Aldrich $NaHCO_3$ solution.

The added NOM was isolated from a concentrated RO-brine solids solution. In order to isolate the NOM, the experimental set-up of the ED experiment was used to extract the dissolved solids salts, resulting in a DOC concentration of 160 [mg/L] and a TDS concentration of 0.90 [g/L]. The evolution of TDS during the abstraction of salts is presented in Appendix B Observations OIC Experiment.

Filtration of the prepared solutions was performed with Millipore $0.20 \cdot 10^{-6}$ [m] filters and $5.0 \cdot 10^{-3}$ [L] syringes.

3.3.2. Experimental OIC procedure

Initially, NOM was added in various concentrations to the initial batch solution: 0.2 [L] demi water. The *NOM addition* ranged 0.0 - 1.0 – 2.0 – 5.0 – 10.0 [mg/L] TOC and remained constant over the experiment. After NOM addition, the pH of the batch solution was corrected and buffered to a fixed value of 8.0 [-] in steps of $5.0 \cdot 10^{-3}$ [L] NaOH solution addition. Subsequently, $7.78 \cdot 10^{-6}$ [L] of $FeCl_3$ solution was added to the batch solution, resulting in a fixed Fe^3 concentration of 8.0 [mg/L]. The Fe^{3+} analysis was verified with measurements for 1.0 – 2.0 – 4.0 and 8.0 [mg/L].

After the addition of Fe^{3+}, the batch solution was mixed thoroughly (to facilitate *coagulation*) for the duration of one minute (empirically determined required duration for floc formation). When the first flocs were formed, the mixing speed was decreased in order to form larger flocs (to facilitate *flocculation*) for the duration of three minutes.

After slow mixing, two samples were taken, of which one was *filtered*, to reject undissolved iron and subsequently determine the dissolved iron concentration content. Finally, both samples were analysed for total Fe concentration. Additional TOC measurements were performed in order to determine TOC removal by the used filters. Each combination was executed in duplicate.

3.4. Nanofiltration experiment

The NF experiment was designed to determine the potential of NF membranes to isolate dissolved NaCl from the RO-brine in the permeate stream using *various membranes and configurations*. To this extend, the following specific research questions were formulated:

- *Does the hydraulic membrane permeability deviate between various configurations and membranes?*
- *What is the TDS yield for the various membranes and configurations?*
- *What is the rejection of contaminants originating from the RO-brine?*

3.4.1. Experimental NF set-up

The experimental NF set-up consisted of a number of various components, with as main component the *NF membranes*. For the PNF runs, single Polyamide Thin-Film Composite material Filmtec NF90-2540 and NF270-2540 membranes were used, with a total filtration area of 2.6 [m^2]. The PNF membranes were placed in a Membraneline® stainless steel PNF membrane housing. For the CNF-HC runs, four sequencing titanium dioxide (TiO_2) Nanofiltration Inopor® nano membranes were used, with a total filtration area of 1.0 [m^2]. The CNF membranes were placed in associating Andreas Junghans stainless steel membrane housings. The relevant characteristics of the membranes are presented in Table 3.

Table 3 - An overview of the relevant NF membrane characteristics (DOW, 2006a; Geraldes et al., 2008; Shang, 2014)

	PNF90 Membrane	PNF270 Membrane	CNF Membranes
Dimensions [m] *Length x Diameter*	1.02 x 0.061	1.02 x 0.061	1.20 x 0.025
Cross sectional area [m^2]	$9.20 \cdot 10^{-4}$	$9.20 \cdot 10^{-4}$	$1.83 \cdot 10^{-4}$
MWCO [Da]	200 - 400 (tight ~ 200)	200 - 400 (loose ~ 400)	450
Max. water flux [$L \cdot m^{-2} \cdot h^{-1}$]	52	52	200

50 [L] feed water was stored in a 80 [L] polypropylene tank and during operation thoroughly mixed by a mechanical mixer. The feed water tank served as accumulation tank for the permeate and concentrate and was therefore also the location for samples from the three flows.

A feed pump, with a working range of 30 – 1200 [L/h] and 0 – 30 [bar], provided the required pressure to the feed water and was controlled by the control center of the set-up: a Divergence OSMO-inspector, more elaborately discussed by Shang (2014). An external Dutchi Motors recirculation pump, with a flow rate of 360 [L/h] was used for the CNF-HC runs, to provide required cross-flow. EC sensors were installed in the permeate and concentrate stream.

Figure 14 presents a schematic overview of the experimental setup, including all components.

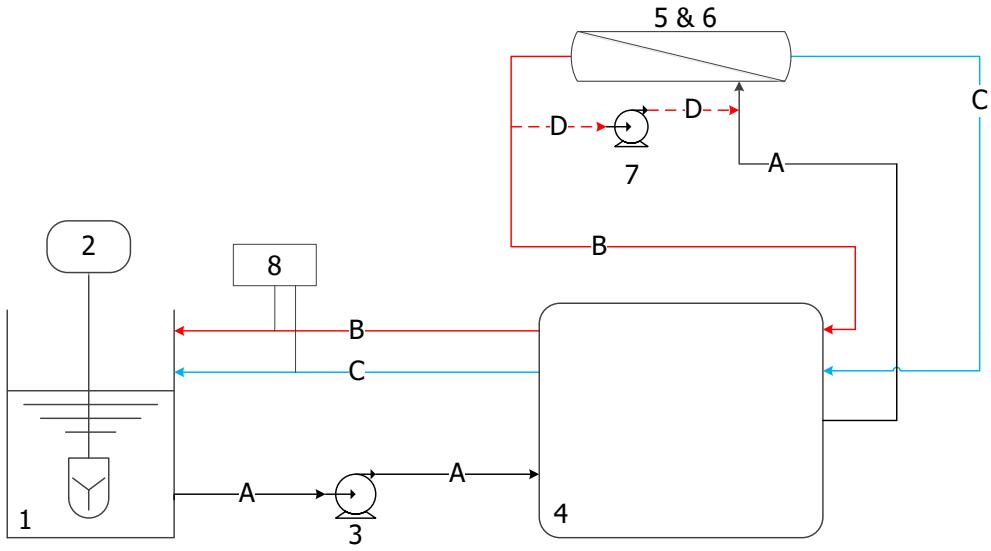

1	Feed water tank	**A**	Feed flow
2	Mixer	**B**	Concentrate flow
3	Feed pump	**C**	Permeate flow
4	OSMO-inspector	**D**	Recirculation flow (CNF-HC)
5	Membrane housing		
6	Nanofiltration membrane		
7	Recirculation pump (CNF-HC)		
8	EC-sensors		

Figure 14 - A schematic presentation of the experimental NF set-up, including all streams and components.

3.4.2. Experimental NF configurations

To execute runs in both dead-end and cross-flow configuration, various procedures needed to be followed, as the PNF membranes and associating housing could not be connected to the external recirculation pump.

The following configurations were executed:

- Polymeric nanofiltration at low cross-flow (PNF-LC) Dead-end
- Polymeric nanofiltration at high cross-flow (PNF-HC) Cross-flow
- Ceramic nanofiltration at high cross-flow (CNF-HC) Cross-flow

The PNF-LC runs concerned a *dead-end* configuration, as the cross-flow is kept to minimum and no additional recirculation has been applied. The PNF-LC was executed with both the polymeric NF90 and NF270 membranes.

The PNF-HC runs concerned a cross-flow configuration, where a higher cross-flow is established by pre-concentration. By concentrating the 50 [L] initial volume with 0.625 [-] and subsequently apply a recovery of 0.20 [-], a higher cross-flow was realized and the aimed recovery was achieved: total permeate production was 35 [L]. This procedure is visualized in Appendix C Additional data NF experiments. The cross-flow velocity in this configuration meets the recommendations of the membrane supplier (DOW, 2006b). The PNF-HC was executed with the NF270 membrane only.

The CNF-HC runs also concerned a cross-flow configuration. In this configuration, an additional recirculation pump was installed in the experimental NF setup, realizing an additional cross-flow without affecting the aimed recovery.

Sampling procedure

For each configuration, samples of feed water, permeate and concentrate were taken strategically, in order to have triplicate measurements. For the PNF-LC and CNF-HC configurations, multiple samples were taken over a period of 48 hours. Samples for the PNF configuration were taken twice over a duration of 1.5 hours, whereas these runs were executed in *triplicate*.

3.4.3. Conditions NF experiments

The various characteristics of the membranes and the various configurations resulted in different operational conditions for the NF experiments. As a general guideline, the *water flux* was set to 19 [$L \cdot m^{-2} \cdot h^{-1}$], equal to the applied settings in the research of Vaudevire et al. (2013). The aimed *recovery* was set to 0.70 [-], for all runs with various membranes and configurations.

The permeate pressure was aimed not to exceed 2.0 [bar]. Temperature was not regulated during the experiment, but continuously measured, because of the influence on the fate of the hydraulic permeability of the membranes. An overview on the specific operational conditions for each NF experiment is presented in Table 4.

Table 4 - An overview of the applied settings in the various NF configurations.

	PNF-LC NF90 & PNF270	PNF-HC NF270		CNF-HC
	Exp.	Pre-conc.	Exp.	Exp.
Feed flow rate [L/h]	70	100	250	30
Permeate flow rate [L/h]	50	50	50	21
External cross-flow [L/h]	-	-	-	360
Cross flow velocity [m/s]	0.02	0.03	0.08	0.59

3.4.4. Cleaning procedure NF

After the experiments with the various membranes, chemical cleaning was carried out using two solutions: NaOH and HCl. Initially HCl was used to remove potential inorganic fouling (scaling products) and subsequently NaOH was used to remove potential organic fouling. For these two solutions, 0.1 [mol/L] concentrations were used and a soaking and a recirculation time of one hour was applied.

In order not to damage the PNF membranes, the pH was kept within the range 2 – 12 [-] (DOW, 2006a), which was assumed to be limiting for all used membranes. After all cleaning phases, the membranes were rinsed thoroughly with demi water, at least for one hour.

3.5. Electrodialysis experiment

The ED experiment was designed to determine the performance of ED to isolate dissolved NaCl from the RO-brine in the concentrate stream using *various types of membranes*. To this extend, the following specific research questions were identified:

- *What is the effect of the LCD on the operation of the ED?*
- *What is the TDS yield and the rejection of contaminants originating from the RO-brine?*

3.5.1. Experimental ED set-up

In the experimental ED set-up a single PCCell 64002 ED cell unit functioned as its core component. The ED cell unit consisted of a membrane stack in between an anode chamber (made of Pt/Ir coated titanium) and a cathode chamber (made of V4A steel) (PCCell, 2014). For the ED experiment, different membrane stacks were used, both supplied by PCCell: a STM stack and a MVM stack. Each stack consisted, in sequencing order, of:

- n-1 Cation exchange membranes (CEM)
- 2 Cation exchange end membranes (CEEM)
- n Anion exchange membranes (AEM)
- 2n Associating spacers

Table 5 - An overview of the relevant ED membranes characteristics (PCCell, 2013).

	Standard CIEXM	Standard AIEXM	Monovalent CIEXM	Monovalent AIEXM
Functional group and ionic form	Sulphonic acid - Na^+	Ammonium - Cl^-	Sulphonic acid - Na^+	Ammonium - Cl^-
Membrane dim. [m] *Length x Height*	0.11 x 0.11	0.11 x 0.11	0.11 x 0.11	0.11 x 0.11
Eff. Mem. dim. [m] *Length x Height*	0.08 x 0.08	0.08 x 0.08	0.08 x 0.08	0.08 x 0.08
Thickness [m]	$160 \cdot 10^{-6}$ - $200 \cdot 10^{-6}$	$180 \cdot 10^{-6}$ - $220 \cdot 10^{-6}$	$100 \cdot 10^{-6}$	$110 \cdot 10^{-6}$
Resistance [Ω/m^2]	~$2.5 \cdot 10^4$	~$2.5 \cdot 10^4$		$20 \cdot 10^4$

The CEEMs and associating spacers were placed at the electrode sides. Subsequently, AEMs and CEMs and associating spacers were placed in a sequencing order to create n=10 diluate and concentrate channels: ten cell pairs in total, resulting in a total effective membrane area of 0.128 [m^2] per stack. An overview of relevant characteristics of both STMs and MVMs is presented in Table 5. The spacers are made of silicone and polypropylene material and have a thickness of $0.5 \cdot 10^{-3}$ [m] (Ben Sik Ali et al., 2013).

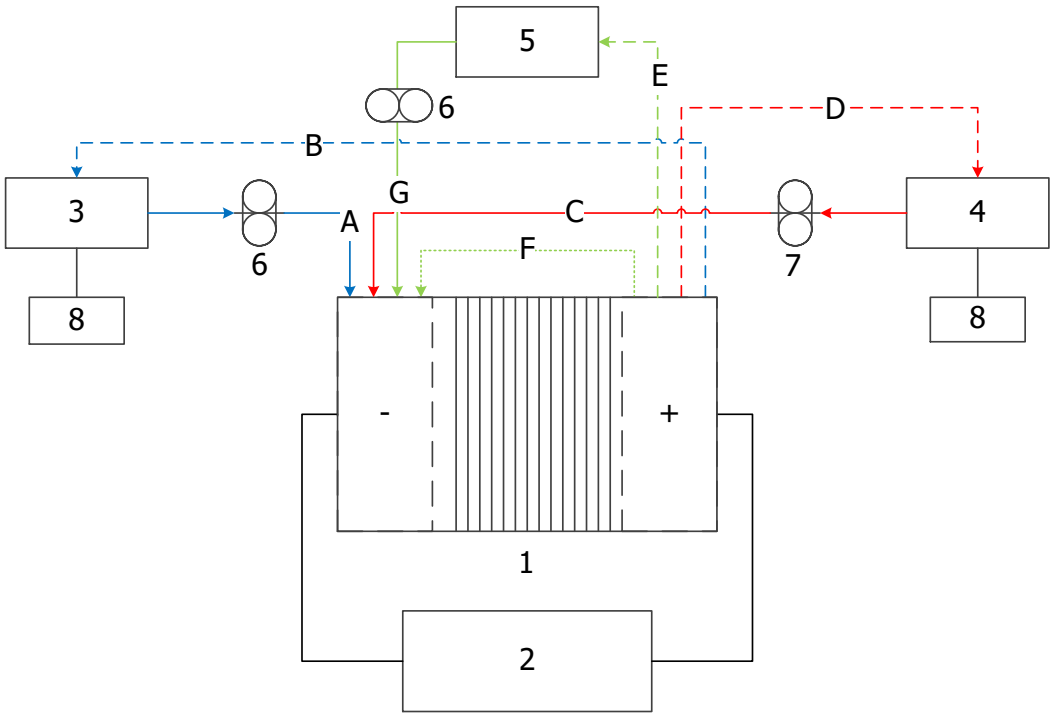

1	Electrodialysis cell	**A**	Diluate in
2	Direct current supply	**B**	Diluate out
3	Diluate jar	**C**	Concentrate in
4	Concentrate jar	**D**	Concentrate out
5	Electrolyte jar	**E**	Electrolyte in
6	Diluate & concentrate pump	**F**	Electrolyte recirculation
7	Electrolyte pump	**G**	Electrolyte out
8	EC-sensors		

Figure 15 – Schematic presentation of the experimental ED set-up, including all streams and components.

The electrical current was provided by a Delta Elektronika direct current (DC) supply, with a potential range of 0 – 30 [V] and a current range of 0 – 0.30 [A]. The various flows were pumped by two Watson Marlow 520S pumps, with 323 pump heads and Marprene tubing, having a flow rate range of 0.25 – 47.00 [L/h], according to performed calibration tests.

Sensors for continuous EC measurements were placed in the diluate and concentrate jars. Figure 15 presents an schematic overview of the experimental setup, including all components.

The initial diluate was represented by 1.0 [L] RO-brine and the initial 1.0 [L] concentrate consisted of a 6.8 [g/L] NaCl solution, resulting in equal TDS concentrations. A concentrated electrolyte solution flows next to the electrodes in order to establish the electrical current and avoid excessive potential in the solution (Strathmann, 2010). The electrolyte consisted of a 85.0 [g/L] $NaNO_3$ solution, following the advice of Vanoppen (2015).

Because water transport due to osmosis and electro-osmosis was expected during the abstraction of salts, the concentrate was collected in a 2.0 [L] jar. Both the diluate and electrolyte were stored in 1.0 [L] glass jars. All streams were continuously mixed with magnetic stirrers on a mixing plate.

3.5.2. LCD determination procedure

The applied current for the experiment was determined according to the *LCD* of the diluate (RO-brine). The LCD was determined according to the empirical method of Cowan et al. (1959).

For the LCD determination, diluate dilutions of 1.0x, 0.8x, 0.6x, 0.4x, 0.2x and 0.1x were prepared. By stepwise increasing (0.05 [A] per minute) the electrical current and logging the potential, the electrical resistance was determined. The LCD determination was stopped when the maximum potential of 30 [V] was reached. For the concentrate a solution of 6.8 [g/L] NaCl was prepared, so the concentrate was never the limiting stream: the TDS in the concentrate increases during the operation. Because only the TDS in diluatedecreases, this stream was corrected according to the LCD.

3.5.3. Experimental ED procedure

The experiment was executed until the EC of the diluate was reduced to ~1.00 [mS/cm]. Initially the maximum applicable electrical current was applied during operation. Subsequently, the applied electrical current was adjusted for the LCD. During operation of the experiment, all streams were *recirculated*, as depicted in Figure 15.

The electrical current and potential were logged manually. Pressure and temperature were not subject of research in the experiment.

Sampling procedure

Right before and after the run, the diluate, concentrate and electrolyte were weighed and sampled. The experiment was executed in *triplicate* for both membrane types.

3.5.4. Experimental ED conditions

The applied flow rate for the diluate and concentrate was fixed to 5.0 [L/h], which gave the highest migration rate of ions in a tested range of 5 – 15 [L/h]. The flow velocity through each single diluate and concentrate channel was of $3.5 \cdot 10^{-3}$ [m/s], corresponding to a residence time in the channels of 23 [s]. The flow rate for the electrolyte was 10 [L/h], double the flow rate of the diluate and concentrate, following the research of Heidekamp (2013).

3.5.5. Cleaning procedure ED

After the experiment, both the STM and MVM membranes were cleaned by recirculation of both a 0.1 [mol/L] HCl and a 0.1 [mol/L] NaOH solution for 1.0 [h], in order to remove potential inorganic (scaling products) and organic fouling, respectively.

3.6. Ion exchange experiment

The IEX experiment was designed to determine the performance of IEX to isolate dissolved NaCl from the RO-brine in the effluent stream using various *ionic forms*. Therefore, the following specific research questions were drafted:

- What is the TDS yield and the rejection of contaminants originating from the RO-brine?
- When does breakthrough occur?
- How efficient is the regeneration procedure?

3.6.1. Experimental IEX set-up

In the experimental IEX set-up, a column enclosing *IEX resin* was the main component. A plastic column was installed, with a height of 0.40 [m], external diameter of 0.02 [m] and wall thickness of $1.0 \cdot 10^{-3}$ [m]. A height of 0.20 [m] of resin was placed in the column, resulting in a bed volume (BV) of $50.9 \cdot 10^{-3}$ [L].

A Lewatit® VP OC 1071 resin was used for this experiment, a strong base, gelular anion exchange resin. The matrix of the resin is crosslinked polyacrylamide and the functional group is quaternary amine (NR_4^+), with chloride (Cl^-) and hydroxide (OH^-) as its optional ionic forms. The ionic form can be changed and restored (regeneration) by eluting the resin with 100 [g/L] NaCl or 70 [g/L] NaOH solutions (Lanxess, 2011).

The physical appearance of this type of resin are white, translucent beads. Table 6 presents an overview of additional relevant physical and chemical data on the used IEX resin.

Table 6 - An overview of the relevant IEX resin characteristics (Lanxess, 2011)

	Strong base anion resin
Bead size [m]	$1.4 - 1.6 \cdot 10^{-3}$
Density [kg/L]	1.09
Total capacity [meq/L]	1.25

Approximately 50 [L] feed water (RO-brine) was stored in a 80 [L] polypropylene tank and during operation thoroughly mixed by a mechanical mixer. The feed water was pumped to the column by a Watson Marlow 120S pump with Marprene tubing, having a flow rate range of 0.06 – 5.70 [L/h], according to performed calibration tests.

For effluent sampling, a Watson Marlow 120S pump was installed and connected to a Biorad 2110 fraction collector, with a total capacity of 80 vials with a volume of $7.5 \cdot 10^{-3}$ [L] each. A third Watson Marlow 120S pump was installed for resin regeneration.

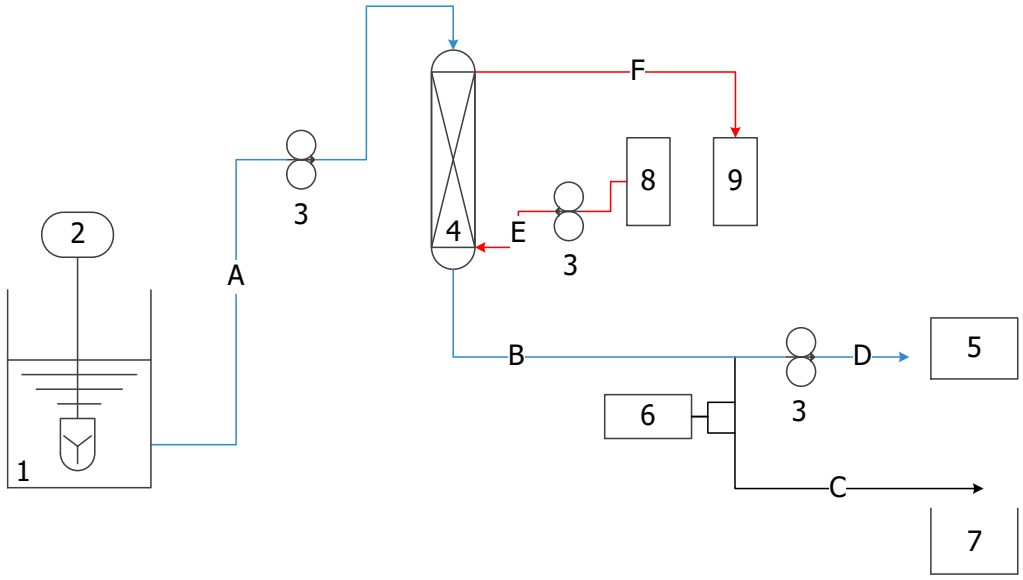

1	Feed water tank	**A**	Feed water stream
2	Mixer	**B**	Effluent stream
3	Peristaltic pump	**C**	Discharge stream
4	IEX resin column	**D**	Sample stream
5	Fraction collector	**E**	Rinse and eluent stream
6	EC sensor & pH sensor	**F**	Brine
7	Sewer drain		
8	Rinse solution & eluent storage		
9	Brine storage		

Figure 16 - A schematic presentation of the experimental IEX set-up, including all streams and components.

For the fast rinse and final rinse demi water was used, whereas and the elution is performed with a 100 [g/L] NaCl solution as eluent as proposed by Grefte (2013). The solutions and brines were stored in 0.5 [L] glass jars.

Finally, a pH-sensor and an EC sensor were installed in the effluent stream. Figure 16 presents a schematic overview of the experimental setup, including all components.

3.6.2. Experimental IEX procedure

The execution of the IEX experiment was performed in a continuous down-flow column configuration for a total throughput of 600 [BV].

Sampling procedure

Right before and after the runs, the column with and without resin was weighed. The sampling pump sampled every 15 [min] for the duration of 1 [min], at a flow rate of 0.45 [L/h]. The fraction collector presented an empty vial every 15 [min], resulting in four samples per hour, which were manually combined to make one sample of 0.03 [L]. When the sampling pump was switched off, the effluent was discharged to the sewer.

The IEX experiment was executed *once* for OH-resin and in *triplicate* for Cl-resin.

3.6.3. Regeneration procedure IEX

After execution of the IEX runs, the resin was regenerated in a counter-current column configuration in three different phases, following the procedure of Alchin et al. (2002):

- Fast rinse
- Elution
- Final rinse

The initial rinse solutions and eluent were pumped through the IEX column, as presented in Figure 16. Initially, potential particulate and suspended solids were washed off in the *fast rinse* phase. Secondly, the original ionic form was restored in the *elution phase* and finally, the resin was rinsed in the *final rinse phase* to remove potential residual contaminants. The brines were stored separately and sampled subsequently.

3.6.4. Experimental IEX conditions

In order to provide good sorption conditions, a contact time of 2 [min] was realised, resulting in a *feed* flow rate of 30 [BV/h] and a flow velocity of 6.0 [m/h], meeting the recommended conditions of the resin supplier (Lanxess, 2011).

Each specific phase in the regeneration procedure was executed under various conditions. The operational conditions and used rinse and elution volumes are presented in Table 7. The conditions are based on the recommended settings by the supplier of the resin (Lanxess, 2011).

Table 7 - An overview of the applied operational conditions during the various phases in regeneration of the IEX-resin.

	Fast rinse	Regeneration	Final rinse
Volume [BV]	4.0	4.0	10.0
Flow rate [BV/h]	27.0	3.0	27.0
Flow velocity [m/h]	5.4	0.6	5.4
Contact time [min]	2.2	20.0	2.2
Bed expansion	50%	0%	50%

3.7. SALEX experiment

The SALEX experiment was designed to determine the potential of mixed solids purification by elution with a saturated NaCl solution. Therefore, the following specific research questions were identified:

- *What is the effect of eluent volumes and bed expansion?*
- *What is the net solids yield and extraction efficiency of contaminants?*
- *What is the quality of the produced residual stream (SALEX-brine)?*

3.7.1. Experimental SALEX set-up

For the experimental SALEX set-up, a glass column was used, with the same dimensions as the column in the IEX set-up: 0.40 [m] in height, an external diameter of 0.02 [m] and wall thickness of $1.0 \cdot 10^{-3}$ [m]. The height of mixed solids in the column was 0.20 [m], resulting in a mixed solids BV of $50.9 \cdot 10^{-3}$ [L].

The used pump for the experimental SALEX set-up was a Watson Marlow 120s with Marprene tubing.

The eluent consisted of a saturated 400 [g/L] NaCl solution and was stored in a 0.5 [L] glass jar. Figure 17 presents an schematic overview of the experimental SALEX setup, including all components.

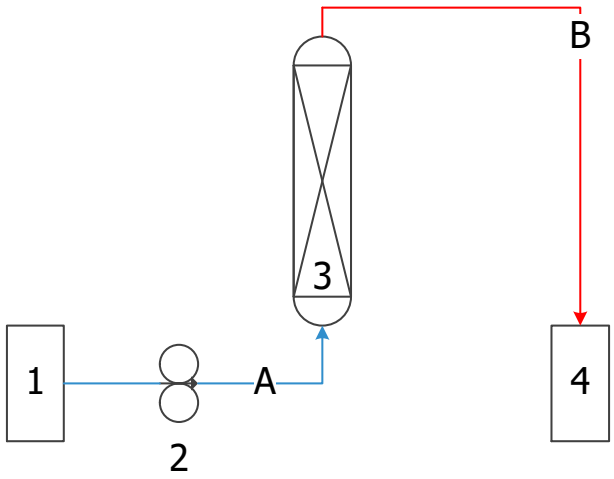

1	Washing solution storage	**A**	Eluent stream
2	Peristaltic pump	**B**	Brine stream
3	Mixed solids column		
4	Brine storage		

Figure 17 - A schematic presentation of the experimental SALEX set-up, including all streams and components.

3.7.2. Experimental SALEX procedure

The mixed solids were placed in the column and the weight of the mixed solids was measured. Subsequently, the mixed solids were eluted with the NaCl solution, in an up-flow column configuration, as schematized in Figure 17.

Sampling procedure

When the eluent was spent, the column was drained and the washed solids were dried in the oven at 100 [°C]. Finally the collected brine and solids were sampled. The washed solids were dissolved in a concentration of 5 [g/L] for analysis.

3.7.3. Experimental SALEX conditions

Various conditions for bed expansion and elution volume were applied for the SALEX experiment, resulting in nine different settings. Table 8 provides an overview of the applied settings.

Table 8 - Overview of tested settings for the SALEX experiment.

Setting ID	Bed expansion [-]	Contact time [min]	Eluent volume [BV]	NaCl in eluent [g]
SALEX 1	0%	8.63	1	20.4
SALEX 2	0%	8.63	2	40.7
SALEX 3	0%	8.63	3	61.1
SALEX 4	25%	1.84	1	20.4
SALEX 5	25%	1.84	2	40.7
SALEX 6	25%	1.84	3	61.1
SALEX 7	50%	1.04	1	20.4
SALEX 8	50%	1.04	2	40.7
SALEX 9	50%	1.04	3	61.1

4. Results and discussion

4.1. Results of organic iron complexation experiment

The initial runs of the OIC experiment were executed without pH buffering by $NaHCO_3$ addition. Directly after $FeCl_3$ addition, the pH dropped rapidly from pH = 8.0 [-] to pH = 4.0 [-], as a result of hydroxide consumption to form $Fe(OH)_3$. Therefore, buffer was added, to stabilize pH during flocculation. In order to rule out removal of NOM by filtration, TOC rejection was tested for all applied concentrations. This resulted in a maximum rejection of 0.15 [-]. All executed runs involved oxidized and buffered solutions with 8.0 [mg/L] Fe^{3+} at an initial pH = 8.0 [-]. The deviating factor in the OIC experiment was NOM and all runs were executed in duplicate. Relevant pH plots (without buffer addition, 0 [mg/L] NOM addition and 10 [mg/L] NOM addition) are presented in Appendix B Observations OIC Experiment.

0 - 1 - 2 [mg/L] NOM addition

The initial runs involved no addition of NOM, assuming that hydrolysis of Fe^{3+} could take place without obstruction. Directly after $FeCl_3$ dosage $Fe(OH)_3$ was formed, resulting in a pH decrease to pH = 6.3 [-] and clearly visible $Fe(OH)_3$ flocs, as presented in Figure 18. Subsequently, samples were taken in order to determine the fraction of dissolved iron. The unfiltered samples had an iron concentration of 8.20 [mg/L], whereas the filtered sample only contained 0.10 ± 0.06 [mg/L] iron, indicating that 0.99 [-] of iron was undissolved. Figure 18 presents the difference in filters before and after filtration of samples containing $Fe(OH)_3$ flocs and the difference between unfiltered and filtered samples.

Figure 18 - Left to right: presence of $Fe(OH)_3$, difference between clean and spent $0.20 \cdot 10^{-6}$ [m] pore sized filters and difference between unfiltered and filtered $Fe(OH)_3$ samples.

Similar results were obtained for the addition of 1 [mg/L] and 2 [mg/L] NOM, because the iron dissolved iron fraction ranged 0.98 – 0.99 [-], achieved under similar conditions and by applying the same procedure. The pH appeared to drop to similar levels as for the runs at no NOM additions, indicating that iron hydrolysed, which was visually verified by detected flocs. According to these results, low NOM concentrations do not have an effect on iron solubility.

5 – 10 [mg/L] NOM addition

For addition of 5 [mg/L] NOM, almost no visible flocs had formed after $FeCl_3$ addition, indicating that the formation of iron flocs was obstructed. The residual iron concentrations of the filtered sample appeared to be significantly higher than the previously executed runs at low NOM addition: 1.94 ± 0.48 [mg/L]. The pH dropped to pH = 6.50 [-], indicating that hydrolysis took place, but to a slightly less extend than for 0 – 2 [mg/L] addition of NOM. For the addition of 5 [mg/L] NOM, only very little $Fe(OH)_3$ flocs were formed. These observations imply smaller floc or stabilized floc formation, which could not be removed by filtration. When stabilized flocs are formed, they tend to repulse each other and obstruct flocculation, resulting in small of $Fe(OH)_3$ flocs with reduced filterability, as explained for colloids by Hendricks (2006). Because 0.77 [-] iron was not rejected by filtration, this fraction was considered to remain dissolved.

The runs with addition of 10 [mg/L] NOM confirmed the expectation that smaller and/or stabilized $Fe(OH)_3$ flocs form in the presence of NOM at concentration higher than 5 [mg/L]. During these runs, the filtered samples contained iron concentrations of 5.01 ± 0.39 [mg/L], resulting in a significant increase of dissolved iron fraction: 0.65 [-] remained dissolved, in presence of 10 [mg/L] NOM. Similar to the runs with 5 [mg/L] NOM addition, the pH decreased to pH = 6.5 [-], indicating iron hydrolysis. Visual inspection resulted in the observation of absence of $Fe(OH)_3$ floc throughout two runs, indicating stabilized $Fe(OH)_3$.

The results are similar as found by Koenings et al. (1976), who researched the effect of colloidal NOM on the hydrolysis of dissolved iron. In this research, inhibition of hydrolysis was found to account for 0.64 [-] of the total iron presence, as this fraction was complexed. The OIC experiment in this thesis achieved very similar results: NOM presence up to 10 [mg/L] provided conditions to keep 0.65 [-] of iron dissolved, whereas in absence of NOM 0.01 [-] was undissolved, of a total of 8.0 [mg/L] Fe^{3+} initially present. Table 9 presents an overview of the iron concentrations and undissolved fraction.

Table 9 – An overview of the iron concentrations, both unfiltered and filtered and the resulting undissolved fraction.

NOM addition	Iron unfiltered [mg/L]	Iron filtered [mg/L]	Dissolved fraction [-]	Visible floc detection
0 [mg/L]	8.20	0.10 ± 0.06	0.01 ± 0.01	Formation of flocs
1 [mg/L]	7.59 ± 0.22	0.13 ± 0.01	0.02	Formation of flocs
2 [mg/L]	7.15 ± 0.20	0.08	0.01	Little formation of flocs
5 [mg/L]	8.52 ± 0.66	1.94 ± 0.48	0.23 ± 0.07	Little formation of flocs (Excessive addition of $FeCl_3$)
10 [mg/L]	7.74 ± 0.08	5.01 ± 0.39	0.65 ± 0.04	No formation of flocs

4.2. Composition of RO-brine and mixed solids

Multiple batches of RO-brine were prepared, resulting in different compositions. Based on mass balance data, supplied by the ZLD WWTP, the total dissolved solids (TDS) concentration of the RO-brine was 6.8 [g/L] and the pH = 8.1 [-]. The majority (> 0.96 [-]) of the TDS consisted of NaCl and $NaHCO_3$, which had stable concentrations over the prepared RO-brine batches for experiments.

The contaminants appeared to deviate significantly between the prepared RO-brine batches, caused by heterogeneity of the shipped solids. Table 10 presents an overview of the average values and the standard deviations of the prepared RO-brine batches in the experiments. Especially the TOC deviated significantly, ranging 21.33 – 51.00 [mg/L], whereas silica deviated to a lower extend: 1.61 – 2.99 [mg/L]. The intention was to measure all metal elements (and silica) simultaneously using ICP-MS analysis equipment, while the presence of sodium was 10^5 times higher than other elements. Furthermore, the analysis centre (WAC) mentioned that the elemental matrix of the samples was very complex and uncertainties. Unfortunately, no reliable iron results were found (< 10 [µg/L]), while the detection limit was 0.15 [µg/L]. The mixed solids composition is presented in 1.2 Problem description.

Table 10 - An overview of the measured content of contaminants in the RO-brine.

	PNF270-LC	CNF-HC	PNF90-LC	PNF270-HC	ED-STM	ED-MVM	IEX
TDS [g/L]	6.8 (added)						
UV254A [1/cm]	0.131 ± 0.013	0.280 ± 0.010	0.142 ± 0.004	0.185 ± 0.004	0.232 ± 0.009	0.232 ± 0.011	0.248 ± 0.005
TOC [mg/L]	21.33 ± 0.96	35.55 ± 2.71	24.81 ± 1.21	35.96 ± 1.74	51.00 ± 1.07	40.31 ± 6.35	34.64 ± 0.35
Silica [mg/L]	-	1.61 ± 0.24	-	2.16 ± 0.06	2.99 ± 0.37	2.92 ± 0.35	2.34 ± 0.58
Iron [mg/L]	N/A	N/A	N/A	N/A	N/A	N/A	N/A

Additional LC-OCD analyses were performed to determine the NOM categories of both the RO-brine and the mixed solids (similar categories as presented in Table 2). The NOM is dominated by the presence of humic acids and building blocks: 0.72 in the RO-brine and 0.55 [-] in the mixed solids. The rest of the NOM appeared to consist substantially as LMW neutrals for 0.22 and 0.32 [-], in the RO-brine and mixed solids respectively. An overview of the relative presence of the NOM categories is presented in Table 11. More detailed data can be found in Appendix A NOM categorization.

Table 11 - An overview of NOM categorization for the RO-brine and the mixed solids.

NOM categories	RO-brine	Mixed solids
Biopolymers	0.02 ± 0.01	0.07 ± 0.06
Humic acids + building blocks	0.71 ± 0.02	0.55 ± 0.13
LMW acid	0.02 ± 0.00	0.05 ± 0.02
LMW neutral	0.22 ± 0.02	0.32 ± 0.06

4.3. Results of nanofiltration experiment

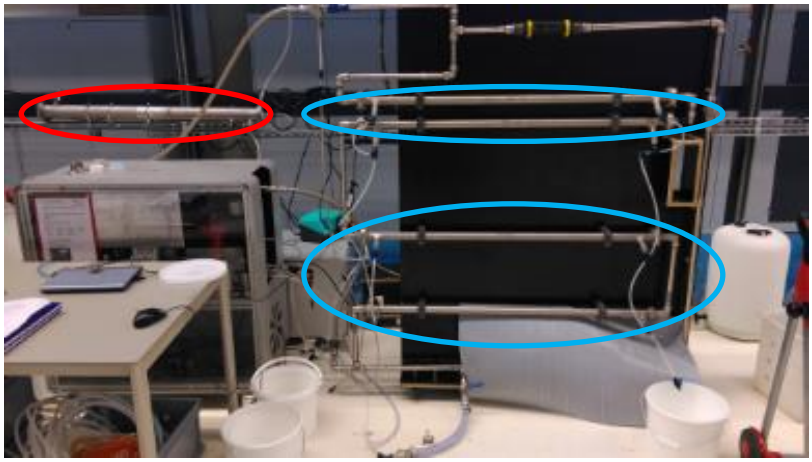

Figure 19 - Impression of the experimental NF set-up, with the PNF (red oval) and CNF (blue ovals) membranes.

Hydraulic membrane permeability of NF membranes

The combination of various NF membranes, having specific characteristics, and various configurations, resulted in unique operational conditions for each run. Because of the initiated long duration for PNF270-LC and CNF-HC, these runs were executed once to gain sufficient data. The shorter lasting experiment of PNF270-HC was executed in triplicate. In Figure 20, the HMP is plotted over run time. Based on these results, it could be derived that a high cross-flow configuration results in 0.23 [-] lower HMP: achieved for PNF270 membranes. The lower HMP in the low cross-flow configuration could be a result of concentration polarization of contaminants, the phenomenon stimulating contaminant diffusion, as mentioned by Hendricks (2006). This is assumed for the contaminants only, because the only difference for the runs was the presence of cross-flow. Concentration polarization of sodium chloride is not of interest, since sodium chloride is rejected at a very low rate.

Since a fixed water flux was applied, the HMP could deviate with respect to viscosity (as a function of temperature) and TMP. The HMP was corrected for a fixed temperature of 25 [°C] and therefore it can be stated that change in HMP was a result of TMP change: a potential fouling indicator. The experiments showed no clear HMP trend, giving no strong evidence of fouling. Fouling was also not expected for the relative short durations of the experiment and the fact that recirculation of the permeate and concentrate was performed. The HMP of the CNF-HC run showed fluctuations, which was a result of unstable pressure regulation of the OSMO-inspector: possibly caused by the installation of the external recirculation pump. The average TMPs for the different configurations were:

PNF270-LC:	11.97 [bar]	PNF90-LC:	16.63 [bar]
PNF270-HC:	9.73 [bar]	CNF-HC:	4.40 [bar]

From the TMP results, it is clear that CNF membranes have a significant higher permeability than PNF membranes, because the TMP is at least 2.2 times lower in high cross-flow configurations to provide a similar water flux. These results are in line with the permeability of CNF membranes found by Shang (2014) and PNF270 membranes by Vaudevire et al. (2013). For this experiment, osmotic pressure was assumed to be negligible, because the high TDS permeability was expected, according to the specific MWCO of the membranes.

Cleaning of the membranes appeared to be efficient, because 0.33 [-] higher HMP for tap water was achieved after cleaning of the PNF270 membranes: see Appendix C Additional data NF experiments.

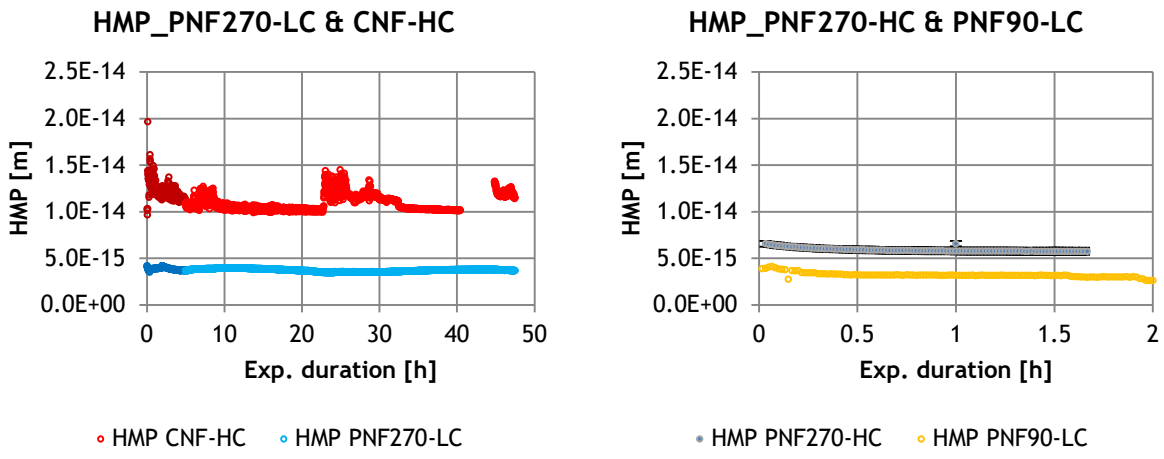

Figure 20 - The evolution of the HMP for all tested membrane and configuration combinations.

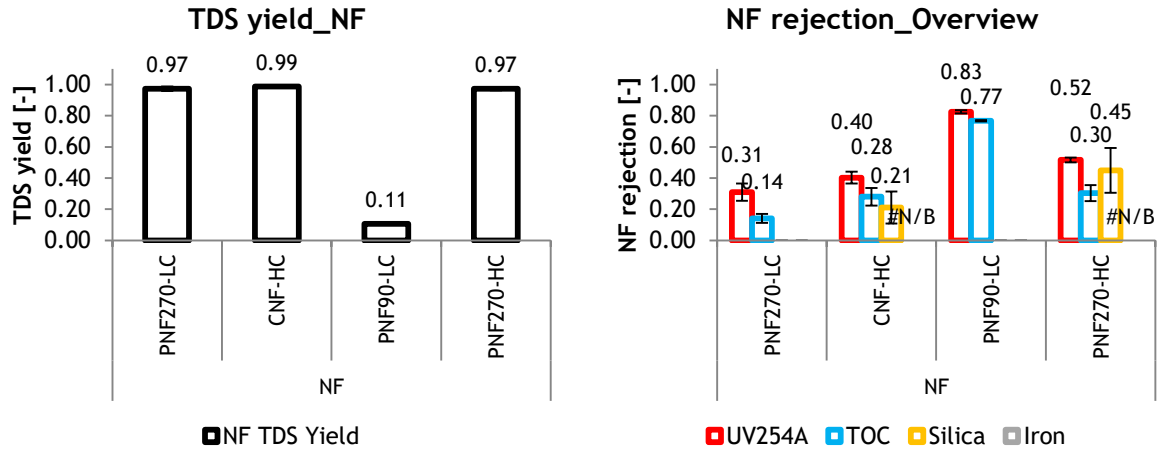

Figure 21 - The TDS yield (left) and contaminants rejection (right) of the NF experiment.

Dissolved solids yield by NF

The TDS yield of the CNF-HC run and the PNF270 runs proved to be very high: 0.99 and 0.97 [-] on average, respectively. The TDS yield was not influenced by cross-flow, according to the results of the PNF270 runs, executed in various configurations. The achieved TDS yield for PNF270 membranes was similar to that achieved by (Kabsch-Korbutowicz et al., 2011), applying a similar research objective. Additionally, the achieved TDS yield for the CNF-HC run was similar to that from the research of (Shang, 2014). This indicated that these two types of membrane are permeable for monovalent ions, such as sodium, chloride and bicarbonate. In these three configurations, the permeate contained 6.73 ± 0.59 [g/L] in the permeate, whereas the feed consistently contained 6.8 [g/L] of TDS.

The TDS yield for the PNF90-LC run appeared to be very low: 0.11 [-], resulting in 0.89 [-] rejection of monovalent ions. This NF membrane is therefore not suitable for the objective in this thesis and was not extensively analysed on rejection of contaminants. An overview of the TDS yields is presented in Figure 21.

Rejection of contaminants by NF

The performance of NOM rejection appeared to deviate between measurements by UV254A and TOC: UV254A measurements consistently indicated higher NOM rejection than TOC, resulting in deviations up to 0.20 [-]. Based on these results, it appeared that aromatic molecules were rejected to a higher extend, since these absorb UV254 light (Stefan A. Huber et al., 2011). The preferential removal of this NOM fraction led to significant colour differences between the feed and permeate flows, as presented in Figure 22.

The contaminant rejection was highest for the PNF90-LC run, which is caused by the low MWCO, as described in the supplier specification (DOW, 2006a). TOC was rejected up to 0.77 [-] on average. For the PNF270 runs, the contaminant rejection was significantly lower, especially for NOM. The application of higher cross-flow appeared to have an effect on the rejection of NOM, because for PNF270-HC a higher fraction of TOC was rejected than for PNF270-LC: 0.30 and 0.14 [-] on average, respectively. Based on these results, the PNF-HC appeared to be the best performing combination of PNF membranes and configurations. The TOC rejection of CNF-HC appeared to be reasonable: 0.28 ± 0.06 [-]. The TOC rejection for CNF-HC and PNF270-HC proved to be very similar, resulting in a permeate TOC concentrations of: 27.11 ± 1.01 [mg/L] and 26.19 ± 2.34 [mg/L], respectively. An overview of the contaminant rejections is presented in Figure 21 and residual contaminant concentrations can be found in Appendix F Additional experimental results.

The rejection results for organic matter deviated from results of the research of Vaudevire et al. (2013), achieving 0.87 [-] rejection of TOC with a PNF270 membrane and Kabsch-Korbutowicz et al. (2011) with similar PNF membranes, resulting in 0.91 [-] rejection. In contrast to the experiment of this thesis, the initial TOC concentration of the reference studies ranged 200 – 1,000 [mg/L] and an even higher cross-flow was applied: 1,000 – 4,000 [L/h]. Shang (2014) achieved 0.81 ± 0.02 [-] rejection of organic matter removal, but expressed as COD, at an initial concentration of ~ 550 [mg O_2/L] using the same CNF membrane, but in TDS concentrations of approximately six times lower. Results of organic matter removal achieved in similar executed researches were not found.

The removal of iron could not be determined, since iron was not detected in neither the RO-brine and the permeate streams, as discussed in 4.2 Composition of RO-brine and mixed solids. Silica was measured in the CNF-HC and PNF270-HC runs and proved to be rejected for 0.21 ± 0.10 and 0.45 ± 0.14 [-], respectively. The permeate concentration of silica for CNF-HC was 1.95 ± 0.24 [mg/L] and 1.40 ± 0.06 for PNF270-HC [mg/L]. Apparently, PNF membranes reject silica to a higher extend than CNF membranes.

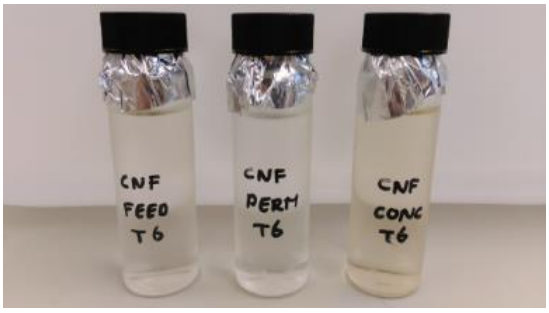

Figure 22 - Colour difference in the CNF-HC feed (left), permeate (middle) and concentrate (right), caused by presence of NOM.

4.4. Results of electrodialysis experiment

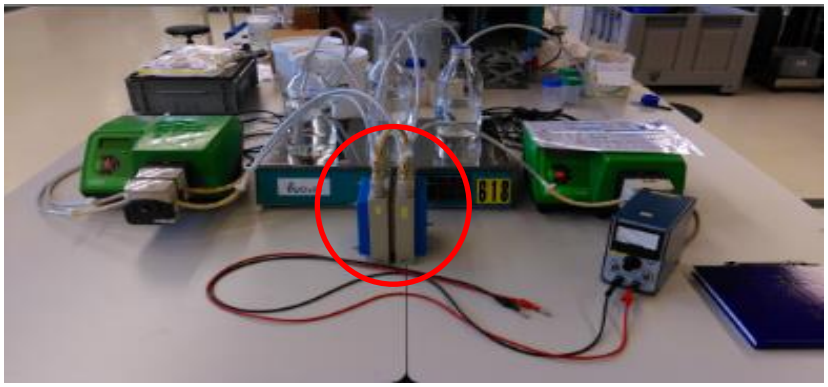

Figure 23 - An impression of the experimental NF set-up, with the ED cell (in red circle).

LCD effect on ED operation

During operation of the ED runs, using various membranes, the current was adjusted based on the LCD, in order to avoid water splitting, assumed to take place at 9.0 – 12.0 [V] (Strathmann, 2010). The results of the determination of the LCD for both membrane types are presented in Appendix D Additional data ED experiment. Runs with both membrane types were executed in triplicate, to gain sufficient data. The initial potential was for all runs was 6.0 [V], corresponding to an electrical resistance of 20 [Ω] at initial applied current of 0.30 [A]. The maximum potential in the water (between the electrodes) during the STM runs was 8.0 and 9.0 [V] for the MVM runs, respectively, corresponding to a maximum electrical resistance of 70 and 90 [Ω] for final applied current of 0.10 [A].

Figure 24 presents the average evolution of the TDS concentration in both the concentrate and diluate streams, for all executed runs. Within an hour, the objective to reduce the EC to 1.00 [mS/cm] was achieved, corresponding to a TDS concentration ranging 0.84 – 0.92 [g/L]. The migration flux proved to be strongly dependent on the applied current density, as a result of the LCD. In Figure 25, the average migration flux and the applied current are presented. The migration flux appeared to decrease when the applied current density was decreased. The same can be derived from the TDS evolution results and the described relation between electrical current and ion migration described by Nikonenko et al. (2014).

The migration flux divided over the applied current density proved to be constant over time for all runs and was slightly higher for the MVM runs. This factors for STM runs was 0.36 ± 0.03 [$mg \cdot s^{-1} \cdot m^{-2} \cdot (A \cdot m^{-2})$] and 0.37 ± 0.04 [$mg \cdot s^{-1} \cdot m^{-2} \cdot (A \cdot m^{-2})$] for the MVM runs.

Dissolved solids yield by ED

The TDS yield was similar for all runs executed with the two membrane types: 0.89 [-], as presented in Figure 26, for an average migration flux of 13 [$mg \cdot s^{-} \cdot m^{-2}$]. The results are in agreement with TDS yields found by Kabsch-Korbutowicz et al. (2011), achieving 0.96 [-] at an initial TDS concentration twenty times higher than for this thesis. The experiment in this thesis achieved 0.89 [-] TDS yield at an initial TDS concentration of 6.8 [g/L]. For each run, new concentrate was used, resulting in a TDS yield of 6.09 [g/L].

The isolation of NOM for the OIC experiment showed that TDS could be reduced from ~ 48 [g/L] to 2.9 [g/L] for a minimal migration flux of 16.7 [$mg \cdot s^{-} \cdot m^{-2}$], see Appendix B Observations OIC Experiment. This flux was achieved at a TDS concentration of the concentrate of ~ 54 [g/L]. This shows that the TDS concentration of the TDS can be significantly higher than the TDS concentration of the diluate, while still effectively ions migrate.

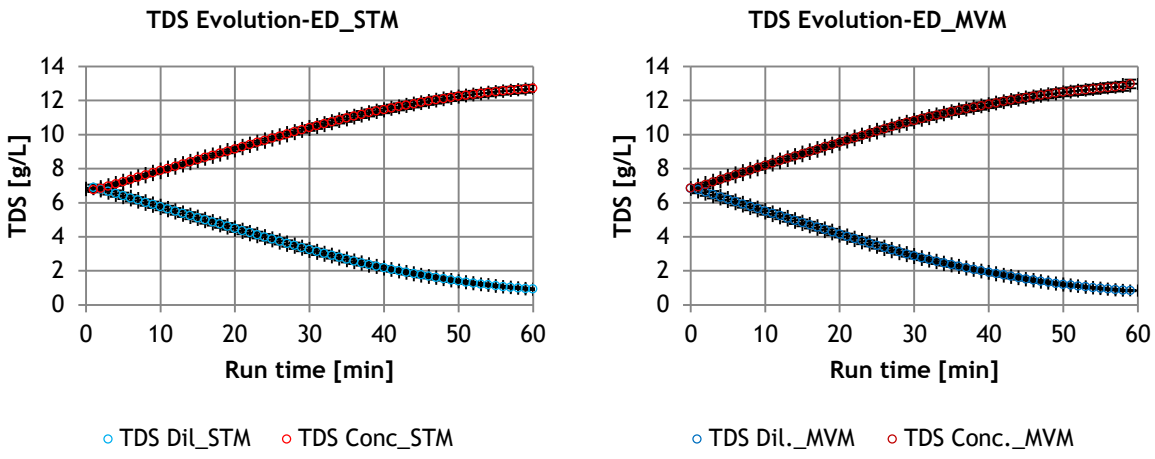

Figure 24 - Average TDS evolution over time of the diluate for all STM (left) and MVM (right) runs.

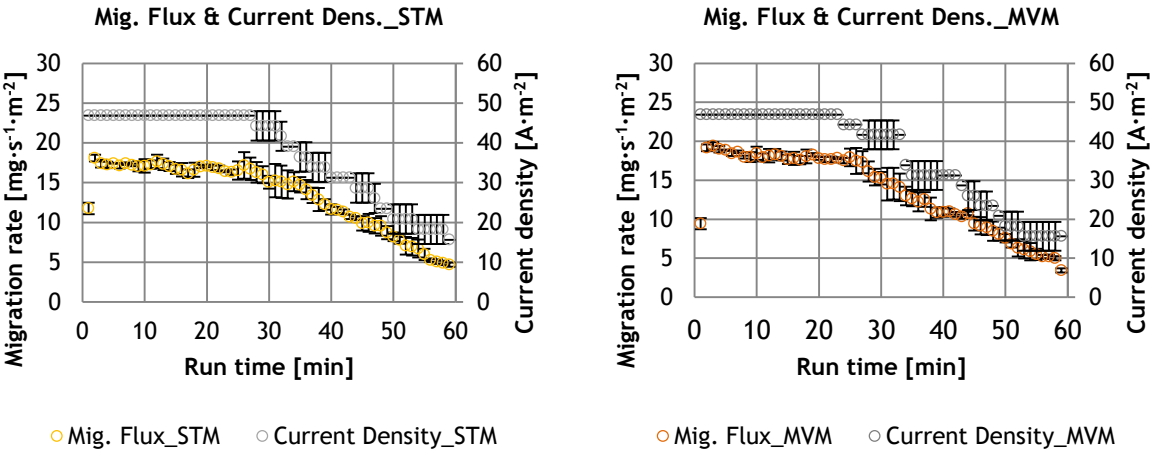

Figure 25 - Average migration fluxes and current density over time for all STM (left) and MVM (right) runs.

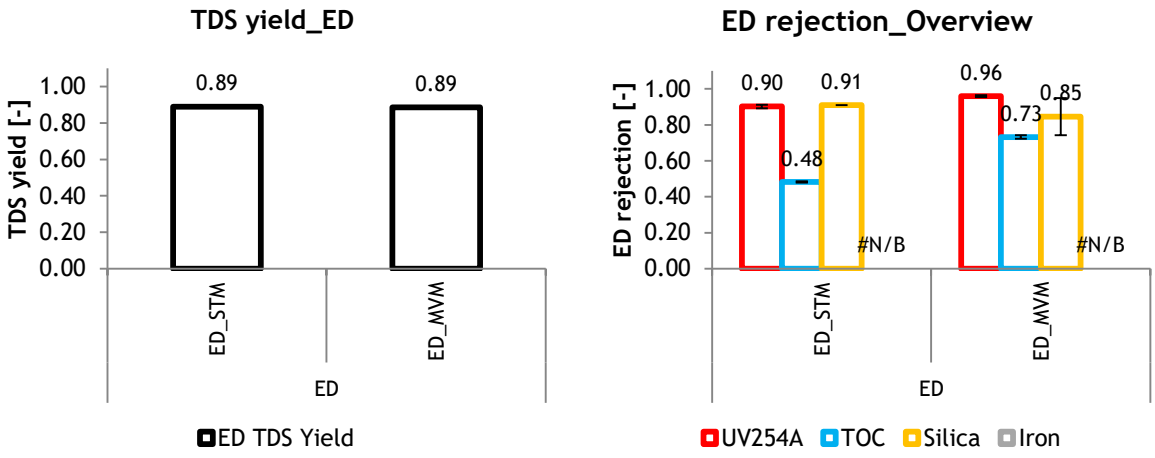

Figure 26 - Average TDS yields (left) and rejection of the contaminants (right) for the ED runs.

Rejection of contaminants by ED

Similar as for the NF experiment, there appeared to be a significant difference in NOM rejection in terms of UV254A and actual TOC. The rejection measured with UV254A proved to be very high for both STM and MVM runs: 0.90 ± 0.01 and 0.96 [-] respectively. This indicates very high rejection of aromatic molecules, because only a very low elevation in the UV254A was measured in the concentrates. This could easily be confirmed by visual inspection of the various streams after the executed runs: the diluate was coloured brownish, whereas the concentrate and electrolyte remain clear, as presented in Figure 27. Kabsch-Korbutowicz et al. (2011) found similarly high colour reduction: up to 0.99 [-], but at a NOM concentration thirty times higher. A significant fraction of the UV254A in the diluate was reduced, but did not show up in the concentrate or electrolyte. It was expected that this fraction adsorbed on the AEMs, which was proven by visual membrane inspection: significant colour change of the AEMs, as presented in Figure 27. Finally, TOC mass balance calculations confirmed this, as presented in Appendix D Additional data ED experiment.

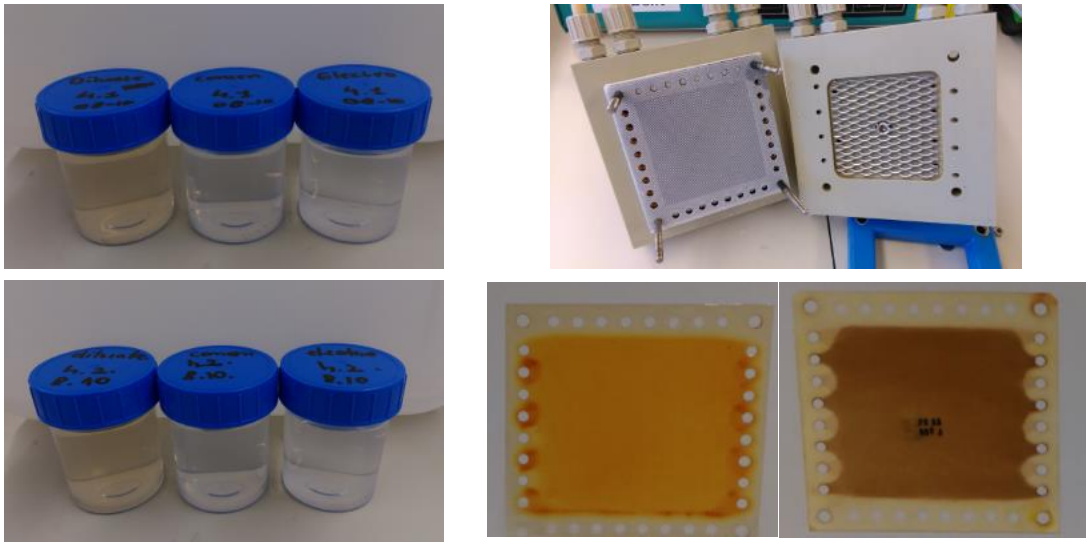

Figure 27 – A visualization of the colour difference of the (from left to right) RO-brine, concentrate and diluate after a successful run (left). The upper right picture presents new AEMs in the ED cell, whereas the lower right picture presents fouled standard AEMs (left) and monovalent selective AEMs (right).

More NOM migrated than expected based on UV254A results, according to the TOC measurements. Apparently, part of the NOM, not detected by UV254A, has monovalent ion characteristics, because it migrated along with the TDS. This can be derived from the observation that the TOC rejection for STMs was lower than for MVMs: 0.48 and 0.73 ± 0.01 [-], respectively. The concentrates contained considerable TOC concentrations, because the concentrate of the STM runs contained 28.36 ± 0.98 [mg/L] TOC and the concentrate of the MVM runs contained 12.52 ± 2.18 [mg/L] TOC. More data on residual contaminant concentrations can be found in Appendix F Additional experimental results by Koprivnjak et al. (2006) showed 0.88 [-] NOM rejection by ED, implying significantly less migration to the concentrate, but achieved for six times low TDS concentrations.

Silica was rejected to a high extend: 0.91 ± 0.05 [-] for STM runs and 0.84 ± 0.09 [-] for MVM runs. According to the data, these high fractions were conserved in the diluate. Unless the low rejection, relatively high silica concentrations were found in the concentrate streams: 2.26 ± 0.37 and 3.15 ± 0.35 [mg/L] respectively. The relatively high initial silica concentrations indicate that the RO-brine contained significantly more silica than the mixed solids. The difference in silica between STM and MVM runs could be a result of the charge of silica: more charged silica could explain the lower rejection for the MVM runs.

4.5. Results of ion exchange experiment

Figure 28 - An impression of the experimental IEX set-up, with the IEX-resin column (red oval).

Ionic form of resin

Initially, the two different ionic resin forms were tested on stability of the ionic form. The hydroxide form proved to be very unstable: the initial pH = 12.3 [-] dropped rapidly to the pH of the feed water: pH = 8.6 [-], as shown in Figure 30. These measurements indicate that the hydroxide ions on the resin were exchanged with ions in the feed water. Because the pH stabilized after approximately 50 [BV], it was assumed that the initial ionic form was exhausted. The run time for the hydroxide ionic form is considered inefficient because regeneration needs to be applied too frequently.

The resin in chloride form proved to be much more stable, based on pH measurements presented in Figure 30, because the feed water consisted of similar ions. The IEX experiment was executed in three similarly operated runs, for a resin in chloride form and RO-brine feed. For all three runs, the initial pH showed a dip for the first 60 [BV]. This dip could be a result of stabilization of the pH sensor. The explanation for the pH evolution was not further researched in this thesis, because the interaction of ions in IEX is complex, especially when the feed water consists of high TDS and various anions (chloride, bicarbonate, potential silica anions and NOM).

Dissolved solids yield by IEX

The TDS yields proved to be very high for the IEX-resin in chloride form: 1.00 [-] on average over 600 [BV]. The TDS of the effluent was continuously equal to the RO-brine TDS concentration. The TDS yields did not change over the treated volume, expressed as BV. It was assumed that when the resin is in chloride form, the dissolved chloride and bicarbonate concentrations of the feed water are unaffected. The TDS yields are presented in Figure 31.

Rejection of contaminants

The rejection of contaminants was determined in three runs for every 60 [BV]. By means of determining the sequencing rejection of NOM over increasing treated bed volumes, a breakthrough curve was developed for UV254A and TOC, as presented in Figure 30. From these results, the rejection of UV254A and TOC decreased over time, indication saturation of the resin. The saturation of the resin could be visually tracked, as a result of colour change, as presented in Figure 32. Because complete rejection of either UV254A or TOC was absent, the resin appeared to breakthrough immediately. Practical breakthrough is considered when the contaminant concentration in the effluent exceeds the set restrictions. This is determined in a later stage.

With respect to the deviating results for NOM, in terms of UV254A and TOC, the differences were not as large for IEX as for ED and IEX: UV254A and TOC rejection were relatively similar, because the highest average difference was 0.09 [-].

The rejection of UV254A and TOC is expressed at 60, 300 and 600 [BV] in Figure 31. The TOC rejection at 60 [BV] was 0.77 ± 0.02 [-] and decreased to 0.73 ± 0.02 [-] at 300 [BV] and 0.55 ± 0.11 [-] at 600 [BV]. The corresponding TOC concentrations in the effluent were 7.95 ± 0.61 [mg/L], 9.31 ± 1.07 [mg/L] and 15.41 ± 0.43 [mg/L], respectively. The rejection of UV254A and TOC proved to be better than found by Kaeocha Eilers (2008): 0.65 [-] and 0.53 [-] respectively, at an initial TOC concentration of 7.2 [mg/L], using the same resin. The results of the experiment in this thesis were also better than achieved by Audenaert et al. (2015): 0.61 [-] TOC rejection for the first 600 [BV] at a twelve times lower TDS concentration. More information on residual contaminant concentrations can be found in Appendix F Additional experimental results.

The relatively high TOC rejection and small difference with UV254A rejection indicated that a great variety of NOM categories are rejected by IEX. Size probably plays a less significant role. As long as the resin affinity of the (apparently) charged organic molecules is higher than for present of ionic form, exchange of these ions takes place.

The removal of silica for the IEX experiment fluctuated strongly, as presented in Figure 30. No clear breakthrough curve could be drafted, since no decreasing rejection trend resulted from the analyse. Moreover, the rejection after various times proved to be negative. This could either indicate that the resin released silica in these stages, or this is again a result of disturbance in the analytical procedure. The complex presence of the many various negatively charged constituents in the RO-brine and their interaction with the IEX-resin make it impossible to assign a clear cause for the fluctuating silica removal by the IEX-resin, over multiple runs.

Similar as for the NF and ED experiments, reliable iron data was not found.

Regeneration of IEX resin

After operation, the spent resins were generated in three stages. These three stages generated a brine with various characteristics, based on NOM presence. Presence of silica and iron was not considered. The first rinse brine appeared to contain suspended NOM, whereas the eluent brine contained the bulk of dissolved NOM and the final rinse contained traces of dissolved NOM. Visual inspection showed that the suspended NOM settled, in contradiction to dissolved NOM in the eluent brine, as presented in Figure 29. According to IEX TOC mass balances, presented in Appendix D Additional data ED experiment, the regeneration was not very efficient: only 0.20 ± 0.01 [-] of NOM was collected in the mixed IEX-brine, consisting of the three separate brines. The regenerated resins were not tested on reuse for contaminant rejection.

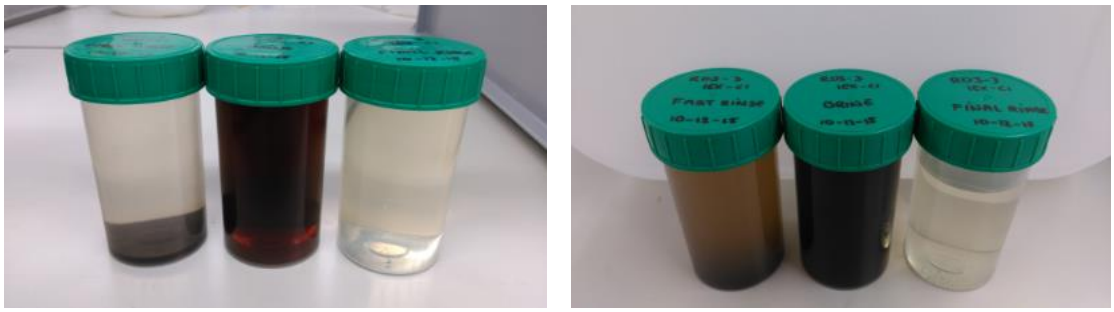

Figure 29 - From left to right: Fast rinse, elution and final rinse brine: settled (left image) and shaken (right image).

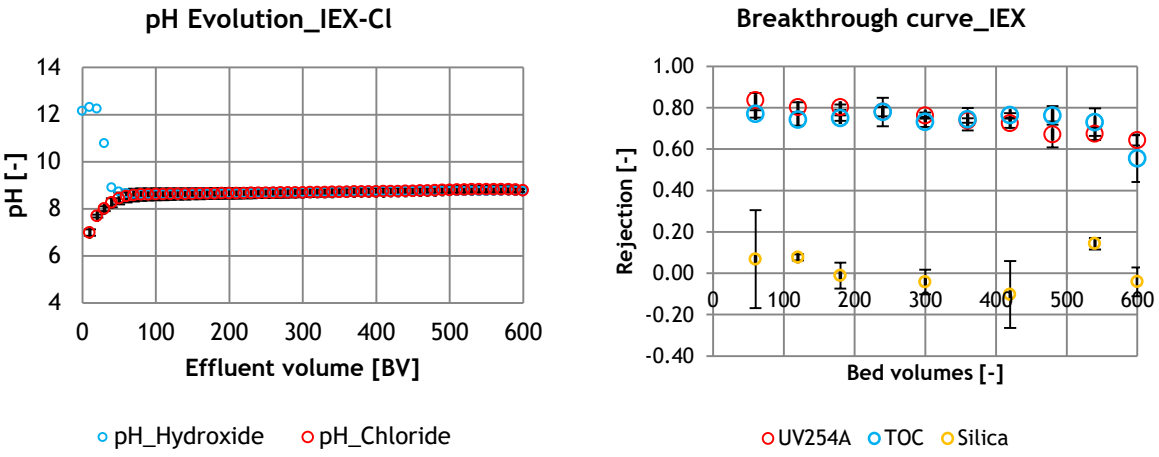

Figure 30 - pH stability according its evolution for hydroxide and chloride ionic forms (left) and the breakthrough curve of the IEX resin in chloride form for UV254A and TOC over 600 [BV] (right).

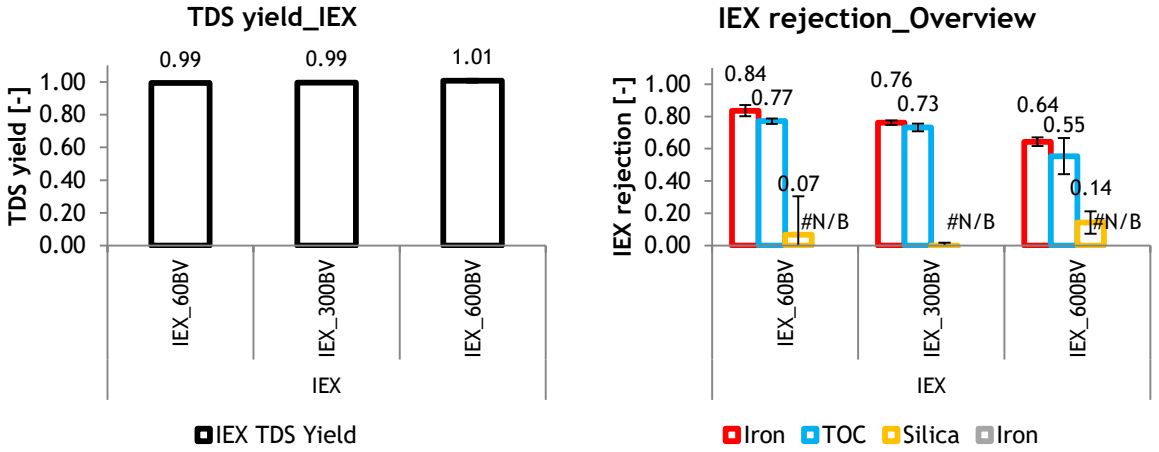

Figure 31 - Average TDS yields (left) and rejection of the contaminants (right) for the IEX runs.

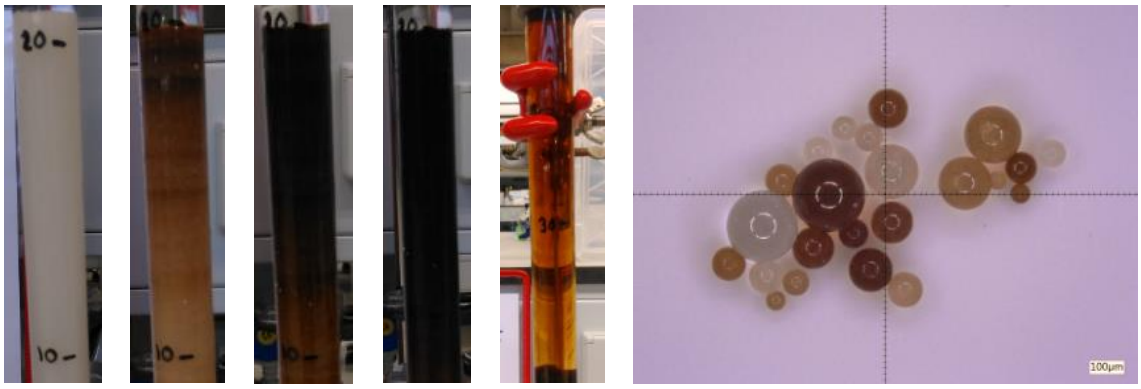

Figure 32 - From left to right: IEX resin at 0, 60, 300 and 600 [BV], elution during generation and regenerated resin at 40x magnification.

4.6. Results of SALEX experiment

(Net) Yield of solids

To determine the yield of solids, the empty columns and dried columns containing (washed) mixed solids were weighed before and after the runs. For a BV of $50.9 \cdot 10^{-3}$ [L], the initial weight of the mixed solids was 46.29 ± 1.72 [g]. The solids yield proved to be in a narrow range: 0.93 ± 0.07 [-] for all combinations, except for the combination of 3BV and 50% bed expansion: 0.52 [-]. This combination of relatively high eluent volume and bed expansion resulted in lower solids yield, because mixed solids were washed away, according to visual inspection.

To determine the net yield of solids, the added NaCl in the eluent was taken into account, resulting in more relevant data. The influence of various eluent volumes proved to be very significant, as presented in Figure 33: usage of more than 1 [BV] of eluent is considered to be inefficient: net yield ≤ 0 [-]. For the usage of 2 [BV] of eluent, the net solids yield was -0.01 ± 0.10 [-] and for the usage of 3 [BV], the net solids yield was even more negative: -0.55 ± 0.18 [-]. Because the application of both 2 [BV] and 3 [BV] results in a negative net solids yield, more solids are required than are finally potentially purified. Therefore, these will be left out of the scope for further analysis and discussion.

Bed expansion did not have a substantial effect on the net solids yield for 1 [BV]. 0% bed expansion resulted in 0.54 [-] net solids yield, whereas 0.51 [-] and 0.56 [-] net solids yield was achieved by 25% and 50% bed expansions, respectively. The results of net solids yield are presented in Figure 33.

Extraction of contaminants

The extraction of contaminants by the SALEX technique proved to deviate over the various applied bed expansions. The extraction of NOM, in terms of TOC, was 0.70 [-] for a bed expansion of 0%, 0.57 [-] for 25% and 0.73 [-] for 50%, indicating that the highest bed expansion facilitates better conditions to elutriate the contaminants. Since these experiments were only executed once, no further verification could be made on the unexpected lower extraction of contaminants by application of 25% bed expansion.

The extraction of silica proved to be very high for all configurations: 0.76 – 0.96 [-]. The highest extraction was achieved for both 25% and 50% bed expansion: 0.96 [-]. Similar as for the NF, ED and IEX experiments, reliable iron rejection and concentrations could not be determined.

Presence of ‘chunks’

During visual inspection, it was observed that larger ‘chunks’ were present in the column during elution, as presented in Figure 34. These chunks appeared to consist of dense contaminated NaCl crystals, as presented in Figure 35. Since these ‘chunks’ are larger than the NaCl crystals in the mixed solids, they are elutriated by the SALEX technique. These ‘chunks’ appeared irregularly, at a low frequency: in 1 out of 9 successful runs, chunks were observed. The ‘chunks’ were not analysed for contaminants extraction.

Visual inspection of the washed solids under the microscope showed significant colour differences, as presented by Figure 35.

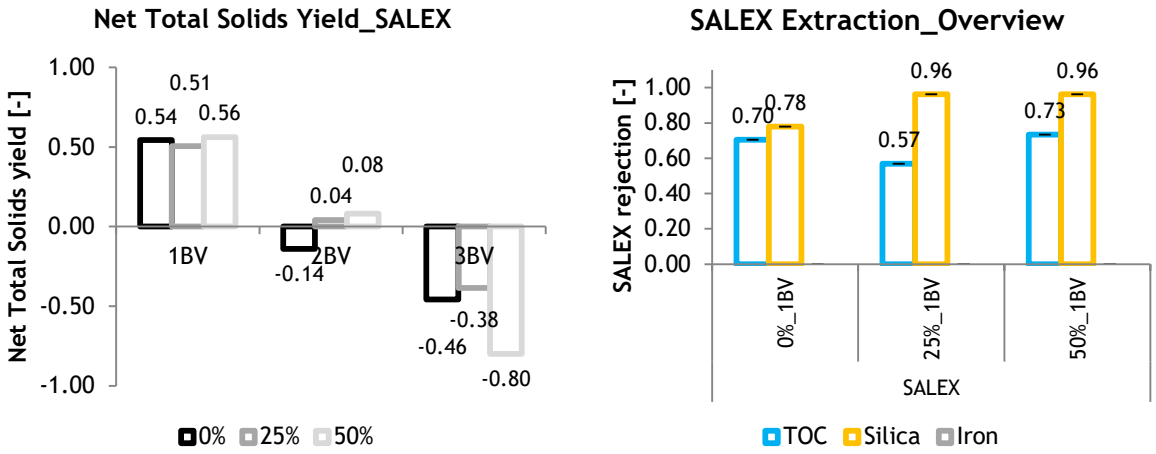

Figure 33 - Average net solids yields (left) and rejection of the contaminants (right) for the SALEX runs.

Figure 34 - Left to right: 0.20 [m] mixed solids in the column, fluidized mixed solids during washing including presence of a 'chunk' and a collection of washed solids, including 'chunks' after a failed attempt.

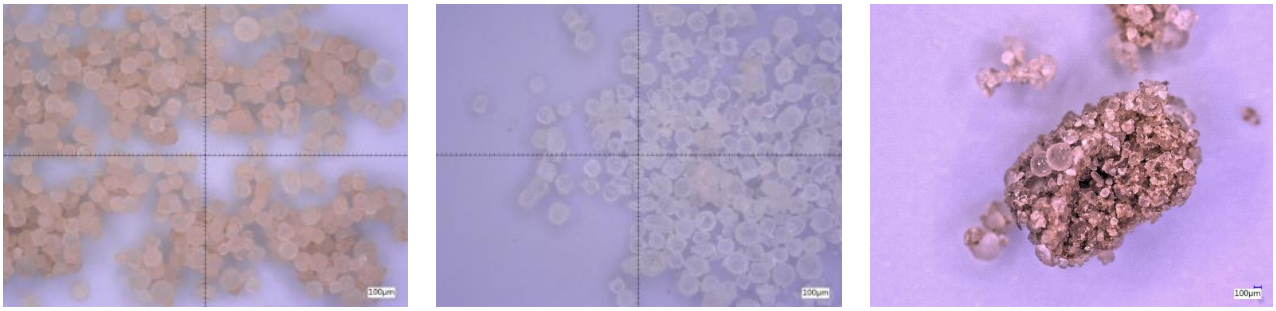

Figure 35 - Brownish mixed solids (left) and whitish washed solids (middle) and a 60x magnification of a 'chunk'.

4.7. Determination of suitable techniques

4.7.1. Determination considerations

The proposed techniques are tested on their performance to produce a high purity (dissolved) NaCl stream. In order to determine the most suitable technique, the QVC limit serves as a guideline, to compare the techniques on their ability to produce high purity NaCl. Additionally, an overview of produced residual streams for each technique is presented in Appendix G Generation of residual streams.

A final, important remark must be made before the techniques are judged on applicability: the RO-brine contained approximately five times more NOM (considered as main contaminant) than the mixed solids: 5.16 ± 0.25 [mg/g] versus 0.99 [mg/g], respectively. This indicates that in the evaporation and crystallization processes in the ZLD WWTP a large fraction of NOM is rejected. According to discussions with company representatives, NOM accumulates in the evaporation and crystallization units, which are occasionally purged. Therefore it is assumed that the allowable dissolved NOM and silica content can be divided by 0.19 [-], resulting in adjusted guidelines for the contaminants in the dissolved state:

- NOM: 1.58 [mg/g] for dissolved, versus 0.30 [mg/g] for solid.
- Silica: 0.005 [mg/g] for dissolved, versus 0.026 [mg/g] for solid.

Iron will be left outside of the scope, since no reliable results were found during the analysis.

The solids yields and rejection of contaminants served as a tool to compare the performance of the proposed techniques. A comparative presentation can be found in Figure 39, Figure 40 and Figure 41. Combining the absolute yields and the absolute concentrations of contaminants in the produced streams (NF permeate, ED concentrate, IEX effluent and washed solids), resulted in the contaminant content, expressed in [mg/g]. From the pre-selection, based on results of the experiments, PNF270-LC appeared to be unsuitable, as the rejection of contaminants was consistently lower than for PNF270-HC. PNF90-HC yielded very little TDS and was therefore considered unsuitable. Finally, IEX in hydroxide ionic form proved to be unstable and was also not suitable. Further selection will be based on comparison of contaminant content to the QVC guidelines (QVC, 2013).

4.7.2. Determination of suitability

All NF configuration were not able to produce a sufficiently pure dissolved NaCl stream, based on both NOM and silica content. ED- STMs neither met the limits for both NOM and silica. ED-MVMs, achieved promising purity results for NOM content, but exceeded the limit for silica content, similar to IEX in chloride form up to 540 [BV]. These two configurations are the two most promising dissolved NaCl isolation techniques.

For the solid purification technique, SALEX proved only to be efficient for washing with 1 [BV], based on the net solids yield. Based on the guidelines restrictions for NOM, the most suitable combination of bed volumes and bed expansion proved to be SALEX using 1 [BV] of eluent. This configuration proved to produce a purity meeting both the limits for NOM and for silica, see Figure 36 and Figure 37.

This finally results in three suitable techniques contributing to produce a high purity NaCl, (partially) meeting the strict guidelines of the QVC.

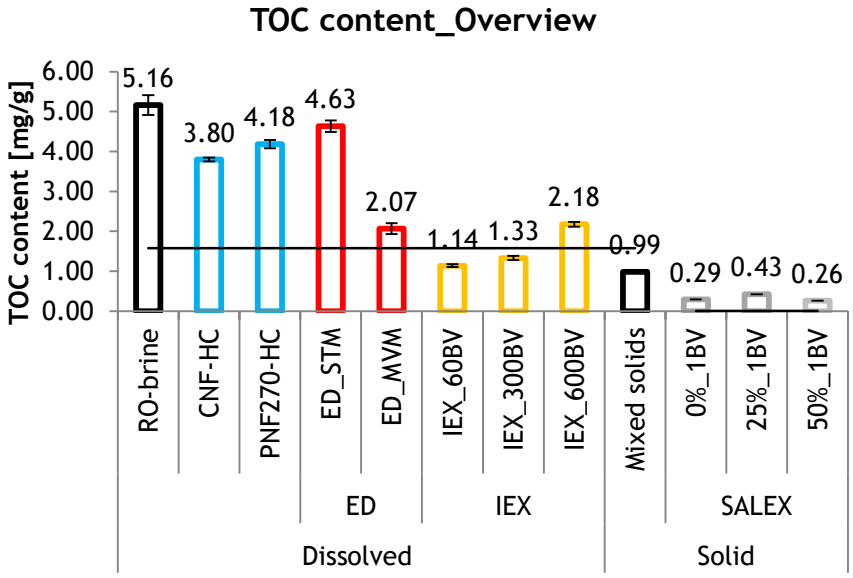

Figure 36 - Overview of the content of NOM per solids, expressed as TOC per solids.

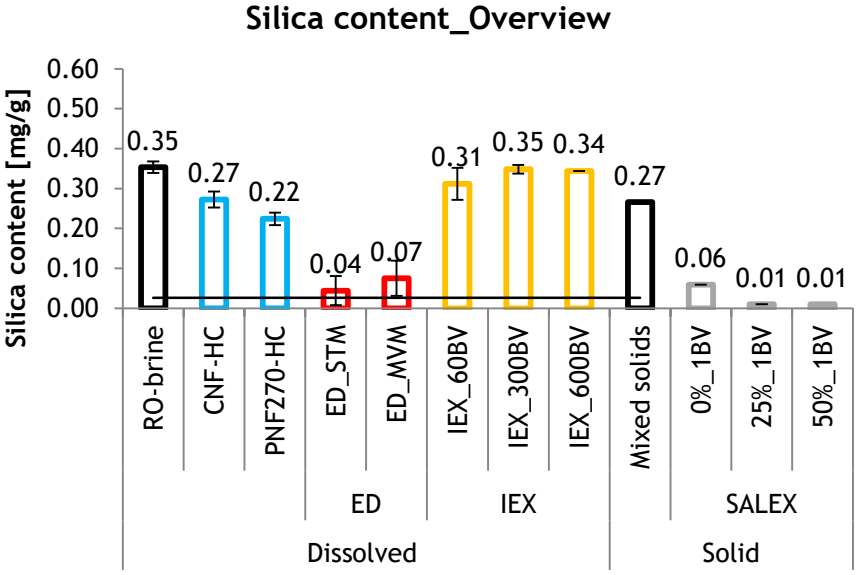

Figure 37 - Overview of the content of silica per solids.

4.7.3. SWOT analysis

The three most promising techniques are assumed to contribute to produce high purity NaCl when they are implemented in the current ZLD WWTP facility. The three techniques have their strengths and weaknesses and therefore a SWOT analysis was conducted to addresses these.

The yield of solids and rejection of contaminants are not taken into account, because the three techniques were already selected on their performance on these topics. Additionally, costs are not taken into account, because no specific knowledge is provided on dimensioning and the presence of energy surpluses or shortages.

ED using MVMs

\+ Strengths: The ED-MVM appeared to remove nearly all constituents giving colour to the solution, according to the UV254A results (~ 0.96 [-]). Therefore, it is assumed that finally whitish solid NaCl can be produced in the ZLD WWTP, with low contamination contents. Additionally, it is possible to concentrate the concentrate at least up to 54 [g/L], as measured in an additional experiment (see Appendix B Observations OIC Experiment). This implies a concentration of the RO-brine of at least eight times, with additional rejection of the contaminants.

– Weaknesses: Since no water is yielded in the concentrate, the volume of the ED-diluate is assumed to be equal to the RO-brine. What is left is a diluted stream of considerable volume, containing biochemically undegradable NOM. Additionally, the operation of ED is not straightforward, because the concentrate should be circulated in order to achieve high concentration. This requires a more complex operation and integration in the ZLD WWTP, where a feed-bleed system might be suitable. This technique did not meet the silica limits.

❖ Opportunities: Since the RO-brine can significantly be concentrated by ED, significant energy savings can be realised, as the evaporators need to evaporate less water. Therefore, an energy balance should be made. The required electrical energy to yield 0.89 [-] of the TDS in the concentrate appeared to be 1.63 [kWh/m^3]. An additional opportunity is the conducted research to membrane selectivity of ion migration by Tanaka et al. (2012), contributing to the rejection performance of the contaminants. A final opportunity is chemical oxidation of the relative low NOM concentration (Murray et al., 2004) and feeding the ED-diluate back to the bio treaters present in the ZLD WWTP.

! Threats: For the ED operation, membranes are the key components, of which fouling was not a topic of this research. According to visual inspection and mass balance calculations, there proved to be organic fouling on the AEMs. The fouling and total lifespan of ED membranes are therefore the major threat for ED implementation (Strathmann, 2010).

IEX in chloride form

\+ Strengths: The implementation of IEX is a straight-forward and well-established. The most common applied configuration is a down-flow resin filter. This configuration implies little energy for pumping or applying an electrical current. Additionally, the IEX-brine produced accounts for only 0.03 [-] of the produced effluent volume, based on the IEX-experiment. This indicates that only a relative small residual stream is produced.

– Weaknesses: The results of the IEX-experiment showed that a regeneration efficiency of 0.20 [-] was achieved, based on mass balance calculations. Based on these results, the regeneration of the IEX resin is assumed to be the main weakness of the technique. Additionally, no additional concentration of the RO-brine is achieved, indicating that still a very large fraction of the water should be reclaimed by evaporation and crystallization. This technique did not meet the silica limits.

❖ Opportunities: Many opportunities lie within the optimization of the regeneration procedure as presented (Hongve et al., 1999). For example, the fast rinse, eluent and final rinse solutions can be reused for other regenerations or different solutions can be used. Additionally, new and more efficient operational configurations are available, facilitation continuous ion exchange and regeneration: SIX configuration (Galjaard et al., 2010). Potentially, NOM can be recovered separately, as presented by Sjoerdsma (2015) using diafiltration (DF).

! Threats: The only actual threat is that regeneration appears to remain inefficient.

SALEX

\+ Strengths: The SALEX technique implementation is simple, because this treatment step can be added at the end of the pipe, where the mixed solids are the final stream in the ZLD WWTP. Additionally, the produced NaCl can directly be re-used in order to purify mixed solids, resulting in a high final net yield. This technique met the QVC guidelines

– Weaknesses: When SALEX is applied, a SALEX-brine will be generated, which is very concentrated with contaminants and NaCl. Additionally, mentioned ‘chunks’ are not elutriated during the experiments and will remain in the washed solids.

❖ Opportunities: In order to decrease the yield of SALEX-brine, the brine can be re-used throughout operation. When the SALEX-brine is assumed to be saturated with contaminants, NaCl can be recovered using NF, which has successfully been achieved by Vaudevire et al. (2013) in a similar brine composition. Another opportunity is the reclamation of humic acids by DF, as presented by Sjoerdsma (2015). ‘Chunks’ can be separate on size exclusion: solids filtration.

! Threats: Potential threats are the resistance of ‘chunks’, suggesting that they are not removed by elutriation or solids filtration.

5. Conclusions

5.1. Contaminants in the mixed solids

The presence of NOM in the mixed solids can be explained by the decay of micro-organisms in the bio treaters of the ZLD WWTP, resulting in various dissolved NOM categories (Lee et al., 2004). This NOM stays dissolved and passes SUF, subsequently ends up in the RO-brine and finally in the mixed solids after evaporation and crystallization. Silica was assumed to end up in the water by environmental influences. The characteristics of silica in water make it likely that is stays dissolved and passes SUF, because the pH is sufficiently low to prevent uncharged silica polymerization (R. Y. Ning, 2003).

Iron was assumed to be absent in both dissolved and undissolved form, based on the physical conditions of the water. Literature research indicated complexation of NOM with iron, where negatively charged dissolved organic molecules serve as ligands to form organic iron complexes. By means of this mechanism, iron can stay dissolved to levels exceeding the solubility product of $Fe(OH)_3$ (Albrektiene et al., 2011). To this extend, the OIC experiment was designed and executed, from which the following was concluded:

- In absence of NOM, 8.0 [mg/L] of Fe^{3+} rapidly formed $Fe(OH)_3$ in oxidized water at pH = 8.0 [-] and is for 0.99 [-] undissolved, according filtration results. During the floc formation, hydroxide was consumed, resulting in a pH drop to pH = 6.3 [-].
- The addition of 1 and 2 [mg/L] NOM did not affect the solubility of iron, because filtration rejected 0.98 – 0.99 [-] of iron, indicating that this fraction was undissolved.
- The addition of 5 and 10 [mg/L] NOM affected the solubility of iron significantly, as on average only 0.77 and 0.34 [-] of iron was rejection by filtration, resulting in a remaining dissolved fraction of 0.23 and 0.64 [-], respectively. For these runs, the pH dropped to pH = 6.5 [-].
- Floc formation was not obstructed by the presence of NOM, because the pH dropped during the runs. Flocculation proved to be obstructed, resulting in very small $Fe(OH)_3$ particles that are considered to be dissolved or colloidal, because they were not rejected by filtration.

➢ Most importantly, it can be concluded that the presence of NOM increased the solubility of iron, because the dissolved iron fraction increased from 0.01 to 0.65 [-] in the presence of 10 [mg/L] NOM corresponding to 0.10 [mg/L] and 5.01 [mg/L], respectively, see Figure 38. This is an increase of approximately fifty times, in terms of iron solubility.

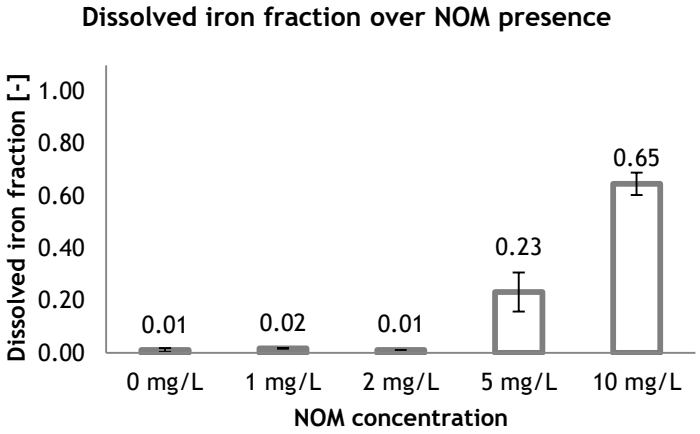

Figure 38 - Overview of the dissolved iron fraction in the presence of various NOM concentrations.

5.2. Isolation of dissolved NaCl

The performance of dissolved NaCl isolation was based on both the yield of (dissolved) solids and the rejection of the contaminants. To this extend, experiments using NF, ED and IEX were executed. As mentioned before, the mechanisms of contaminant rejection were not subject of research in this thesis. Generally, it can be concluded that no reliable iron measurements could be used, because the analysis was probably disturbed by high presence of sodium.

For a clear overview: the results on (dissolved) solids yield are summarized in Figure 39, NOM rejections are summarized in Figure 40 and silica rejections are summarized in Figure 41.

5.2.1. NF experiment

The NF experiment consisted of various tested membranes (polymeric and ceramic) and configurations: low cross-flow (dead-end) and high cross-flow, for which the HMP, TDS yield and contaminant rejection were determined as performance indicators. From this experiment, the following can be concluded:

Hydraulic membrane permeability

- The HMP appeared to deviate significantly over the various tested configurations, which was a function of the TMP, because the water flux was fixed and the HMP was corrected for temperature. The application of a high cross-flow configuration showed a relative decrease in TMP of 0.23 [-] for PNF270 membranes, with respect to a low cross-flow (dead-end) configuration.
- The HMP for CNF membranes appeared to be 2.2 times lower than for PNF270 membranes for high cross-flow conditions, indicating that the CNF membranes are more water permeable than the tested PNF membranes.

Dissolved solids yield

- PNF90 membranes proved to be unsuitable to isolate dissolved NaCl, because this type of membrane only yielded TDS for 0.11 [-].
- The TDS yield for PNF270-LC, CNF-HC and PNF270-HC was similarly high: 0.97, 0.99 and 0.97 [-], respectively.

Rejection of contaminants

- The rejection of NOM appeared to deviate significantly between in terms of UV254A and TOC: 0.14 ± 0.06 [-] over the executed runs. For all runs, it was found that NOM rejection, in terms of UV254A, was always higher than actual TOC. This implies that NOM categories containing aromatic molecules are removed to a higher extend than other NOM categories.
- PNF270-LC performance consistently worse than CNF-HC and PNF270-HC on the rejection of NOM, whereas the last two mentioned performed equally moderately, suggesting that a low cross-flow configuration suffers from more contaminant passage over the membrane. This is potentially caused by concentration polarization of the contaminants: accumulation of contaminants near membrane.
- The rejection of silica was considerable for CNF-HC and PNF270-HC: 0.21 [-] and 0.45 [-], respectively. From these results it can be concluded that PNF membranes reject silica to a higher extend than CNF membranes.

5.2.2. ED experiment

The ED experiment involved various types of membranes (standard and monovalent-selective) to determine the performance of ED on dissolved NaCl isolation. Based on this experiment, the following can be concluded:

LCD effect on ED operation

- Due to correction of the applied current density to the LCD, the potential never exceeded 9 [V] in all executed runs, which is the critical point for undesired water splitting.
- The migration factor proved to be slightly higher for MVMs membranes: 0.37 [$mg \cdot s^{-1} \cdot m^{-2} \cdot (A \cdot m^{-2})$]over 0.36 [$mg \cdot s^{-1} \cdot m^{-2} \cdot (A \cdot m^{-2})$] for STMs on average.
- The ion migration flux proved to be directly linked to the applied current density. By correcting for the LCD, the ion migration flux decreased simultaneously with the applied current density.

Dissolved solids yield

- The aimed TDS yield of 0.89 [-] was achieved within an hour and proved to be equal for all runs, with various membranes. The average migration flux was 13 [$mg \cdot s^{-} \cdot m^{-2}$].
- Higher TDS yield, up to > 0.99 [-] appeared to be possible, but the migration flux and therefore duration decreases significantly. Additional half an hour is required to yield the final 0.10 [-].
- The concentrate can be concentrated to at least 47 [g/L], where considerably high migration flux of 17 [$mg \cdot s^{-} \cdot m^{-2}$] was achieved for a diluate TDS concentration of 2.9 [g/L].

Contaminant rejection

- Aromatic molecules were rejected by ED to high extend: 0.90 and 0.96 [-] for STMs and MVMs, respectively. As the TOC rejection was consistently lower, there appeared to be a preferential rejection for NOM categories containing aromatic molecules.
- MVMs appeared to have significantly better NOM rejection characteristics than STMs.
- STMs appeared to reject silica to higher extend than MVMs, which is probably caused by the charge of silica: more charged silica results in lower rejection.
- Fouling of AEMs (adsorption of NOM) was observed throughout the runs by visual inspection and verified mass balances.

5.2.3. IEX experiment

Ionic form of resin

- The application of resin with hydroxide as ionic form is not suitable for the isolation of dissolved NaCl because the ionic form is rapidly replaced by chloride from the feed water. For the treatment of water with a high TDS concentration, this phenomenon should be considered.

Dissolved solids yield

- The TDS yield for 600 [BV] RO-brine using IEX in chloride form appeared to be 1.00 [-] on average. Because during IEX, the ionic strength of the water remains constant and the TDS contains similar ions are the ionic form, the TDS proved to remain unaffected.

Rejection of contaminants

- The rejection of NOM in terms of UV254A and TOC did not deviate significantly, in contrast to the NF and ED experiment: 0.06 ± 0.02 [-] difference. Apparently, the effect of preferential rejection is applicable to less extend for IEX and a wider variation of NOM is adsorbed.
- The rejection of contaminants decreased over the amount of treated bed volumes.
- Poor silica rejection was achieved by IEX, which is probably caused by higher selectively for other negatively charged constituents or a low presence of charged silica.
- Official breakthrough occurred immediately, because no contaminant-free effluent was produced. Practical breakthrough, related to the limited contaminant content appeared to occur after 540 [BV] of produced effluent.
- The regeneration of the IEX proved to be inefficient, because only 0.20 [-] of the adsorbed NOM was found in the IEX-brine.

5.3. Purification of mixed solids

SALEX was experimentally tested to purify the contaminated mixed solids. Based on the results of the SALEX experiment, the following conclusions can be drawn:

- The solids yield achieved in the SALEX experiment proved to be high: 0.93 [-], on average. Because the SALEX technique required solids to prepare eluent, the solids yield needed to be corrected for the preparation of eluent, resulting in 0.54 [-] on average. The application of more than 1 [BV] of eluent proved to be inefficient, because the net solids yield was negative for the application of 2 and 3 [BV]: more solids were required to prepare eluent than were yielded.
- The application of 50% bed expansion resulted in slightly elevated contaminant extraction: 0.73 [-] maximally.
- Silica proved to be rejected to a very high extend, indicating that the silica was probably present on the outside of the NaCl crystals and could therefore easily be elutriated.
- The mixed solids appeared to contain chunks, which could not be elutriated and remained in the washed solids during the runs in the experiment.

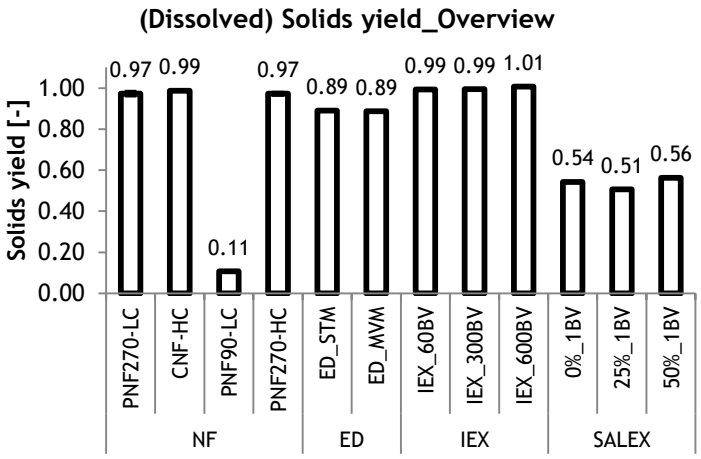

Figure 39 - Overview of (dissolved solids) yield achieved by the various tested techniques.

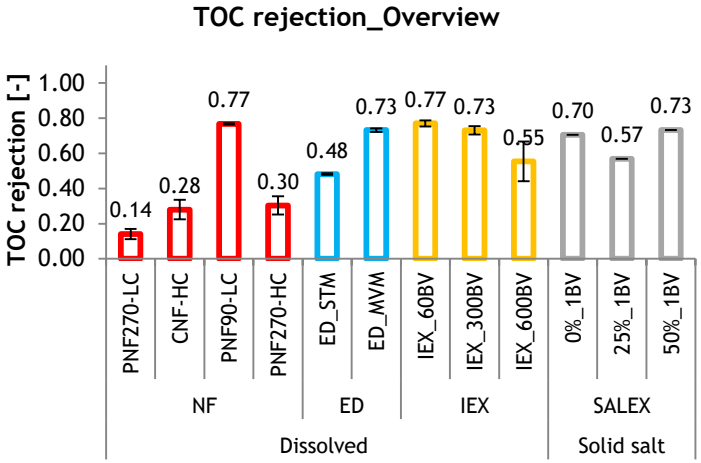

Figure 40 - Overview of UV254A (left) and TOC (right) rejection achieved by all tested techniques.

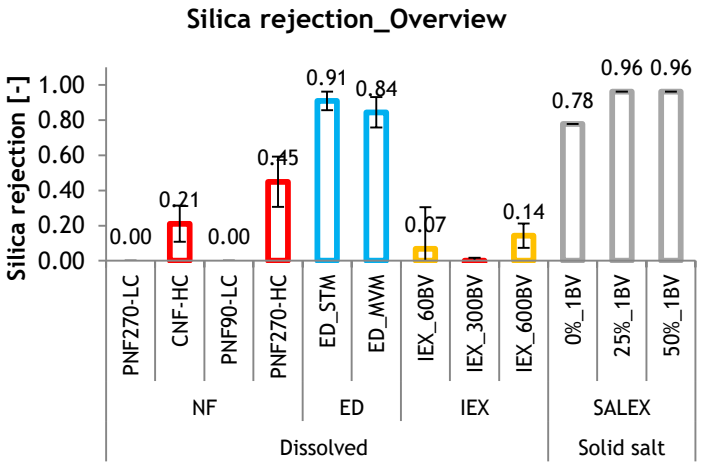

Figure 41 - Overview of silica (left) and iron (right) rejection achieved by all tested techniques.

5.4. Determination of suitable techniques

The comparison of techniques contributing to produce of high purity were compared based on contaminant content per total amount of solids. Based on this comparison, the following conclusions can be drawn:

- The contaminant content, based on NOM, in the RO-brine appeared to be more than five times the contaminant content in the mixed solids. Therefore it was assumed that the evaporation and crystallization processes in the ZLD WWTP reject a fraction of the contaminants. The limit for dissolved streams was therefore corrected with respect to solid streams, as presented in Table 12.
- ED-MVM and IEX-Cl proved to be able to produce a stream meeting dissolved contaminant content limit for NOM and were therefore selected as suitable techniques.
- SALEX proved to be able to produce a solid stream meeting the contaminant content guidelines for NOM and silica and was therefore selected as final suitable technique.

Table 12 - Overview of the minimum contaminant content in the various produced streams. N/A = not available.

	RO-brine	Limit dissolved	PNF270-HC	CNF-HC	ED-STM	ED-MVM	IEX-540BV
TOC [mg/g]	4.91	**1.58**	4.08	3.75	4.49	1.57	1.38
Silica [mg/g]	0.34	**0.026**	0.20	0.26	0.37	0.47	0.27
Iron [mg/g]	N/A	**0.053**	N/A	N/A	N/A	N/A	N/A

	Mixed solids	Limit solid	SALEX-50%
TOC [mg/g]	0.99	**0.30**	0.26
Silica [mg/g]	0.27	**0.005**	< 0.010
Iron [mg/g]	N/A	**0.01**	N/A

Finally, a SWOT analysis has been conducted for these techniques, to address strengths, weaknesses, opportunities and threats. A summary of this SWOT analysis is presented in Table 13.

Table 13 – An overview of the results of the SWOT analysis on ED-MVM, IEX-Cl and SALEX.

	Strengths	Weaknesses	Opportunities	Threats
ED-MVM	+ Near complete colour reduction + Additional RO-brine concentration	– Large residual stream volume – Complex integration – Did not meet silica limits	❖ Energy savings concentration ❖ Improving membrane selectivity	! Membrane fouling
IEX-Cl	+ Easy operation + Small volume residual stream	– Poor regeneration efficiency – No additional concentration RO-brine – Did not meet silica limits	❖ Innovation in operation and regeneration IEX ❖ Potential NOM recovery	! Poor regeneration of resin
SALEX	+ Easy integration + Direct re-use of NaCl + Met all purity limits	– Concentrated residual stream – Presence of 'chunks'	❖ Staged re-use of SALEX-brine ❖ Potential NOM recovery ❖ Solids filtration	! Resistance of 'chunks'

6. Recommendations

The presence of the contaminants in the mixed solids is considered to be inevitable, according the probable origins and the characteristics. Therefore, the implementation of one of the three selected techniques is required. The QVC limit served as a quality guidelines for this thesis. According to the purity of the SALEX salt product, the strengths drafted in the SWOT analysis and considerable weaknesses and threats, SALEX is recommended as suitable technique to contribute to produce high purity NaCl in the ZLD WWTP.

To this extend, several more specific recommendations on the implementation are drafted, considering a suitable, promising configurations and potential research questions which need to be addressed. Recommendations on dimensions is not considered since additional data needs to be collected to this extend.

The application of dissolved intervention technique proved to produce NaCl of lower purity and had much more threats, according to the SWOT analysis. Nevertheless, in Appendix H Proposal for NaCl isolation techniques, recommendations for the implementation of the two most promising dissolved intervention techniques (ED-MVM and IEX-Cl) are presented.

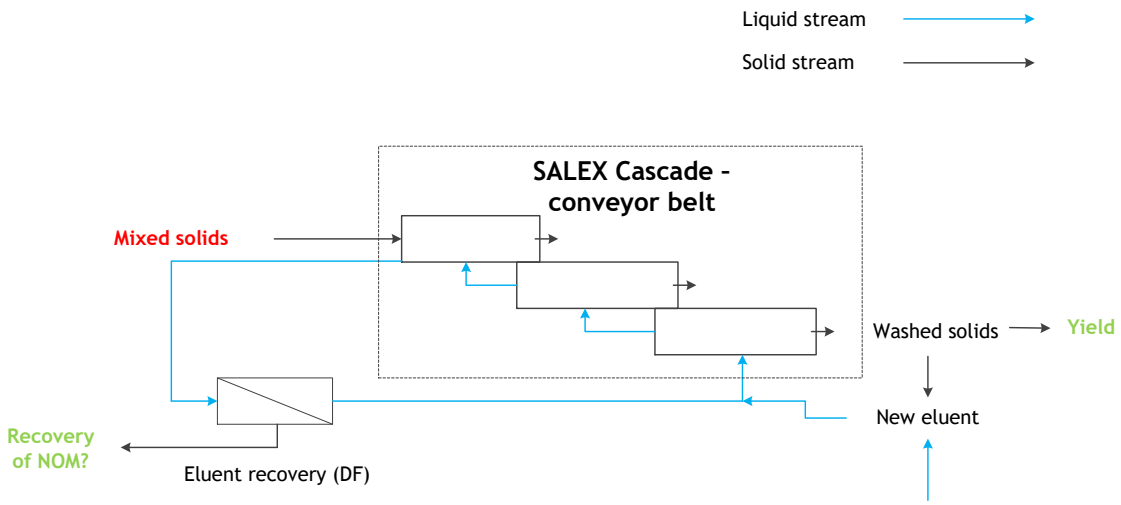

Figure 42 - A schematic presentation of the proposed SALEX configuration, including all relevant streams.

For the implementation of the SALEX technique, a cascade conveyor belt configuration is proposed, as schematized in Figure 42. In this configuration, the mixed solids are horizontally displaced in multiple stages, in order to meet desired contact time with the eluent. Within the horizontal displacement, screen filtration is possible to reject the 'chunks' based on size.

The eluent flows in an up-flow configuration through the porous conveyor belts to achieve bed expansion during the horizontal displacement. The bottom stage in the cascade contains the cleanest mixed solids and therefore the cleanest eluent is inserted here in the first place. Subsequently, the eluent is re-used and flows to the middle stage in the cascade to wash the second cleanest mixed solids. Finally, the most contaminated mixed solids are washed with the least clean eluent in the top stage of the cascade. By means of recirculation of the SALEX-brine, the volume of eluent can significantly be reduced, with respect to the results of the SALEX-experiment in this thesis.

The SALEX-brine is discharged after it has been used to its maximum potential and subsequently the dissolved NaCl can be recovery by DF, in a similar way as the IEX-brine treatment. The recovered NaCl from the SALEX-brine can be re-use in the preparation of new eluent.

The recommended bed expansion is 50%, according to the experimental results. In order to implement a certain SALEX configuration, multiple additional research topics should be resolved in bench-scale experiments followed by a pilot plant, including:

- Recirculation potential of the SALEX-brine.
- Elutriation of contaminants during a horizontal displacement of mixed solids.
- Solid filterability of 'chunks'.

Bibliography

Acevedo, C. R., et al. (2010). *Silica removal from brine by using ion exchange*. Paper presented at the World Environmental and Water Resources Congress 2010: Challenges of Change - Proceedings of the World Environmental and Water Resources Congress 2010.

Ahmed, M., et al. (2003). Feasibility of salt production from inland RO desalination plant reject brine: A case study. *Desalination, 158*(1–3), 109-117. doi: http://dx.doi.org/10.1016/S0011-9164(03)00441-7

Akhavan, A. C. (2009). Chemical Properties. Retrieved 24-07-2015, 2015, from http://www.quartzpage.de/gen_chem.html

Alberti, F., et al. (2009). Salt production from brine of desalination plant discharge. *Desalination and Water Treatment, 10*(1-3), 128-133.

Albrektiene, R., et al. (2011). *The removal of iron-organic complexes from drinking water using coagulation process*. Paper presented at the 8th International Conference on Environmental Engineering, ICEE 2011.

Alchin, D., & Wansbrough, H. (2002). Ion Exchange Resins: The New Zealand Institute of Chemistry.

Alexander, G. B., et al. (1954). The solubility of amorphous silica in water. *Journal of Physical Chemistry, 58*(6), 453-455. doi: 10.1021/j150516a002

Andrade Becheleni, E. M., et al. (2015). Water recovery from saline streams produced by electrodialysis. *Environ Technol, 36*(1-4), 386-394. doi: 10.1080/09593330.2014.978898

Audenaert, W. T. M., et al. (2015). Removal of natural organic matter (NOM) by ion exchange from surface water for drinking water production: a pilot-scale study. *Desalination and Water Treatment*, 1-12. doi: 10.1080/19443994.2015.1061457

Baghoth, S. A., et al. (2008). An urban water cycle perspective of natural organic matter (NOM): NOM in drinking water, wastewater effluent, storm water, and seawater. *Water Science and Technology: Water Supply, 8*(6), 701-707. doi: 10.2166/ws.2008.146

Baker, R. W. (2000). *Membrane Technology and Applications*. New York: McGraw-Hill.

Beckett, R., et al. (1987). Determination of molecular weight distributions of fulvic and humic acids using flow field-flow fractionation. *Environmental Science & Technology, 21*(3), 289-295. doi: 10.1021/es00157a010

Bellona, C., et al. (2004). Factors affecting the rejection of organic solutes during NF/RO treatment—a literature review. *Water Research, 38*(12), 2795-2809. doi: http://dx.doi.org/10.1016/j.watres.2004.03.034

Belton, D. J., et al. (2012). An overview of the fundamentals of the chemistry of silica with relevance to biosilicification and technological advances. *FEBS Journal, 279*(10), 1710-1720. doi: 10.1111/j.1742-4658.2012.08531.x

Ben Sik Ali, M., et al. (2013). Iron removal from brackish water by electrodialysis. *Environmental Technology, 34*(17), 2521-2529. doi: 10.1080/09593330.2013.777081

Bergna, H. E. (1994). Colloid Chemistry of Silica *The Colloid Chemistry of Silica* (Vol. 234, pp. 1-47): American Chemical Society.

Bergna, H. E., & Roberts, W. O. (2005). *Colloidal Silica: Fundamentals and Applications* (Vol. 131).

Bolto, B., et al. (2002). Removal of natural organic matter by ion exchange. *Water Research, 36*(20), 5057-5065. doi: http://dx.doi.org/10.1016/S0043-1354(02)00231-2

Bruland, K. W., & Rue, E. L. (1999). Iron: Analytical methods for the determination of concentrations and speciation *IUPAC Working group on iron in the oceans*. Santa Cruz: Institute of Marine Sciences.

Cob, S. S. (2014). *Towards Zero Liquid Discharge in drinking water production*. (PhD), Delft University of Technology, Delft.

Cowan, D. A., & Brown, J. H. (1959). Effect of Turbulence on Limiting Current in Electrodialysis Cells. *Industrial & Engineering Chemistry, 51*(12), 1445-1448. doi: 10.1021/ie50600a026

de Leeuw, K. (2013). *Recycling of Industrial Water: The journey of Pearl GTL*. Paper presented at the Vakantiecursus Delft, the Netherlands.

de Ridder, D., et al. (2014). Solutions for COD-removal in zero liquid discharge. Delft: Delft University of Technology.

De Sacadura Bretes, M. (1985).

DOW. (2006a). FILMTEC™ Membranes *FILMTEC NF90&270 Nanofiltration Elements for Commercial Systems*: The DOW Chemical Company.

DOW. (2006b). FILMTEC™ Membranes *System Design: Membrane System Design Guidelines for Commercial Elements*: The DOW Chemical Company.

Firdaous, L., et al. (2007). Transfer of monovalent and divalent cations in salt solutions by electrodialysis. *Separation Science and Technology, 42*(5), 931-948. doi: 10.1080/01496390701206413

Galjaard, G., & Koreman, E. (2010). SIX®: A New Resin Treatment Technology for Drinking Water. *Water Practice & Technology, 01*. doi: DOI: 10.2166/wpt.2009.076

Geraldes, V., et al. (2008). Spiral-wound module nanofiltration of surface river water. *E-Water*.

Grefte, A. (2013). *Removal of Natural Organic Matter Fractions by Anion Exchange: Impact on drinking water treatment processes and biological stability*. (PhD Dissertation), Delft University of Technology, Delft.

Griffin, S. J., et al. (2011). *The Advantage of Mixed Salt Crystallizers in Zero Liquid Discharge (ZLD) Wastewater Treatment Systems*. Paper presented at the IWC-98-50.

Hach-Lange. (2013). Working procedure: LCK321 Iron (Vol. AD_321): Hach-Lange.

Heidekamp, M. (2013). *Mild desalination of cooling tower blowdown water with electrodialysis and membrane capacitive deionization: a comparative study*. (MSc), Delft University of Technology, Delft.

Hem, J. D., & Cropper, W. H. (1959). Survey of ferrous-ferric chemical equilibria and redox potentials *Water Supply Paper* (- ed.).

Hendricks, D. (2006). *Water Treatment Unit Processes: Physical and Chemical*: CRC Press.

Hongve, D., et al. (1999) Experiences from operation and regeneration of an anionic exchanger for natural organic matter (NOM) removal. *Vol. 40. Water Science and Technology* (pp. 215-221).

Huber, S. A. (2002). *Differences in the Composition of Organic Impurities in Ground and Surface Waters: Consequences for the Preparation of Boiler Feed Water*. Paper presented at the Chemistry 2002: International conference on water chemistry in nuclear reactors systems - operation optimisation and new developments, France.

Huber, S. A., et al. (2011). Characterisation of aquatic humic and non-humic matter with size-exclusion chromatography – organic carbon detection – organic nitrogen detection (LC-OCD-OND). *Water Research, 45*(2), 879-885. doi: http://dx.doi.org/10.1016/j.watres.2010.09.023

Jeppesen, T., et al. (2009). Metal recovery from reverse osmosis concentrate. *Journal of Cleaner Production, 17*(7), 703-707. doi: http://dx.doi.org/10.1016/j.jclepro.2008.11.013

Kabsch-Korbutowicz, M., et al. (2011). Application of UF, NF and ED in natural organic matter removal from ion-exchange spent regenerant brine. *Desalination, 280*(1–3), 428-431. doi: http://dx.doi.org/10.1016/j.desal.2011.06.068

Kaeocha Eilers, A. (2008). *Ion exchange for NOM removal in drinking water treatment*. (MSc), Delft University of Technology, Delft.

Kawakubo, S., et al. (2002). Speciation of iron in river water using a specific catalytic determination and size fractionation. *J Environ Monit, 4*(2), 263-269.

Keller, M. (2004). Softening: Iron Removal by Ion Exchange—Standing on Solid Ground. *Water Conditioning & Purification, 46*(6), 20-24.

Koenings, J. P., & Hooper, F. F. (1976). The influence of colloidal organic matter on iron and iron-phosphorus cycling in an acid bog lake1. *Limnology and Oceanography, 21*(5), 684-696. doi: 10.4319/lo.1976.21.5.0684

Kopeliovich, D. (2012). Pourbaix diagrams. Retrieved 04-08-2015, 2015, from http://www.substech.com/dokuwiki/doku.php?id=pourbaix_diagrams

Koprivnjak, J. F., et al. (2006). Coupling reverse osmosis with electrodialysis to isolate natural organic matter from fresh waters. *Water Research, 40*(18), 3385-3392. doi: http://dx.doi.org/10.1016/j.watres.2006.07.019

Korshin, G. V., et al. (1999). Use of differential spectroscopy to evaluate the structure and reactivity of humics. *Water Science and Technology, 40*(9), 9-16. doi: http://dx.doi.org/10.1016/S0273-1223(99)00634-4

Lanxess. (2011). Lewatit® VP OC 1071 *X_Lewatit* (2011-10-13 ed.): Lanxess Energizing Chemistry.

Lee, N., et al. (2004). Identification and understanding of fouling in low-pressure membrane (MF/UF) filtration by natural organic matter (NOM). *Water Research, 38*(20), 4511-4523. doi: 10.1016/j.watres.2004.08.013

Matilainen, A., et al. (2011). An overview of the methods used in the characterisation of natural organic matter (NOM) in relation to drinking water treatment. *Chemosphere, 83*(11), 1431-1442. doi: 10.1016/j.chemosphere.2011.01.018

Meyers, P. (1999). Behavior of silica in ion exchange and other systems *October 18-20*. Pittsburgh, PA: International Water Conference.

Mickley, M., & WateReuse, F. (2008). *Survey of high-recovery and zero liquid discharge technologies for water utilities*. Alexandria, Va.: WateReuse Foundation.

Miller, W. S., et al. (2009). Understanding Ion-Exchange Resins For Water Treatment Systems: GE Water & Process Technologies.

Murray, C. A., & Parsons, S. A. (2004) Advanced oxidation processes: Flowsheet options for bulk natural organic matter removal. *Vol. 4. Water Science and Technology: Water Supply* (pp. 113-119).

NASA. (2014). NASA Goddard Instrument Makes First Detection of Organic Matter on Mars [Press release]. Retrieved from https://www.nasa.gov/content/goddard/mars-organic-matter

Nathoo, J., et al. (2009). *Freezing your brines off: Eutectic Freeze Crystallization for brine treatment*. Paper presented at the International Mine Water Conference, Pretoria, South Africa.

Nikonenko, V. V., et al. (2014). Desalination at overlimiting currents: State-of-the-art and perspectives. *Desalination, 342*, 85-106. doi: http://dx.doi.org/10.1016/j.desal.2014.01.008

Ning, R. Y. (2003). Discussion of silica speciation, fouling, control and maximum reduction. *Desalination, 151*(1), 67-73. doi: 10.1016/S0011-9164(02)00973-6

Ning, R. Y., & Tarquin, A. J. (2010). Crystallization of salts from super-concentrate produced by tandem RO process. *Desalination and Water Treatment, 16*(1-3), 238-242. doi: 10.5004/dwt.2010.1098

Olariu, R. (2015). *Treatment of cooling tower blowdown water – The effect of biodispersant on the ultrafiltration membrane*. (MSc), Delft University of Technology, Delft.

PCCell. (2013). PCA Ion Exchange Membranes: Technical Data Sheet. Heusweiler: PCCell GmbH.

PCCell. (2014). PC Cell ED 64 0 02 *Electrodialysis Cell Unit*. Heusweiler, Germany: PCCell GmbH.

Pérez-González, A., et al. (2012). State of the art and review on the treatment technologies of water reverse osmosis concentrates. *Water Research, 46*(2), 267-283. doi: http://dx.doi.org/10.1016/j.watres.2011.10.046

QVC. (2013). Quality restrictions for sodium chloride. Qatar: Qatar Vinyl Company Ltd.

Roberts, D. A., et al. (2010). Impacts of desalination plant discharges on the marine environment: A critical review of published studies. *Water Research, 44*(18), 5117-5128. doi: http://dx.doi.org/10.1016/j.watres.2010.04.036

Rue, E. L., & Bruland, K. W. (1995). Complexation of iron(III) by natural organic ligands in the Central North Pacific as determined by a new competitive ligand equilibration/adsorptive cathodic stripping voltammetric method. *Marine Chemistry, 50*(1–4), 117-138. doi: http://dx.doi.org/10.1016/0304-4203(95)00031-L

Saracco, G., & Zanetti, M. C. (1994). Ion transport through monovalent-anion-permselective membranes. *Industrial & Engineering Chemistry Research, 33*(1), 96-101. doi: 10.1021/ie00025a013

Sedivy, V. M. (1996). Purification of salt for chemical and human consumption. *Industrial Minerals*.

Shang, R. (2014). *Ceramic Ultra- and Nanofiltration for Municipal Wastewater Reuse*. (Dissertation), Delft University of Technology, Delft.

Shapiro, J. (1964). Effect of Yellow Organic Acids on Iron and Other Metals in Water. *Journal (American Water Works Association), 56*(8), 1062-1082. doi: 10.2307/41264269

Sjoerdsma, P. (2015). *Color in drinking water: from interfering substance into valuable commodity*. Paper presented at the NOM6 Congress, Malmo.

Specht, C. H., & Frimmel, F. H. (2000). Specific Interactions of Organic Substances in Size-Exclusion Chromatography. *Environmental Science & Technology, 34*(11), 2361-2366. doi: 10.1021/es991034d

Strathmann, H. (2010). Electrodialysis, a mature technology with a multitude of new applications. *Desalination, 264*(3), 268-288. doi: http://dx.doi.org/10.1016/j.desal.2010.04.069

Tanaka, N., et al. (2012). Organic fouling behavior of commercially available hydrocarbon-based anion-exchange membranes by various organic-fouling substances. *Desalination, 296*, 81-86. doi: http://dx.doi.org/10.1016/j.desal.2012.04.010

Valero, F., et al. (2011). Electrodialysis Technology - Theory and Applications. In M. Schorr (Ed.), *Desalination, Trends and Technologies*: InTech.

Vandezande, P., et al. (2008). Solvent resistant nanofiltration: Separating on a molecular level. *Chemical Society Reviews, 37*(2), 365-405. doi: 10.1039/b610848m

Vanoppen, M. (2015, 25-09-2015). [Discussion on Electrodialysis Experiments].

Vaudevire, E., & Koreman, E. (2013). *Ion exchange brine treatment: closing the loop of NaCl use and reducing disposal towards a zero liquid discharge*. Paper presented at the Win4Life, Tinos Islands, Greece.

White, M. J., et al. (2010). Reverse Osmosis Pre Treatment of High Silica Waters. In G. P. Water (Ed.), *Water & Process Technologies* (Vol. TP1058EN).

Xu, T., & Huang, C. (2008). Electrodialysis-based separation technologies: A critical review. *AIChE Journal, 54*(12), 3147-3159. doi: 10.1002/aic.11643

Zaman, M., et al. (2015). Downstream processing of reverse osmosis brine: Characterisation of potential scaling compounds. *Water Research, 80*, 227-234. doi: 10.1016/j.watres.2015.05.004

Zhang, Y., et al. (2011). Electrodialysis on RO concentrate to improve water recovery in wastewater reclamation. *Journal of Membrane Science, 378*(1–2), 101-110. doi: http://dx.doi.org/10.1016/j.memsci.2010.10.036

Appendices

Appendix A NOM categorization

NOM categorization mixed solids

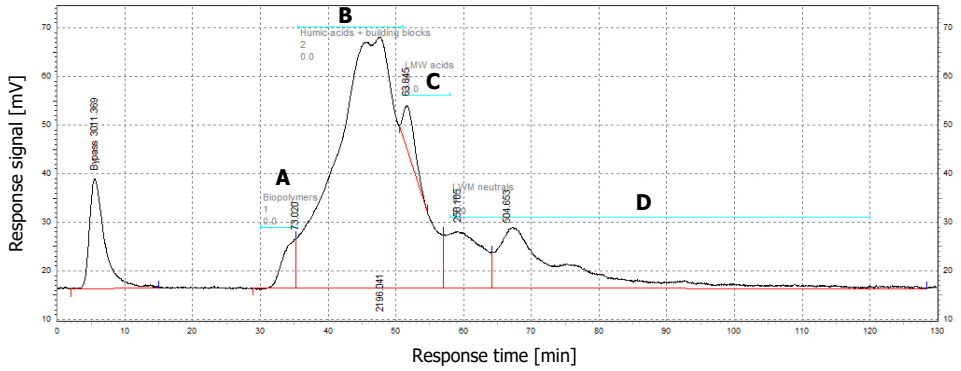

Figure 43 - NOM categorization RO-brine first analysis

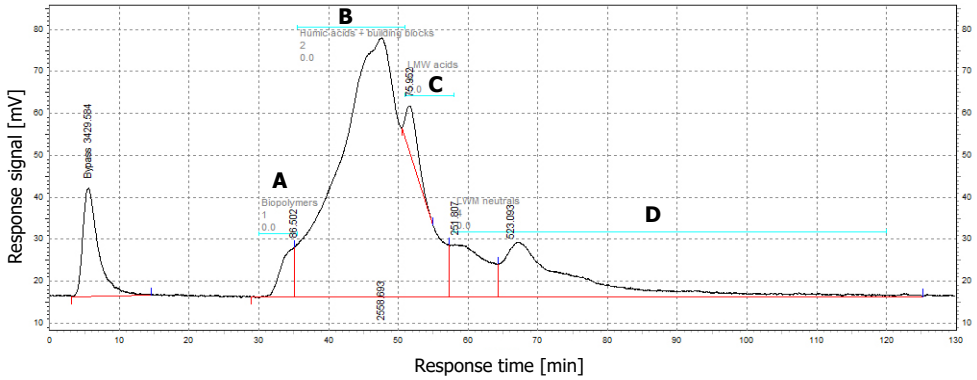

Figure 44 - NOM categorization RO-brine second analysis

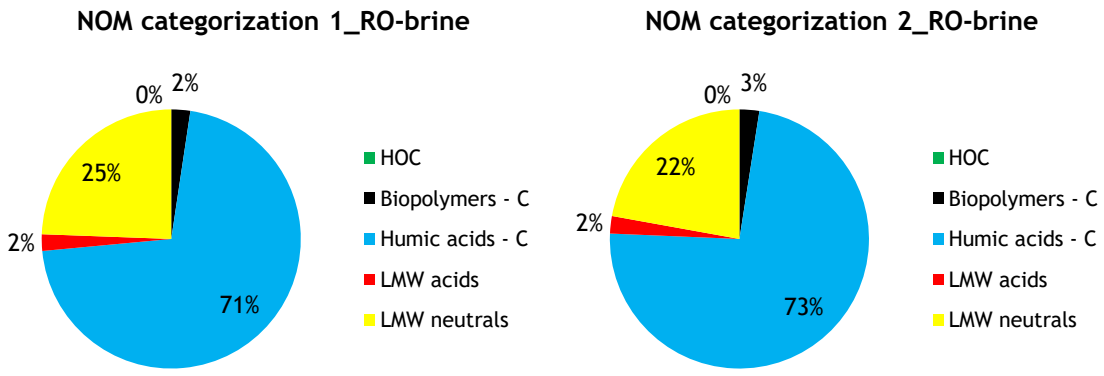

Figure 45 - Relative distribution of NOM presence in the RO-brine.

NOM categorization mixed solids

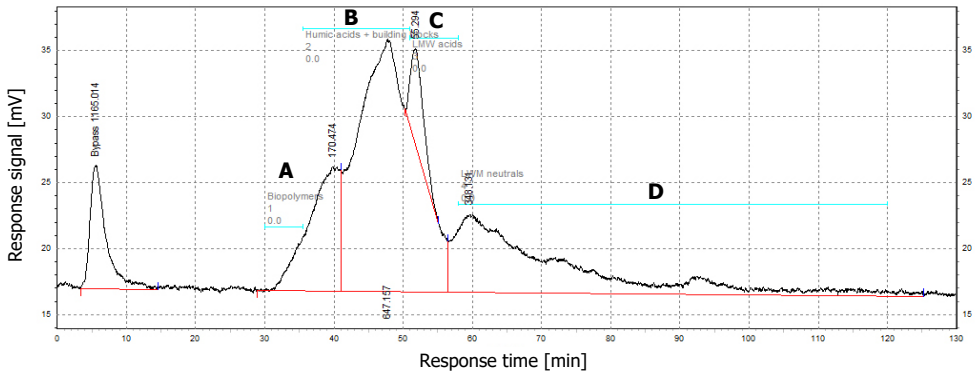

Figure 46 - NOM categorization mixed solids first analysis.

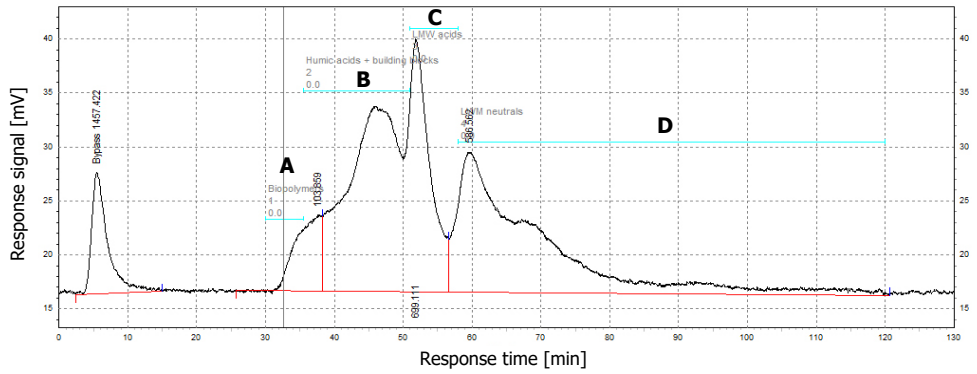

Figure 47 - NOM categorization mixed solids second analysis.

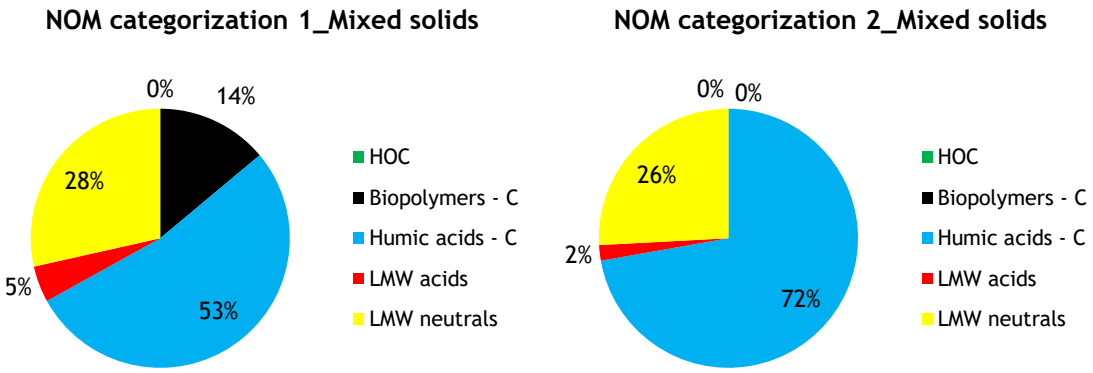

Figure 48 - Relative distribution of NOM presence in the mixed solids.

Appendix B Observations OIC Experiment

Isolation of NOM

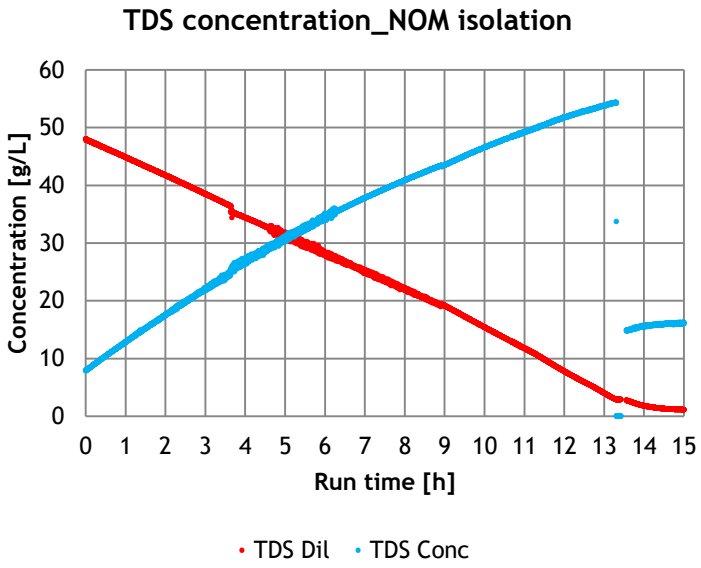

Figure 49 - Evolution of the TDS concentration in the diluate (concentrated RO-brine solids solution) and concentrate (NaCl solution). After 13.5 hours, the concentrate solution was changed to see an effect on migration flux for various concentrate solutions.

pH evolution during the experiments

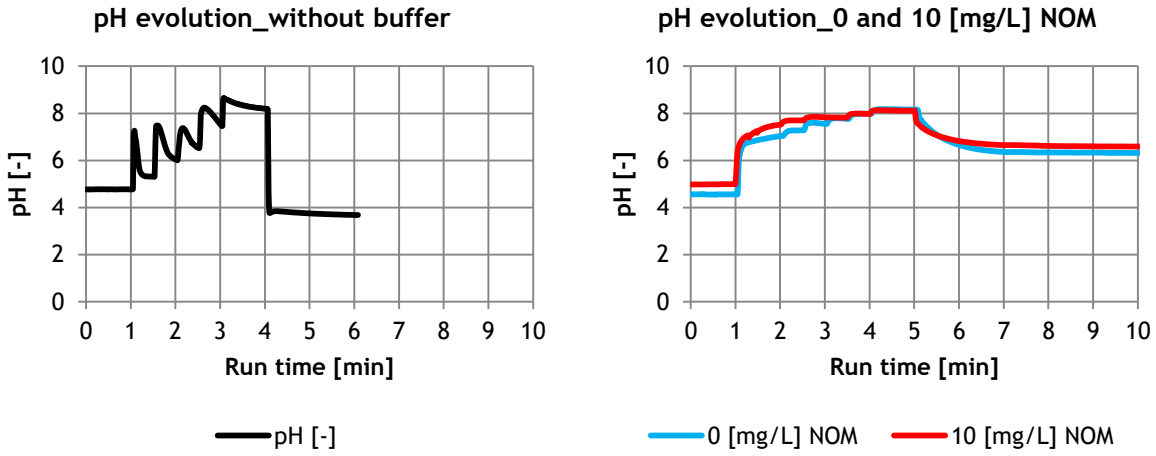

Figure 50 - Left: Evolution of the pH, with and without addition of buffer: pH dropped directly to pH < 4.0 [-]. Right: Evolution of the pH for 0 and 10 [mg/L] NOM addition. Final pH is slightly higher for 10 [mg/L] NOM addition: pH = 6.5 [-] over pH = 6.3 [-] fo

Appendix C Additional data NF experiments

Procedure of PNF270-HC runs

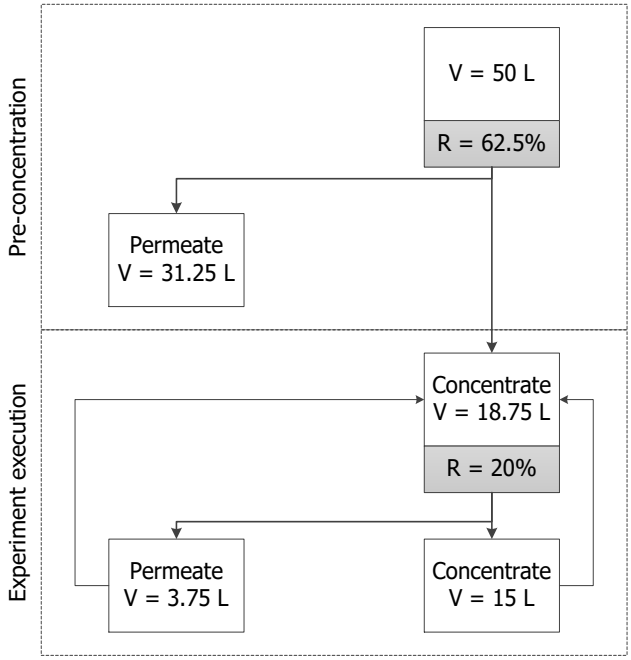

Figure 51 - A schematic visualization of the pre-concentration procedure, applied for the PNF270-HC runs.

Chemical PNF270 membrane cleaning

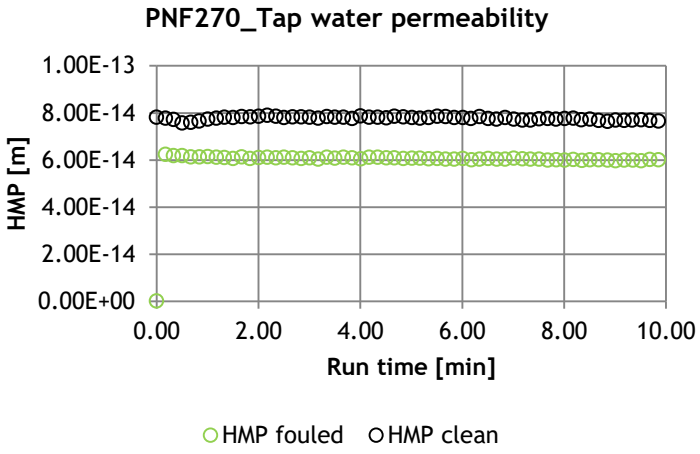

Figure 52 - The HMP for the fouled and clean PNF270 membrane for tap water at 8 [L/m2/h] and 21 [°C]. Feed pressure was approximately 4.0 [bar].

Appendix D Additional data ED experiment

Limiting current density tests

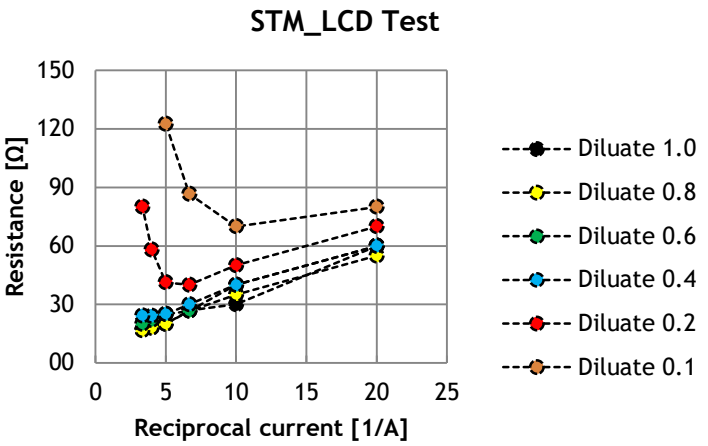

Diluate [-]	TDS [g/L]	LCD [A/m^2]
1.0	6.75	47
0.8	5.70	47
0.6	3.67	47
0.4	2.93	39
0.2	1.52	23
0.1	0.88	23

Figure 53 - The LCD results for the STMs, including corresponding TDS concentrations.

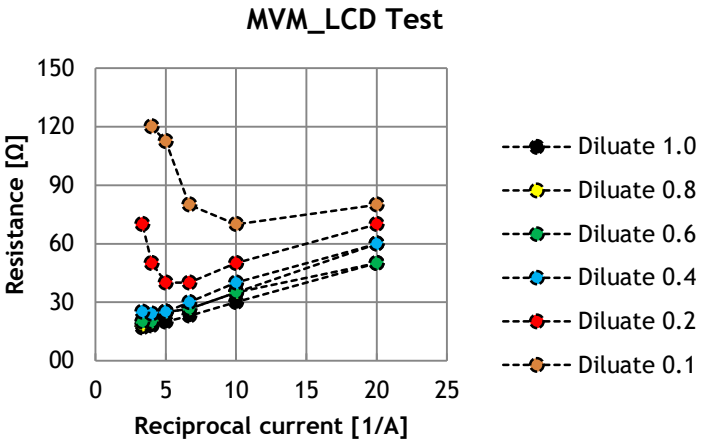

Diluate [-]	TDS [g/L]	LCD [A/m^2]
1.0	6.63	47
0.8	5.64	47
0.6	3.87	39
0.4	2.43	39
0.2	1.18	23
0.1	0.60	16

Figure 54 - The LCD results for the MVMs, including corresponding TDS concentrations.

TOC balance

Table 14 - Overview of the TOC in the diluate and concentrate for the runs using STMs, resulting in adsorbed TOC. The concentrations in the electrolyte proved to be negligible: very low and stable.

	ID	TOC [mg/L]	TOC_Change [mg/L]	Adsorbed TOC [mg/L]
Run 1	STM Dil 1.1	50.30	36.32	10.46
	STM Dil 1.2	13.97		
	STM Conc 1.1	1.80	25.86	
	STM Conc 1.2	27.67		
Run 2	STM Dil 3.1	52.51	36.65	9.17
	STM Dil 3.2	15.85		
	STM Conc 3.1	2.26	27.48	
	STM Conc 3.2	29.74		
Run 3	STM Dil 4.1	50.18	36.21	10.35
	STM Dil 4.2	13.97		
	STM Conc 4.1	1.80	25.86	
	STM Conc 4.2	27.67		

Table 15 – Overview of the TOC in the diluate and concentrate for the runs using MVMs, resulting in adsorbed TOC. The concentrations in the electrolyte proved to be negligible: very low and stable.

	ID	TOC [mg/L]	TOC_Change [mg/L]	Adsorbed TOC [mg/L]
Run 1	MVM Dil 2.1	47.88	30.88	18.17
	MVM Dil 2.2	17.00		
	MVM Conc 2.1	2.05	12.71	
	MVM Conc 2.2	14.76		
Run 2	MVM Dil 4.1	40.70	20.45	9.00
	MVM Dil 4.2	20.26		
	MVM Conc 4.1	1.79	11.44	
	MVM Conc 4.2	13.23		
Run 3	MVM Dil 5.1	32.34	14.93	6.63
	MVM Dil 5.2	17.41		
	MVM Conc 5.1	1.26	8.30	
	MVM Conc 5.2	9.56		

Appendix E Additional data IEX experiment

Regeneration efficiency determination

Bed volumes	Acc. loaded TOC [mg]	Acc. loaded TOC [mg]	Acc. loaded TOC [mg]
0	0	0	0
60	81	77	82
120	162	154	155
180	240	230	235
240	331	308	308
300	409	381	386
360	490	450	468
420	570	530	545
480	648	616	619
540	718	701	691
600	760	771	751

	Recovered TOC [mg]	Recovered TOC [mg]	Recovered TOC [mg]
Fast rinse	29.4	24.1	14.4
Eluent	129.5	121.0	125.6
Final rinse	4.2	4.0	3.6
Total	163.1	149.1	143.6
Efficiency	**0.21**	**0.19**	**0.19**

Table 16 - Results of three generation runs, where TOC is chosen as recovered pollutant.

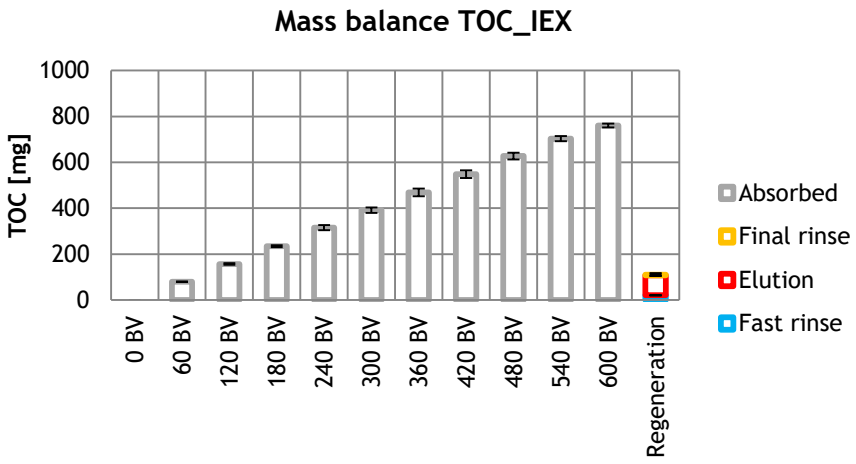

Figure 55 - Overview of average loaded and recovered TOC for the executed regeneration runs.

Appendix F Additional experimental results

Residual dissolved contaminant concentrations

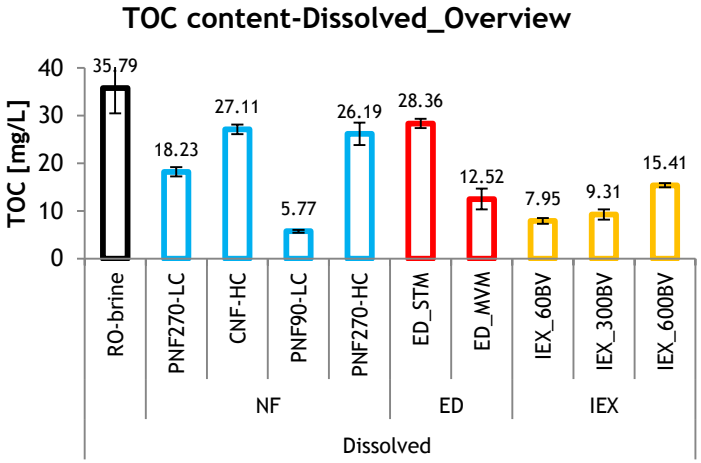

Figure 56 - An overview of the residual TOC concentrations in the respective isolated NaCl streams.

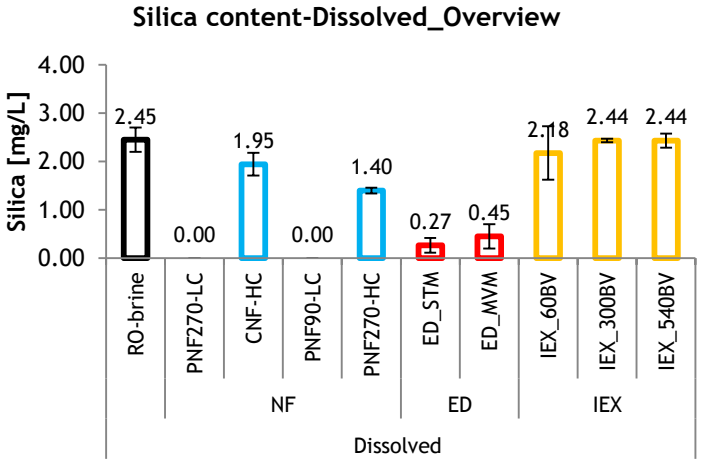

Figure 57 - An overview of the residual silica in the respective isolated NaCl streams.

Appendix G Generation of residual streams

During the application of all proposed techniques to produce high purity (dissolved) NaCl, residual streams are produced, including:

- Nanofiltration: NF-concentrate
- Electrodialysis: ED-diluate
- Ion exchange: IEX-brine
- SALEX: SALEX-brine

The composition and fraction of the feed stream is of importance, because these streams need to be processed as well in ZLD process. In TDS, the bulk is considered to be NaCl and $NaHCO_3$, unless noted different.

For NF a recovery of 0.70 [-] was applied during both CNF-HC and PNF-HC, resulting in a fraction of 0.30 [-] of the feed stream for the residual concentrate stream. The composition of the NF-concentrates is derived from performed measurements and mass balance calculations, based on rejection, recovery and feed concentrations. This stream can be considered as moderately concentrated.

No significant fraction of water is abstracted from the ED-diluate: only by potential osmosis and co-migration. This stream is therefore relatively large, but contains low TDS concentrations, because these were mostly abstracted during the ED process. TOC, iron and silica concentrations in the ED-diluate were derived from performed measurements. This stream can be considered as diluted.

The IEX-brine is a mixture of the three mentioned brines (fast rinse, elution and final rinse). The IEX-brine considered a total volume of 14 [BV] for 600 [BV] produced effluent, which is a relative small fraction of the feed stream. The composition of the IEX-brine is based on measurements and the used eluent and rinse TDS concentrations. This stream can be considered as very concentrated.

In the application of the SALEX technique, the SALEX-brine is the considered residual stream. Because the feed stream in SALEX consisted of solids, the fraction is also expressed in solids: amount of NaCl used for eluent preparation and washed solids amount. The concentration is expressed as a solution and corresponding composition in terms of contaminants is derived from measurements. This stream can be considered as extremely concentrated.

Table 17 presents an overview of the compositions and fractions of the respective streams.

Table 17 - Summary of composition of the various produced residual stream, with average concentration of TDS and contaminants.

	CNF-HC	PNF-HC	ED-STM	ED-MVM	IEX-Brine	SALEX-brine
Fraction of feed stream	0.30	0.30	~ 0.99	~ 0.99	0.03	0.48
TDS [g/L]	7.3	7.3	6.1	6.1	29	400
TOC [mg/L]	45	42	15	18	166	596
Silica [mg/L]	2.7	1.5	2.7	3.3	14	27
Iron [mg/L]	N/A	N/A	N/A	N/A	N/A	N/A

Appendix H Proposal for NaCl isolation techniques

Electrodialysis implementation proposal

The ED technique is proposed to be implemented in a feed-and-bleed configuration, where the concentrates is concentrated throughout operation. The diluate passes through various ED-stacks, resulting in gradually decreasing TDS concentration. Since the TDS concentration decreases, the applied current density is reduced in each sequencing ED-stack, according to the LCD. Finally, when the aimed TDS yield is achieved, the diluate can potentially be oxidized chemically, in order to oxidize the contaminants. This diluted, oxidized stream can subsequently be fed back to the bio-treaters in the ZLD WWTP.

The most diluted concentrate will flow through the last ED-stack (lowest applied current density) and is gradually concentrated, as it is partially recirculated and partially flowing to the next ED-stack. The most concentrated concentrate flows through the first ED-stack (highest applied current density) and is collected in a concentrate tank. When the aimed concentration has been achieved, the concentrate flows to the evaporators and crystallizers, to recover high purity NaCl.

Part of the recovered NaCl can be re-used directly for new concentrate preparation, which is fed to a different concentrate tank. By means of this configuration, energy used in the evaporation process can be saved, which can be used in the operation of the ED. Finally, yielded solid NaCl can be exported.

Data obtained from the ED-experiment, such as the LCD determination, ion migration fluxes per applied current density and rejection of contaminants can be used for the design. In order to implement this ED configuration, multiple additional research topics should be resolved in bench-scale experiments followed by a pilot plant, considering:

- Mass balance for the system to determine potential yields, (recirculation) flow rates and TDS concentrations in all streams.
- Concentration behaviour and migration efficiency in the various stacks.
- Potential to chemically oxidize the contaminants in the diluate.

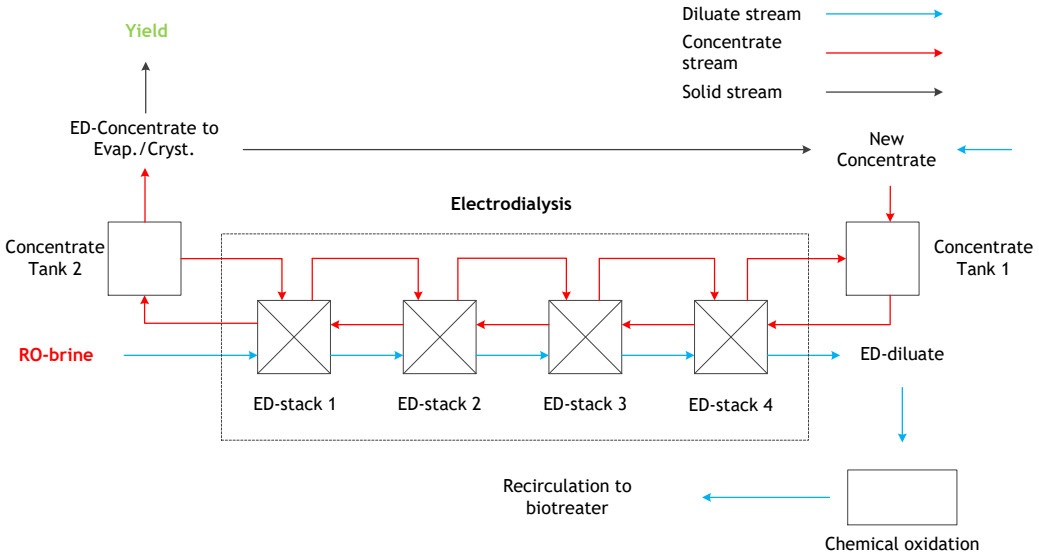

Figure 58 - A schematic presentation of the proposed ED configuration, including all relevant streams.

Ion exchange implementation proposal

The IEX technique is proposed to be implemented in suspended ion exchange (SIX) configuration, according the designed principle of PWN Technologies (Galjaard et al., 2010). This configuration is chosen since a down-flow column configuration appeared to come with a significant drawback: insufficient achieved regeneration. Since the saturation of the IEX bed gradually travels down the bed, saturation difference occur over the bed height, as presented in visual inspection results. To overcome this problem, a SIX configuration is proposed, making use of direct regeneration.

In this configuration, the RO-brine will be mixed with fresh IEX-resin in chloride form and flows through a plug-flow system, to achieve the required contact time of two minutes to reject the required amount of contaminants. Subsequently, the resin and RO-brine, will be separated by a sieve or coarse filter (SF). The treated RO-brine can subsequently be evaporated and crystallized, to produce high purity NaCl, which can be re-used as IEX-resin eluent and the solid yield can potentially be exported. The separated IEX-resin can partially be re-circulated or is regenerated immediately. At this point, the IEX-brine can be filtered by diafiltration in order to potentially recover NOM, in a similar way as performed by Vitens (Sjoerdsma, 2015). Another way to recover dissolved NaCl from a with contaminants concentrated IEX-brine is PNF (Vaudevire et al., 2013). This configuration potentially results in a closed loop, with exception of required water to produce new eluent and the final yield of solid NaCl as output.

Data from the IEX-experiment on rejection of contaminants can be used for the design. To this extend, it is recommended to maintain a contact time of two minutes and the usage of Lewatit VP OC 1071 resin is recommended. In order to implement a certain IEX configuration, multiple additional research topics should be resolved in bench-scale experiments followed by a pilot plant, considering:

- Suitable techniques to separate the IEX-resin from the effluent and to recover NaCl from concentrated IEX-brine.
- Mass balance for the system to determine potential yields and recirculation flows.

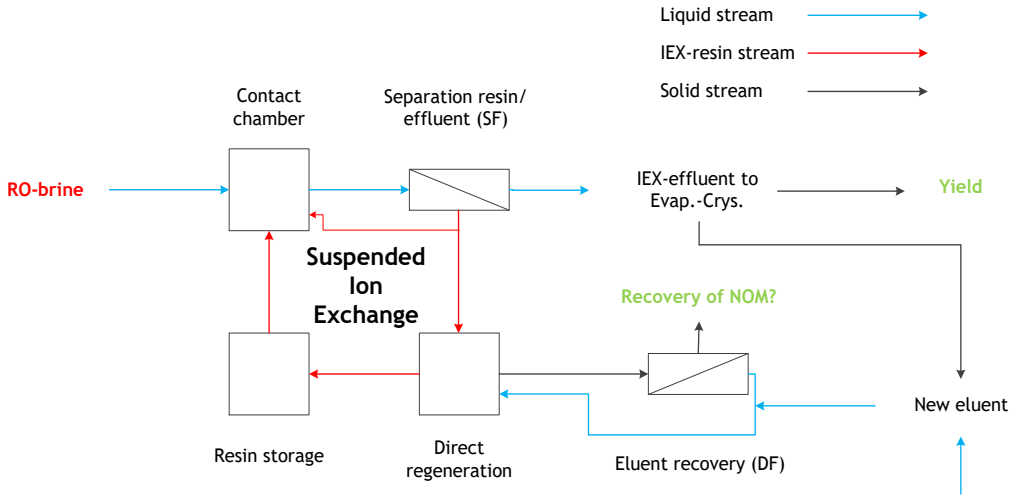

Figure 59 - A schematic presentation of the proposed IEX configuration, including all relevant streams.